AD NUMBER

ADB027806

LIMITATION CHANGES

TO:

Approved for public release; distribution is unlimited.

FROM:

Distribution authorized to U.S. Gov't. agencies only; Test and Evaluation; APR 1978. Other requests shall be referred to Air Force Rome Air Development Center, Attn: RBTV, Griffiss AFB, NY 13441.

AUTHORITY

radc, usaf ltr, 8 nov 1982

(2) LEVEL I

RADC-TR-78-75
Final Technical Report
April 1978

PRECISION ANTENNA MEASUREMENT SYSTEM (PAMS) ENGINEERING SERVICES

Graham A. Walker

Actron

ROME AIR DEVELOPMENT CENTER
Air Force Systems Command
Griffiss Air Force Base, New York 13441

RADC-TR-78-75 has been reviewed and is approved for publication.

APPROVED: Merton E. Cook
MERTON E. COOK
Project Engineer

APPROVED: Joseph J. Naresky
JOSEPH J. NARESKY
Chief, Reliability and Compatibility Division

FOR THE COMMANDER: John P. Huss
JOHN P. HUSS
Acting Chief, Plans Office

If your address has changed or if you wish to be removed from the RADC mailing list, or if the addressee is no longer employed by your organization, please notify RADC ((RBTV), Griffiss AFB NY 13441. This will assist us in maintaining a current mailing list.

Do not return this copy. Retain or destroy.

UNCLASSIFIED

SECURITY CLASSIFICATION OF THIS PAGE (When Data Entered)

REPORT DOCUMENTATION PAGE

READ INSTRUCTIONS BEFORE COMPLETING FORM

1. REPORT NUMBER: RADC-TR-78-75	2. GOVT ACCESSION NO.	3. RECIPIENT'S CATALOG NUMBER
4. TITLE (and Subtitle): PRECISION ANTENNA MEASUREMENT SYSTEM (PAMS) ENGINEERING SERVICES		5. TYPE OF REPORT & PERIOD COVERED: Final Technical Report. 19 Apr 74 - 14 Oct 75
		6. PERFORMING ORG. REPORT NUMBER: B7785030-1000
7. AUTHOR(s): Graham A. Walker		8. CONTRACT OR GRANT NUMBER(s): F30602-74-C-0241
9. PERFORMING ORGANIZATION NAME AND ADDRESS: Actron, 700 Royal Oaks Drive, Monrovia CA 91016		10. PROGRAM ELEMENT, PROJECT, TASK AREA & WORK UNIT NUMBERS: J. O. 21140301
11. CONTROLLING OFFICE NAME AND ADDRESS: Rome Air Development Center (RBTV), Griffiss AFB NY 13441		12. REPORT DATE: April 1978 13. NUMBER OF PAGES: 112
14. MONITORING AGENCY NAME & ADDRESS (if different from Controlling Office): Same		15. SECURITY CLASS. (of this report): UNCLASSIFIED 15a. DECLASSIFICATION/DOWNGRADING SCHEDULE: N/A

16. DISTRIBUTION STATEMENT (of this Report)

Distribution limited to U.S. Government agencies only; test and evaluation; April 1978. Other requests for this document must be referred to RADC (RBTV), Griffiss AFB NY 13441.

17. DISTRIBUTION STATEMENT (of the abstract entered in Block 20, if different from Report)

None

DDC RECEIVED JUL 12 1978 B

18. SUPPLEMENTARY NOTES

RADC Project Engineer: Merton E. Cook (RBTV)

19. KEY WORDS (Continue on reverse side if necessary and identify by block number)

Antenna Measurements
Propagation
Radar Cross Section (RCS)
Signal Sources
Data Processing
Test Facilities

20. ABSTRACT (Continue on reverse side if necessary and identify by block number)

This final report documents the hardware modifications, software programs, analysis efforts and hardware study concepts, which were performed on the Precision Antenna Measurement System (PAMS) and associated airborne instrumentation. The PAMS and airborne instrumentation are fully described in technical reports RADC-TR-73-233 and RADC-TR-74-174.

DD FORM 1 JAN 73 1473 EDITION OF 1 NOV 65 IS OBSOLETE

UNCLASSIFIED

SECURITY CLASSIFICATION OF THIS PAGE (When Data Entered)

PREFACE

This is the Final Technical Report for the PAMS Engineering Services. The effort reported herein was performed during the period of 19 April 1974 through 14 October 1975.

The Final Technical Report covers the work performed by Actron, Division of McDonnell Douglas Corporation, 700 Royal Oaks Drive, Monrovia, California and was submitted in fulfillment of Contract F30602-74-C-0241 and was written by Graham A. Walker.

Acknowledgement is made here to William G. Duff of Atlantic Research Corporation, Alexandria, Virginia of his efforts in the preparation of the "Site Evaluation and Propagation Analysis for the Precision Antenna Measurement Program" which is included as Appendix III to this report.

The principal contributors to the PAMS Engineering Services were: Program Manager, Robert B. Alterman; Project Engineer, Graham A. Walker; Alan D. Reed, who did the programming and Marcus Lewinstien who was responsible for the system error analysis.

A special note of appreciation is extended to Mr. M. E. Cook for his valuable guidance and support throughout the program.

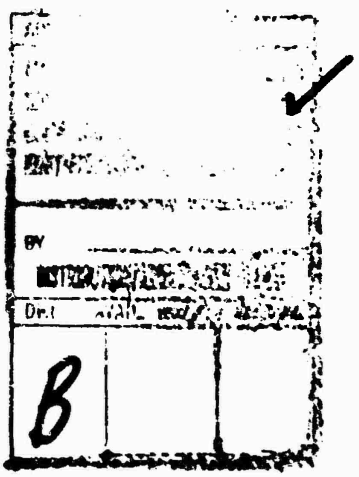

TABLE OF CONTENTS

LIST OF ILLUSTRATIONS

LIST OF ILLUSTRATIONS (CONTINUED)

LIST OF TABLES

TABLE OF CONTENTS

LIST OF ILLUSTRATIONS

LIST OF ILLUSTRATIONS (CONTINUED)

LIST OF TABLES

LIST OF ILLUSTRATIONS

LIST OF TABLES

LIST OF ILLUSTRATIONS

LIST OF ILLUSTRATIONS (CONTINUED)

EVALUATION

This technical report documents the hardware enhancements, software programs, analysis efforts, and hardware study concepts which were performed on the Precision Antenna Measurement System (PAMS) and associated airborne instrumentation. The minor hardware modification provided extreme flexibility in system configuration; thereby, enabling custom data collection and retrieval which satisfied the users complex test requirements. Detailed studies of calibration/alignment hardware, system error analysis, propagation analysis and radar cross section measurements were conducted to identify and analyze hardware, software and environmental limitations of the system which are evident during dynamic airborne antenna evaluations. The hardware study has identified a cross section measurement capability, which can be easily integrated into the present system configuration at minimal costs. The cross section measurements program can be conducted simultaneously while collecting airborne antenna patterns or weapon system evaluations.

Merton E. Cook

MERTON E. COOK
Project Engineer

SECTION I

INTRODUCTION AND SUMMARY

1.1 INTRODUCTION

The PAMS Engineering Services Program was initiated to provide technical support for experimental testing, and dynamic engineering evaluations of airborne antenna systems utilizing the Precision Antenna Measurement System and associated airborne instrumentation.

The support level included the modification of existing PAMS instrumentation, new computer programs, and analyses of the PAMS and its environment. The program also included the operation and maintenance of the PAMS; however, this aspect will not be reported on in this document.

1.2 SUMMARY

Section II of this report covers all of the major activities performed under the PAMS Engineering Services. Detailed analyses of the PAMS calibration and alignment, error analysis, propagation analysis, and radar cross section measurements which were previously submitted as separate reports are included in this document as appendixes I through IV.

SECTION II

PAMS ENGINEERING SERVICES

2.1 TECHNICAL SUPPORT

The Engineering Services program provided for a broad spectrum of technical support for the PAMS and the associated airborne instrumentation. The effort was divided into ten general categories which are listed below.

1. Operation
2. Programming Services
3. Minor Modifications
4. Calibration/Alignment
5. Test Planning, Analysis and Reports
6. Installation Design
7. Error Analysis
8. Propagation Analysis
9. Maintenance
10. Data Processing

The operation and maintenance of the PAMS was provided by a resident Actron field representative. His duties also included training on all PAMS instrumentation, software/programming checkout, minor programming, software maintenance, and assistance in the test planning and installation of airborne instrumentation for flight tests.

The flight test programs conducted at the Verona Test Annex, the PAMS project engineer from Actron was on site to provide assistance with the test plan and the analysis and evaluation of data.

The major effort of the program was centered on Tasks 2, 3, 4, 7, and 8 and these activities are reported on in the following paragraphs. A brief description of a data enhancement approach is given for Task 10. Those areas which dealt with on-site support, primarily Tasks 1, 5, 6, and 9 will not be covered in this report.

2.2 PROGRAMMING SERVICES

During the course of the program there were three significant new programs added to the PAMS software library. These were (1) Parallax Correction, (2) X-Y

Analog Plot Program, and (3) Flight Path Simulator Program. In addition, a number of revisions were made to existing programs to enhance data and extend the system range for special test requirements.

2.2.1 Parallax Correction

The Data Acquisition program was revised to incorporate a dynamic parallax correction program. Previous parallax correction was accomplished in the PAMS Calibration Program during data reduction. An algorithm was written that corrected the horizontal and vertical amplitude data when the parallax angle was less than three degrees. The degree of parallax was determined by the slant range of the target to the FPS-16 track radar where the critical range was approximately 7.5 nautical miles. The amplitude was compensated as a function of the antenna pattern beam rolloff. This method provided a moderate improvement in amplitude measurements over most of the frequency range except at the high and low frequency limits of an antenna and several discrete frequencies where the algorithm did not accurately match the beam shape. In order to remove the deficiencies, a new parallax correction program was written and incorporated into the PAMS library.

The new parallax correction routine operates in a dynamic mode and is resident in the Data Acquisition Program. The parallax angle is derived from the azimuth, elevation, and range data from the FPS-16 radar. The data is translated to the PAMS antenna coordinate system and then input to the digital comparator which derives an error signal to steer the PAMS antenna to the desired position in space. The corrected values of the pointing angle are made available to display, list, or output to the magnetic tape. The parallax correction operates continuously during a data run; however, it is suppressed during calibration. The dynamic parallax program is selected by putting the φ sense switch on the computer console in the up position. The program operates in real time to eliminate most errors in the pointing angle. An analysis of the parallax correction routine was made to determine if any errors were introduced during data acquisition. The error introduced by the algorithm itself is negligible compared to the error caused by the uncertainty in the vehicles position relative to the tracking radar. The analysis did indicate that some error does occur at low altitudes when the site is near nadir. The azimuth error is greatest when the vehicle under test is on a NE to SW leg running over the site. The condition is due to a combination of radar range rates and computer speed. In order to minimize the errors it is recommended that the vehicle should stay outside a "forbidden" zone whose approximate locus is illustrated in figure 1.

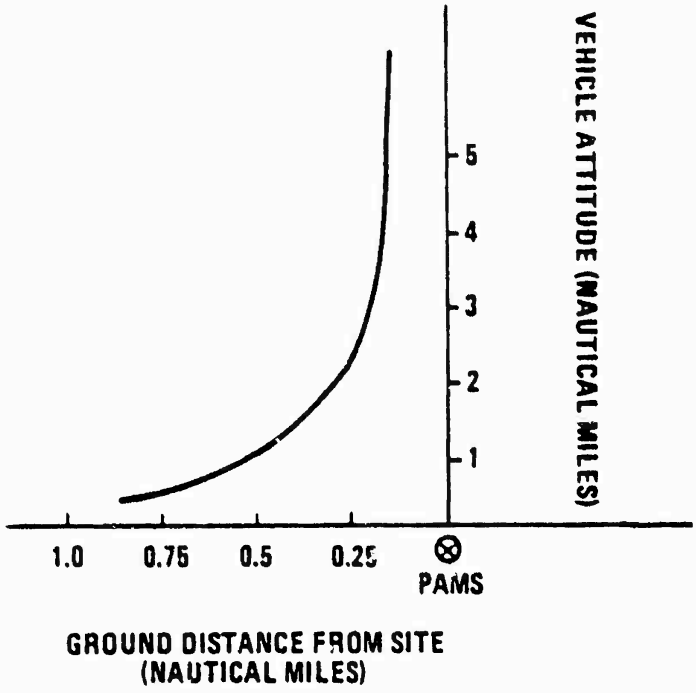

Figure 1. Approximate "Forbidden Zone" Locus

2.2.2 X-Y Analog Plot Program

The X-Y Analog Plot Program (PAMS PLOTR) can be used to plot any of the eleven variables listed below, using data taken from any of three magnetic tapes (Calibration, Merge, and AMS) against a common time base.

TAPE	VARIABLE
CAL or AMS	1. Vehicle heading in degrees
	2. Vehicle pitch in degrees
	3. Vehicle roll in degrees
CAL	4. Vehicle azimuth relative to the PAMS antenna
	5. Vehicle elevation relative to the PAMS antenna
	6. Vehicle range from the PAMS antenna in nautical miles
	7. Frequency in MHz
	8. Horizontal Chaff in $db/m^2/m^3$ Reflectivity in db/m^2 Power Density in dbW MHz Integrated Power in dbW MHz Power in dbW
	9. Vertical Chaff db/m^2 m^3 Reflectivity in db m^2 Power Density in dbW MHz Integrated Power in dbW MHz Power in dbW

MERGE	10. Azimuth of the PAMS antenna relative to the vehicle in degrees or chaff width in feet 11. Elevation of the PAMS antenna relative to the vehicle in degrees or chaff height in feet

The purpose of the program was to display large amounts of data from the three tapes in a way that would make unusual or erroneous data easier to locate. Each plot is for a particular cursor, run, and time span, which is specified by the user. The vehicle attitude angles are taken directly from the AMS tape, if that tape is used, so the AMS calibration (offset angles added to roll and pitch, compass correction, and magnetic deviation correction for heading) won't be included.

A maximum of ten variables may be plotted on the same page, using a common time axis. The first plot will be positioned at the bottom of the page, the second will be displaced toward the top of the page, by the width of the first plot, and so forth for each parameter plotted. The run number, cursor number, plot variable and units, and labeled X-Y axis are plotted for reference. A typical plot is shown in figure 2, where a total of eight variable were plotted.

2.2.3 Flight Path Simulator (FLIPS)

The Flight Path Simulator Program (FLIPS) was written to predict the azimuth and elevation antenna coverage that will result for a proposed flight path when used with the PAMS. The program provides a relatively rapid means of designing the flight path to achieve the desired antenna coverage. The program maximizes the useful data taken, while minimizing the mission flight time. The technique provides a cost effective method of performing flight tests. The program simulates the movement of an antenna-carrying vehicle through a user specified path in three dimensional space. The azimuth and elevation coordinates of the PAMS antenna, relative to the vehicle are computed at regular intervals of simulation time using N point averages to minimize the density of plotted points (N is a multiple of 8). In order to verify the input data to the program the vehicle locus, projected into a horizontal (X, Y) plane, can be plotted as a user option. The theory of flight path simulation is fully explained in the Final Technical Report - PAMS Airborne Instrumentation RADC-TR-74-174 (AD922-537L). Tables 1, 2, 3, and 4 illustrate typical readouts for cloverleaf, parallel fly bys, skidding turn, and coordinated turn, respectively. The actual plots showing elevation coverage as a function of azimuth angle are given in figure 3 through 6.

2.2.4 Miscellaneous Programming

2.2.4.1 Two Variable Polar Plot

The two variable polar plot routine was modified to allow the user to vary the scale of the plot. This enables the user to compare data taken at the PAMS facility with data taken elsewhere, by adjusting the scale factors so that an overlay may be made. Two sizes which are commonly used are the NAV-4 and standard which are shown in figures 7 and 8, respectively.

TABLE 1. CLOVERLEAF PLOT

```
PAMS CLOVERLEAF PLOT
 INPUT FROM PAPER TAPE (Y,N)?

 RUN   1
 MIN,MAX AZ=   117.57   146.27       MIN,MAX EL=     6.63    10.24
 RUN   2
 MIN,MAX AZ=   255.11   271.72       MIN,MAX EL=     7.37     8.56
 RUN   3
 MIN,MAX AZ=    58.33    94.79       MIN,MAX EL=     7.37     8.56
 RUN   4
 MIN,MAX AZ=   214.27   242.43       MIN,MAX EL=     6.68    10.24
 RUN   5
 MIN,MAX AZ=    11.23    22.51       MIN,MAX EL=     6.39    11.97
 RUN   6
 MIN,MAX AZ=   157.51   160.32       MIN,MAX EL=     6.37    11.92
 RUN   7
 MIN,MAX AZ=   297.35   325.91       MIN,MAX EL=     6.63    10.26
 RUN   8
 MIN,MAX AZ=    35.32   121.36       MIN,MAX EL=     7.36     8.56
 RUN   9
 MIN,MAX AZ=   238.14   274.62       MIN,MAX EL=     7.36     8.56.
 RUN  10
 MIN,MAX AZ=    34.39    62.63       MIN,MAX EL=     6.69    10,26
 RUN  11
 MIN,MAX AZ=   191.23   202.39       MIN,MAX EL=     6.37    11.92
 RUN  12
 MIN,MAX AZ=   337.49   347.77       MIN,MAX EL=     6.39    11.97
 MISSION TIME =  2/12/ 3.1
   21754. DATA POINTS     276. AVERAGED POINTS
STOP
```

TABLE 2. PARALLEL FLY BY PLOT

```
PAMS FLIPS PLOT (PARALLEL FLY BY)
 INPUT FROM PAPER TAPE (Y,N)?

 RUN   1
 MIN,MAX AZ=   172.31   237.79       MIN,MAX EL=     3.72    44.46
 RUN   2
 MIN,MAX AZ=    17.39   192.17       MIN,MAX EL=     3.53     7.25
 RUN   3
 MIN,MAX AZ=   179.15   337.73       MIN,MAX EL=     3.72    14.39
 RUN   4
 MIN,MAX AZ=    35.74   154.13       MIN,MAX EL=     3.54     4.96
 RUN   5
 MIN,MAX AZ=   325.23   314.74       MIN,MAX EL=     3.21     3.71
 RUN   6
 MIN,MAX AZ=    32.75   147.17       MIN,MAX EL=     3.43     3.74
 MISSION TIME =  1/27 23.7
   24377. DATA POINTS     274. AVERAGED POINTS
STOP
```

FOR INFORMATION PURPOSES ONLY

TABLE 3. SPIRAL CLIMB, SKIDDING TURN PLOT

```
PAMS SPIRAL CLIMB, SKIDDING
 INPUT FROM PAPER TAPE (Y,N)?

 RUN   1
 MIN,MAX AZ=      .72   356.47       MIN,MAX EL=     1.92     3.85
 RUN   2
 MIN,MAX AZ=      .72   356.47       MIN,MAX EL=     3.61     7.58
 RUN   3
 MIN,MAX AZ=      .72   356.47       MIN,MAX EL=     5.31    11.25
 RUN   4
 MIN,MAX AZ=      .72   356.47       MIN,MAX EL=     7.21    14.83
 RUN   5
 MIN,MAX AZ=      .72   356.47       MIN,MAX EL=     8.63    18.29
 RUN   6
 MIN,MAX AZ=      .72   356.47       MIN,MAX EL=    10.36    21.63
 RUN   7
 MIN,MAX AZ=      .72   356.47       MIN,MAX EL=    12.22    24.81
 RUN   8
 MIN,MAX AZ=      .72   356.47       MIN,MAX EL=    13.65    27.84
 RUN   9
 MIN,MAX AZ=      .72   356.47       MIN,MAX EL=    15.26    30.71
 RUN  10
 MIN,MAX AZ=      .72   356.47       MIN,MAX EL=    16.85    33.43
 MISSION TIME =  7/30/10.5
   5711. DATA POINTS     757. AVERAGED POINTS
STOP
```

TABLE 4. SPIRAL COORDINATED TURN PLOT

```
PAMS SPIRAL COORDINATED TURN
 INPUT FROM PAPER TAPE (Y,N)?

 RUN   1
 MIN,MAX AZ=     1.69   357.72       MIN,MAX EL=      .32   358.88
 RUN   2
 MIN,MAX AZ=     2.67   358.24       MIN,MAX EL=      .32   359.47
 RUN   3
 MIN,MAX AZ=     3.67   359.37       MIN,MAX EL=      .31   359.82
 RUN   4
 MIN,MAX AZ=      .79   357.30       MIN,MAX EL=      .32   359.31
 RUN   5
 MIN,MAX AZ=     1.92   357.86       MIN,MAX EL=      .32   359.52
 RUN   6
 MIN,MAX AZ=     2.94   359.12       MIN,MAX EL=      .31   359.35
 RUN   7
 MIN,MAX AZ=      .19   356.25       MIN,MAX EL=      .35   359.22
 RUN   8
 MIN,MAX AZ=     1.25   357.36       MIN,MAX EL=      .34   359.77
 RUN   9
 MIN,MAX AZ=     2.31   358.47       MIN,MAX EL=      .32   359.25
 RUN  10
 MIN,MAX AZ=     3.32   359.59       MIN,MAX EL=      .33   359.92
 MISSION TIME =  7/30/10.5
   5711. DATA POINTS     757. AVERAGED POINTS
STOP
```

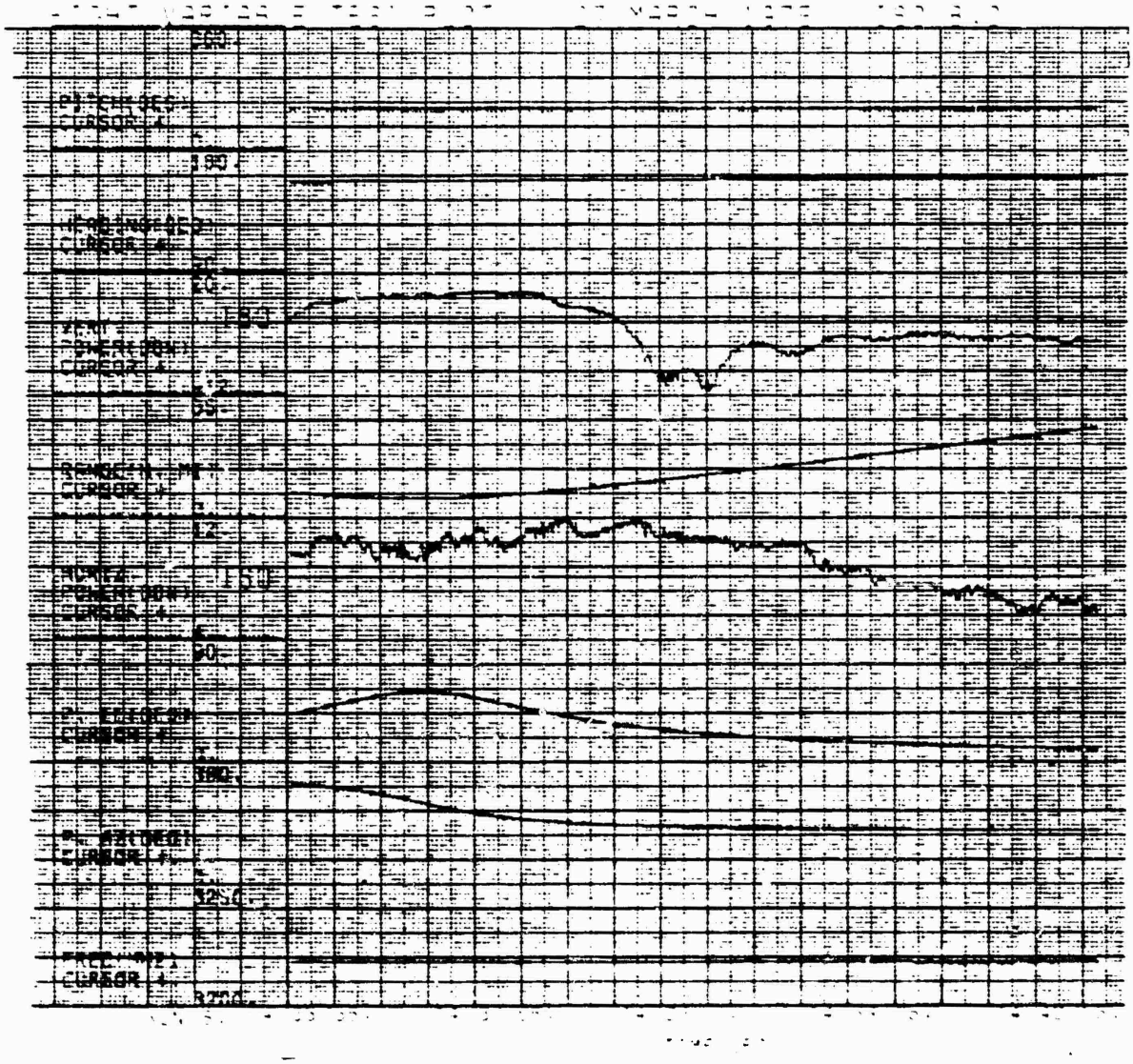

Figure 2. Flight Variable-Test Plot

2.2.4.2 Angular Resolution and Range Extension

A decision was made to use angular data from the shaft encoders of the FPS-16 radar instead of the angular synchro outputs to increase the resolution. The synchro outputs would be maintained as a backup system. In addition, new test requirements made it necessary to extend the range capability of the PAMS data acquisition program.

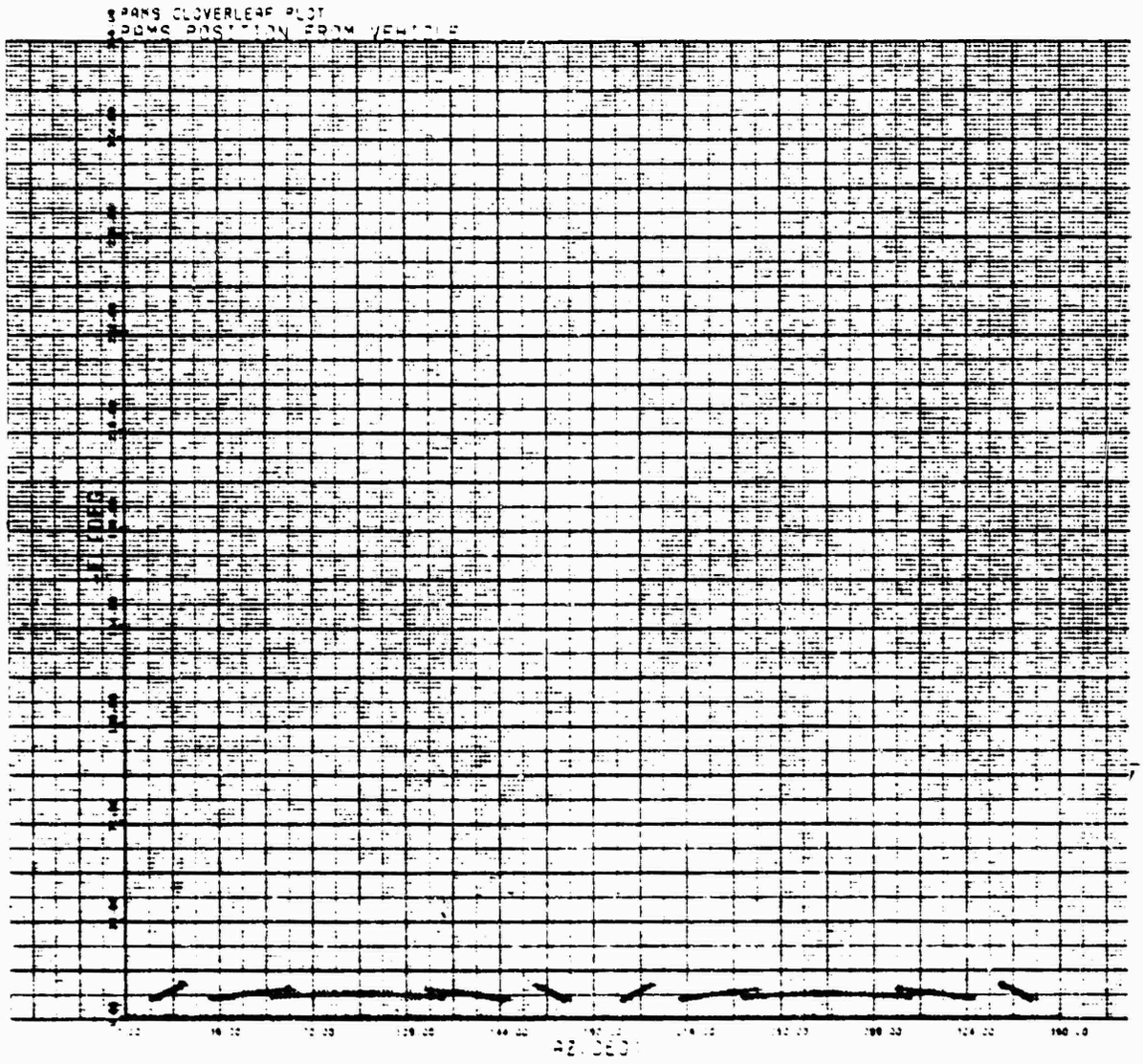

Figure 3. Cloverleaf Plot

The original angular inputs to the PAMS from the FPS-16 were through synchros and synchro-to-digital converters which had a BCD output. This format had a resolution of ±0.02 degree with the least significant bit (LSB) being 0.04 degree. Using the first 15 most significant bits from the serial digital output of the shaft encoders resulted in a binary format with the LSB being 0.011 degree with a new resolution of ±0.006 degree.

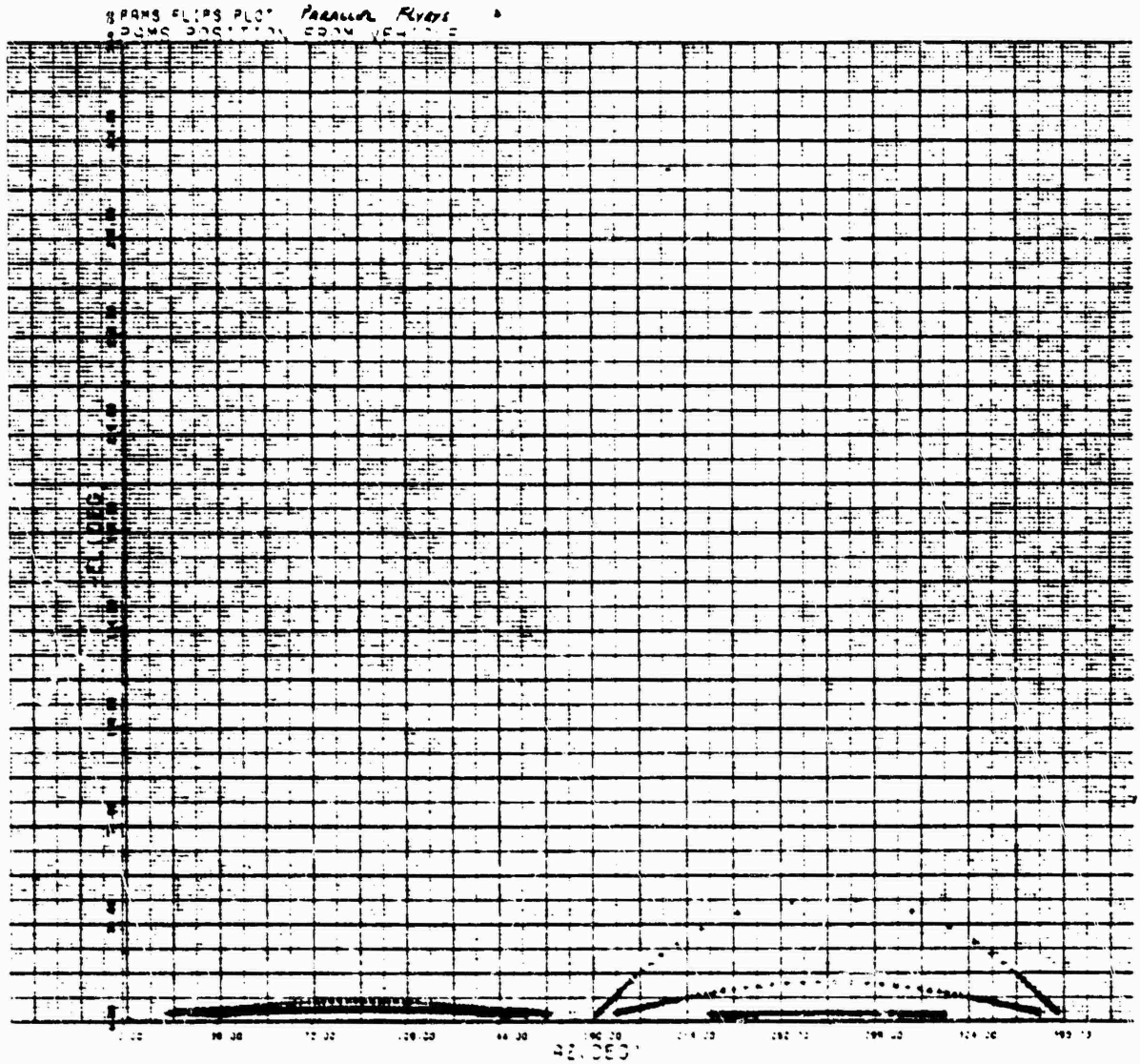

Figure 4. Parallel Flyby Plot

The original range input was in a binary format with a maximum range of 126.4 nautical miles. The LSB was 7.8125 yards, giving rise to a resolution of 7.8125 yards. In order to increase the range it was necessary to utilize more of the significant bits and drop some of the lesser significant bits. This approach was used to avoid the need for double precision calculations in the range. This resulted in an increase in the data acquisition range to 505.6 nautical miles with the LSB and resolution being 15.625 yards. Double precision would have improved the resolution but would have increased the computational time of the parallax correction routine to the point where updating of the pointing angle could not be accomplished.

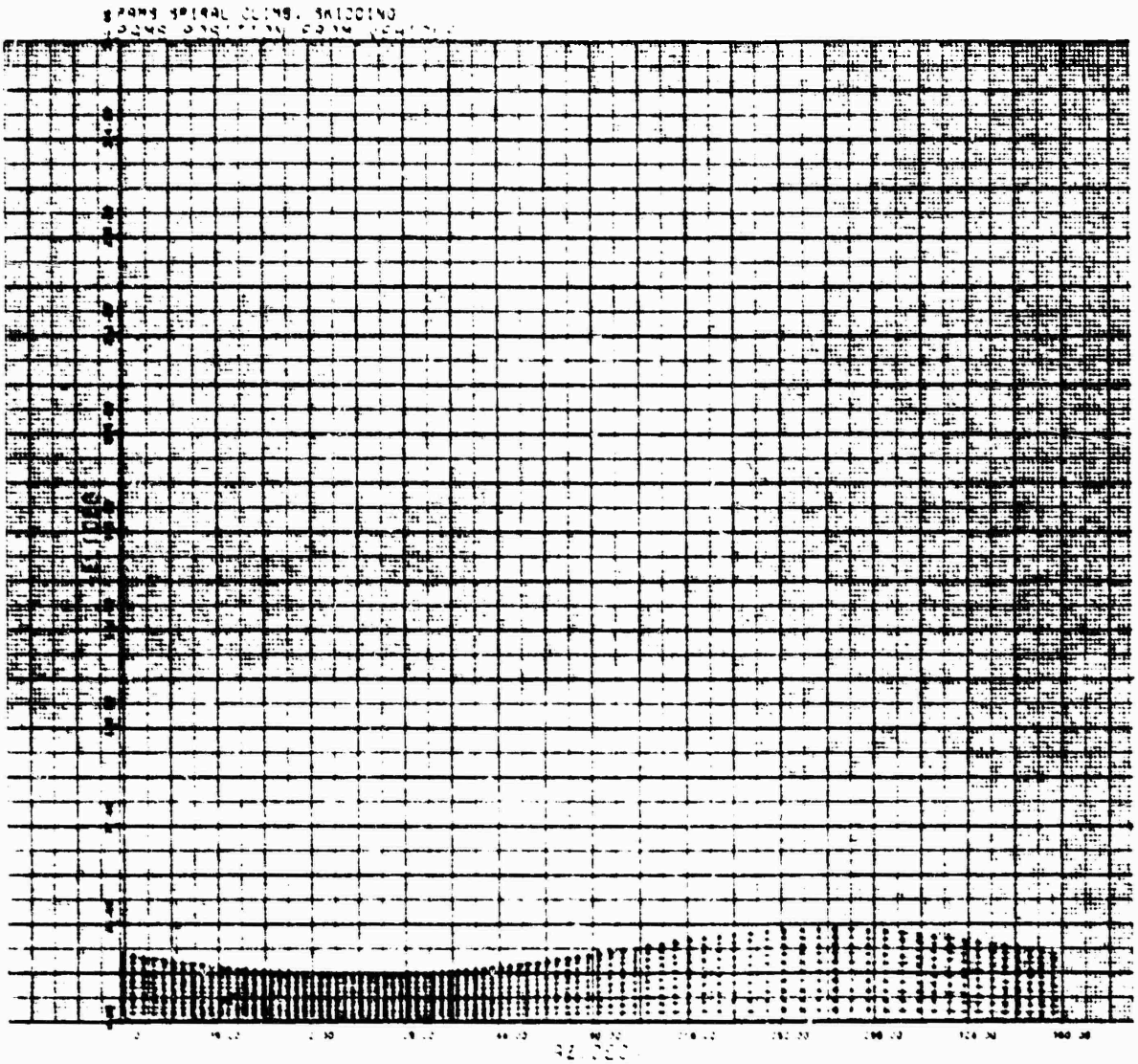

Figure 5. Spiral Climbs, Skidding Plot

The actual modifications made in the PAMS in order to use the angular shaft encoders and extend the range capabilities are described in paragraph 2.3 of this report.

2.3 MINOR MODIFICATIONS

During the PAMS Engineering Services program, several modification tasks were initiated to extend the capability of both the ground system and the airborne instrumentation. The first of these modifications was the changeover of the azimuth

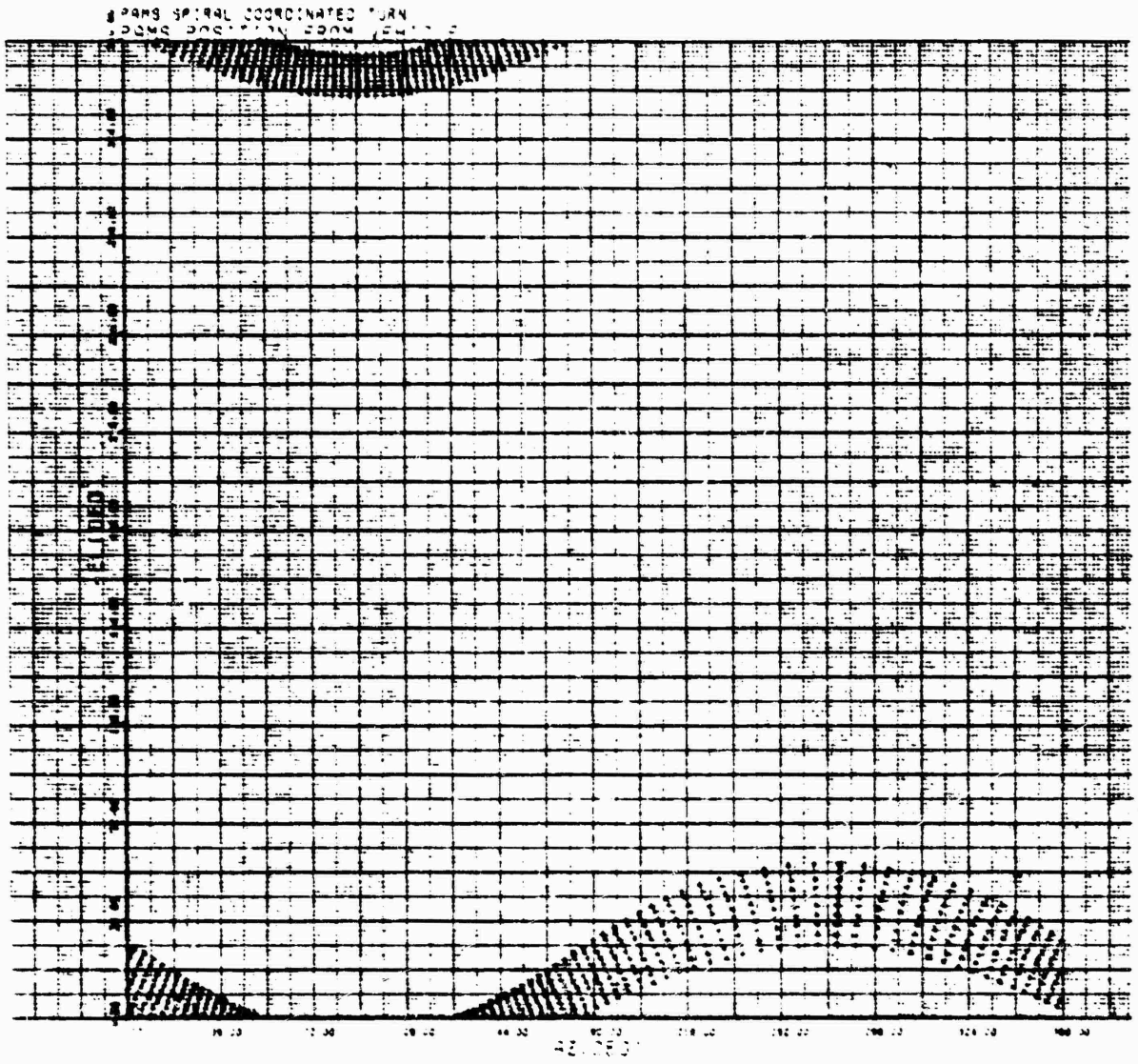

Figure 6. Spiral Coordinated Turn Plot

and elevation angular inputs from synchros to shaft encoders and the extension of the range. The second major task involved the modification of the airborne signal sources to incorporate frequency lockout, remote switching for antenna selection, output YIG oscillator tuning voltages, and incorporate the capability of remote control. These modifications are described in the following paragraphs.

2.3.1 Angular Resolution and Range Extension

The original design of the PAMS used the angular output of FPS-16 synchros for azimuth and elevation information. This data was input to synchro-to-digital converters which output the data in a digital BCD format for slaving the PAMS antennas to the FPS-16 radar. In order to obtain better angular resolution, it was

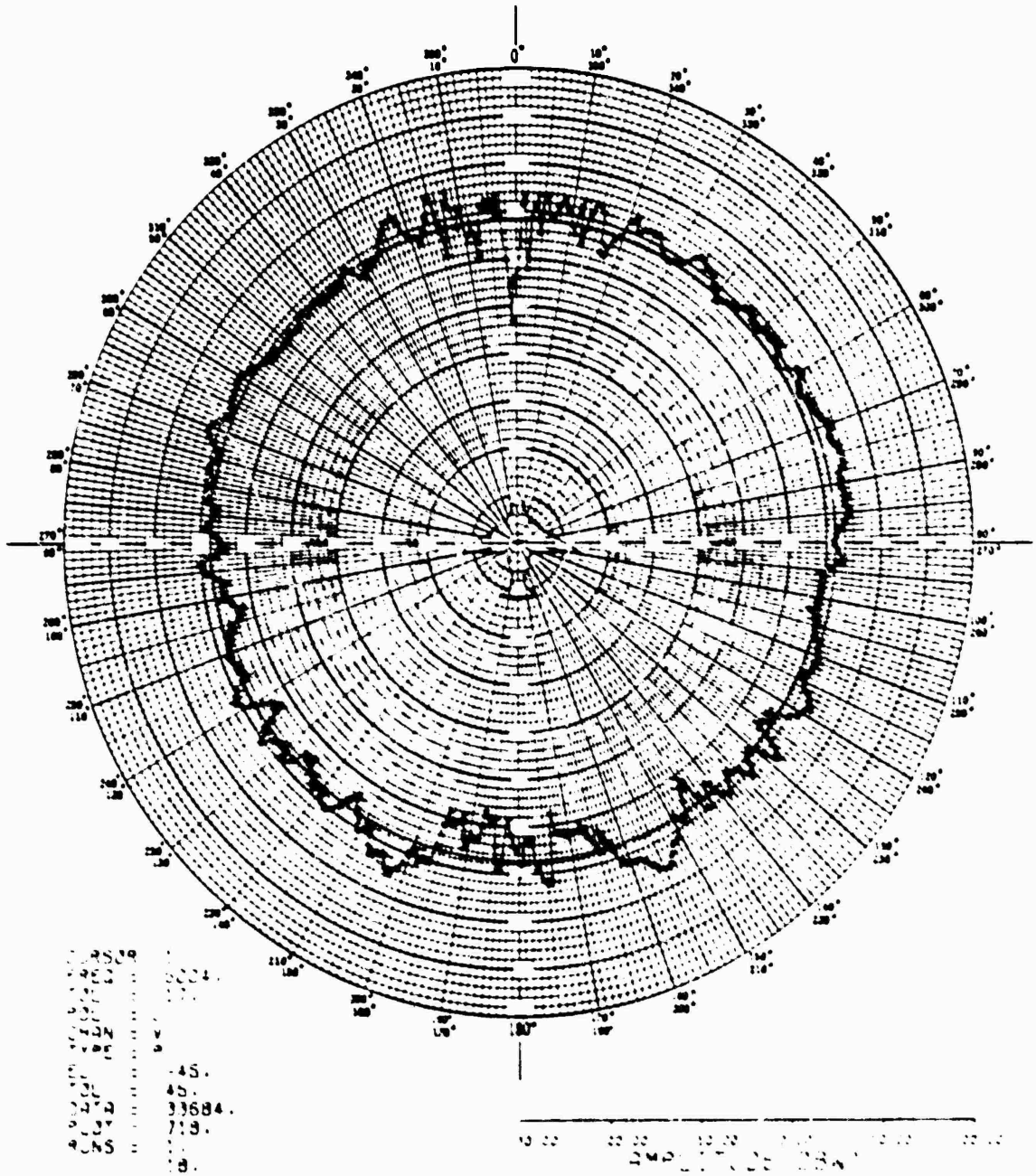

Figure 7. Two Variable Polar Plot - NAV-4

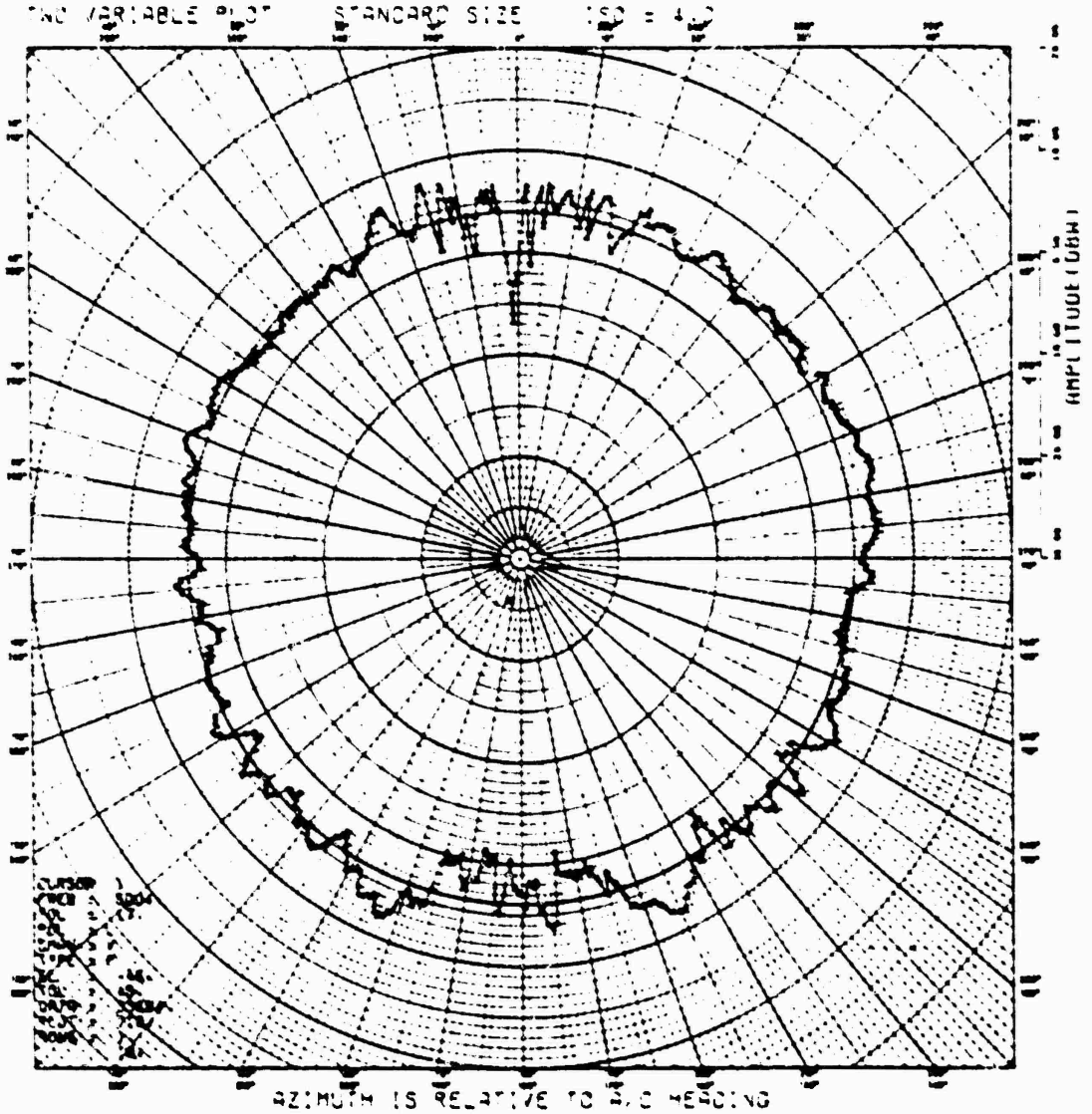

Figure 8. Two Variable Polar Plot - Standard

necessary to use the serial digital output of the FPS-16 shaft encoders. Since digital data was directly available in a binary format it was possible to clock the bits into a shift register and take the data out in parallel for processing. The data is clocked in using the same clock pulse from the FPS-16 as is used to clock in the range. The two least significant bits were dropped and only bits 2^2 through 2^{15} used. This gave 2^{15} = 360 degrees or a resolution of ±0.006 degree. The modification was implemented using standard XDS FJ14 8 bit shift registers in a serial in-parallel out configuration. The cards were installed in spare slots in the signal processor section of the console. A new cable was fabricated for inputting the

data into the 40 bit data card in the data acquisition computer. Using this approach, it was possible to use the synchro inputs as a backup system simply by switching cables. Both the azimuth and elevation shaft encoder inputs were implemented using the same circuitry. The modification is illustrated in figure 9.

The range modification was essentially one requiring different outputs from the range registers. In order to increase the range it was necessary to use some of the higher order bits of the range input from the FPS-16. In order to eliminate the necessity of using double precision in the range computations it was also necessary to drop some of the lesser significant bits. To achieve this, it was only necessary to rewire the output of the range circuit for the right bit output. This enabled the range to be increased from 126.4 nautical miles to 505.6 nautical miles. Although there was a four-to-one increase in range there was only a two-to-one increase in range resolution i.e., 7.8125 yards to 15.625 yards.

These modifications required that the software be altered to accept the new parameters in both the data acquisition and parallax correction routines as described in paragraphs 2.2.1 and 2.2.4.2.

2.3.2 Airborne Signal Source Modifications

The desirability of incorporating additional capabilities in the airborne signal sources came about from the results of numerous flight tests and predicated requirements for future tests. The four modifications which were implemented are listed below.

1. Lockout of undesired frequencies.
2. Stepping logic for multiple antenna selection.
3. Remote output of RF tuning voltage.
4. Remote control.

These modifications are detailed in the following paragraphs.

2.3.2.1 Frequency Lockout

The original design of the signal sources had provisions for automatic stepping of the frequency in any one of nine different ranges. In each range there were eight discrete frequencies each with a dwell time of 0.5 second, giving rise to a four-second period. Experience gained from flight tests indicated that the maximum number of eight frequencies were never used. Typically, four frequencies were sufficient to describe an antennas characteristics as a function of frequency. In addition, it was desirable to have the ability to suppress RF radiations in unauthorized frequency bands.

In the original configuration, data was taken at a desired frequency every four seconds. This inherently was a dominating factor in the flight time required to secure sufficient data. In addition, it also put some restrictions on the vehicle's

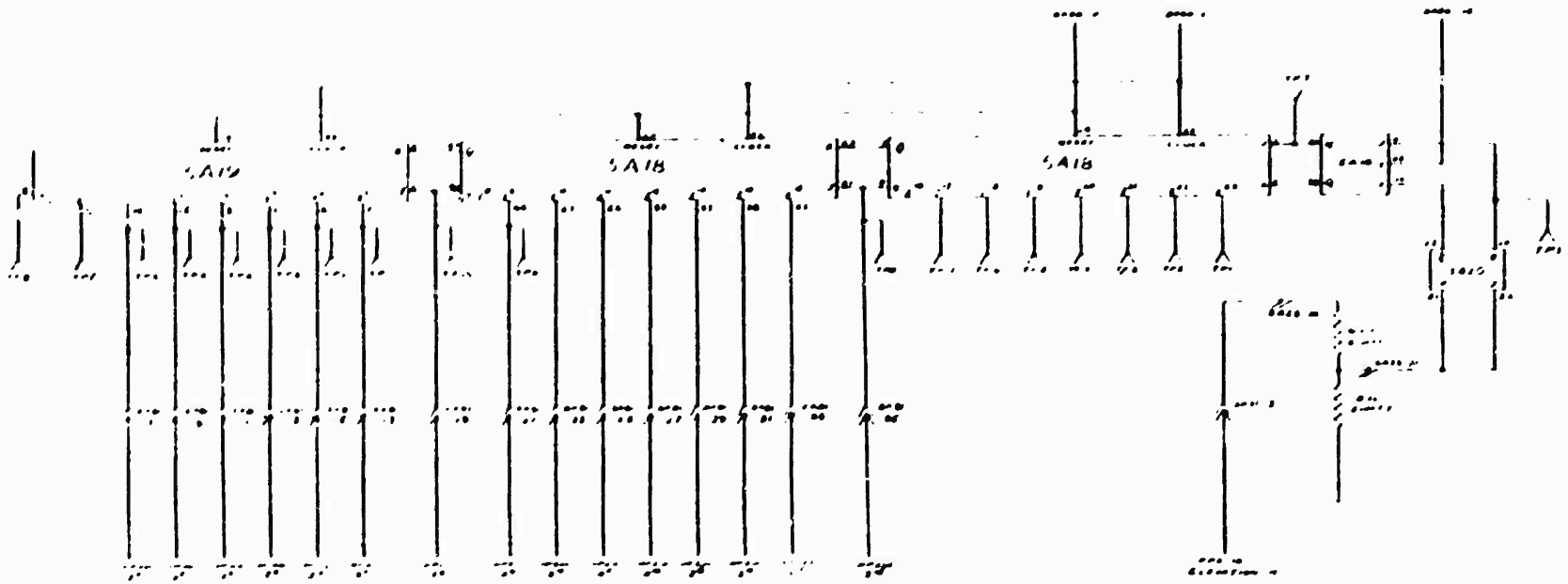

Figure 9. Processor Logic, Elevation Encoder Schematic, FPS-16 Interface

speed and maneuvering ability. Too fast and the data points would become widely separated and additional runs would be required to fill in the holes. With the ability to disable unwanted frequencies, the period would be decreased accordingly. For example, using four instead of eight frequencies the period would be reduced from four to two seconds. Consequently, the flight time could be reduced by a factor of two or twice as much data could be collected in the same time. The implementation of the modification is shown in figures 10 and 11. A new circuit card was fabricated to incorporate the additional electronics and added to the existing circuitry in the signal sources. The card is shown in figure 12. Frequency lockout is obtained by placing a ground on the multiplexed circuits U1 and U2 of figure 10. This produces a lockout signal from U2 to U1 of figure 11 which advances the count and skips the undesired frequency. The clock then continues to run normally until another lockout pulse is received and again advances the count. When the count is advanced, the clock input in the A/D Converter (U5 of figure 11) is also advanced and the YIG tuning voltage is set to the level of the next frequency which was selected to radiate. Although it is possible to lock out all eight frequencies, it is recommended that only six be used. If only one frequency is desired, the Manual Mode should be selected.

2.3.2.2 Stepping Logic for Multiple Antenna Selection

The capability for providing remote stepping logic to energize multiple port coaxial switches for activating multiple test antennas was incorporated on the new circuit card. This enables multiple antennas to be tested during a flight using a common signal source, considerably reducing flight time and instrumentation.

The remote switching logic consists of U3, U4, and U5 along with Q1 through Q8 in figure 10 and shares some of the same multiplex circuitry as the frequency lockout. In normal operation the multiplexed output of U1 is decoded to drive Q1 through Q8 in the same sequence as the frequency steps F1 through F8. If one or more of the frequencies are locked out the switch driver corresponding to those frequencies is disabled. This permits data to be sorted on a frequency basis which can readily be identified with a specific antenna. Switch driver outputs can be OR'd for multiple frequency operation of several antennas depending upon test requirements.

2.3.2.3 Remote YIG Tuning Voltage Output

The YIG tuning voltage was brought to the outside so that the voltage could be monitored and/or recorded for test purposes. This was easily accomplished by tapping the tuning input line and buffering the output with a voltage follower, U7 of figure 11.

2.3.2.4 Remote Control

The remote control modification provides for all of the signal source front controls to be located in the cockpit of the test aircraft. In addition, all of the operating functions of the TWT amplifier used with the signal sources were incorporated into the remote control capability. The front panel functions of signal sources which were remoted were power ON/OFF, select fixed or step frequency, manual tuning for fixed frequency selection, and single frequency incrementing for step frequency selection. The TWT amplifier functions are identified with status lamps.

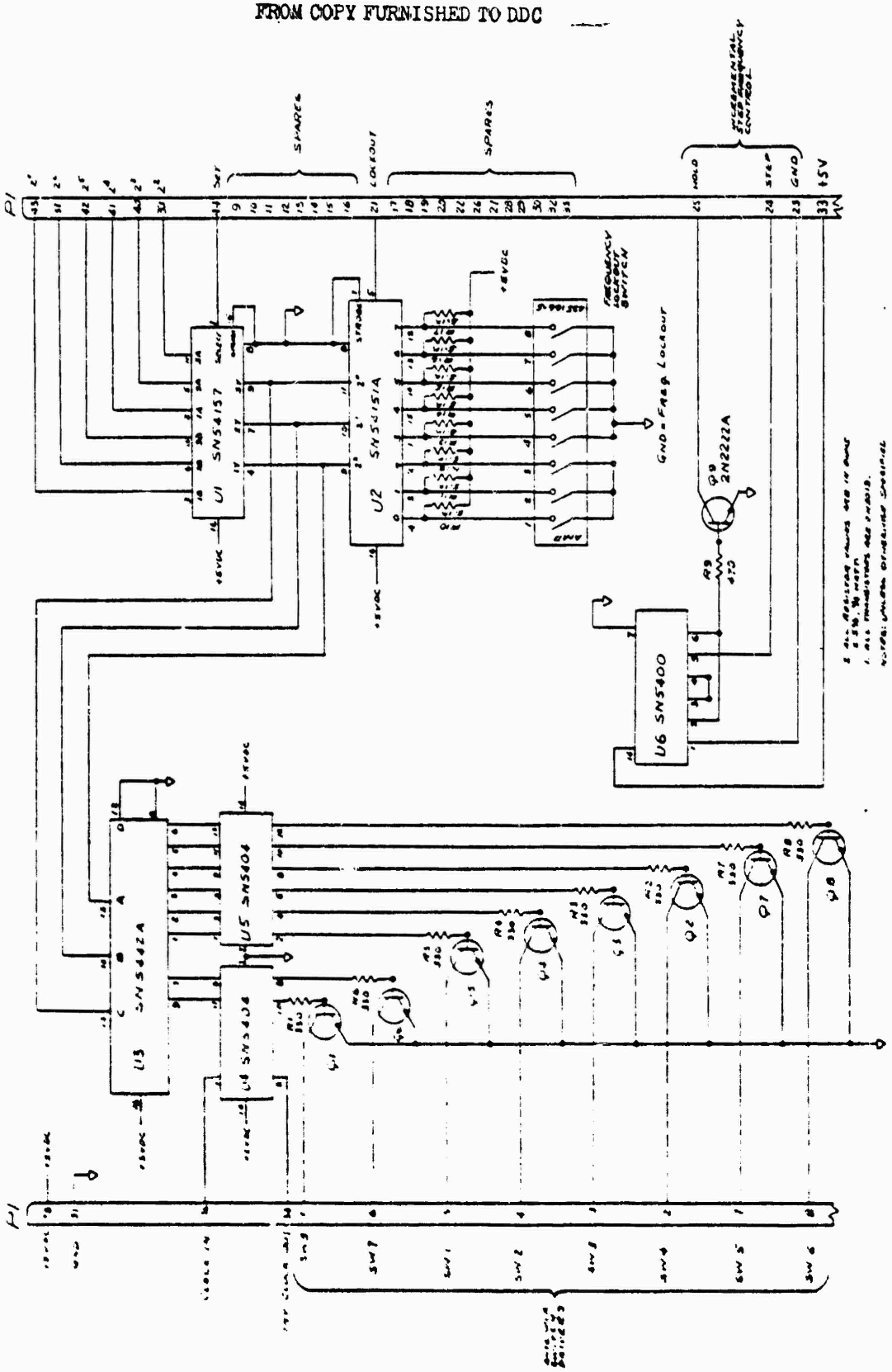

Figure 10. AS^2 Logic, Schematic Diagram

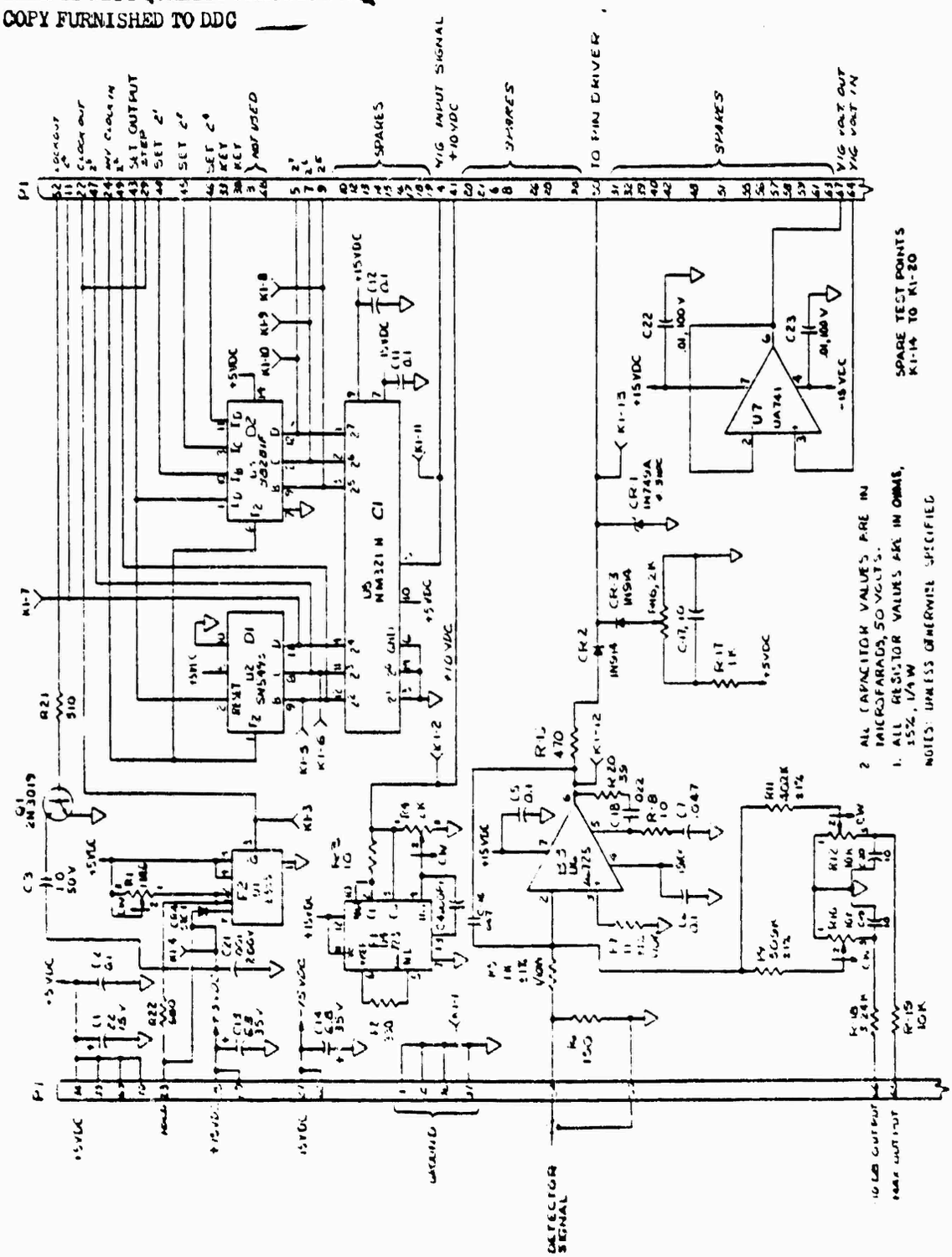

Figure 11. AS^2 Control, Schematic Diagram

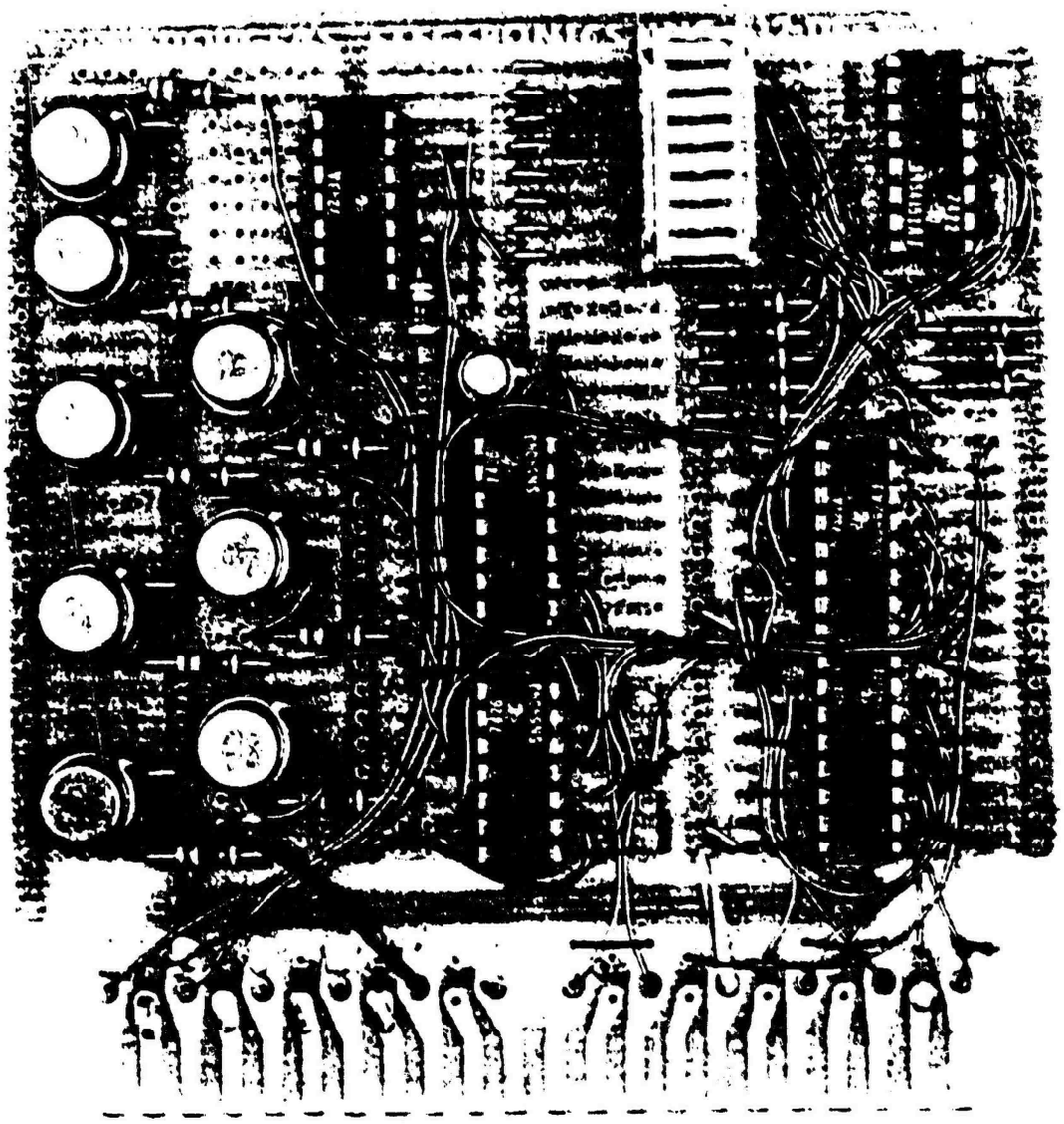

Figure 12. New Frequency Lockout and Antenna Select Logic Card

Filament ON, Timer ON, and High Voltage ON, and an RF ON/OFF switch. A proposed layout for the remote control panel is illustrated in figure 13. The remote control capability was achieved by using parallel inputs to the control input connectors. To use the remote control, all lines go from the remote control box directly to the AS^2 control cards in the signal source. For manual or local operation the front panel controls are jumpered in the input connector. All the modifications were incorporated in the signal sources; however, the remote control box itself was not fabricated although all the hardware and design were supplied. This was done because of the numerous cockpit configurations which would have had to been provided.

The signal sources with all the modifications incorporated have been successfully flown in a series of flight tests.

2.4 CALIBRATION AND ALIGNMENT

During the program an engineering report was requested concerning the requirements for implementing a collimation tower with remote instrumentation for the calibration and alignment of the PAMS. This report was previously submitted and is included in this final report as Appendix I.

2.5 SYSTEM ERROR ANALYSIS

One of the tasks initiated during the Engineering Services was an Error Analysis of the PAMS. This was done and submitted as an Engineering Report. It is resubmitted here as Appendix II.

2.6 PROPAGATION ANALYSIS

Concurrent with the system error analysis was a propagation analysis. This was performed by Atlantic Research under a subcontract to the PAMS Engineering Services and was previously submitted as an Engineering Report. It is resubmitted here as Appendix III.

2.7 RADAR CROSS SECTION

A report on the radar cross section measurement capability and recommendations for improving RCS measurement was requested during the program. This report was not previously submitted and is incorporated in this report as Appendix IV.

2.8 DATA ENHANCEMENT

At this time, the PAMS data processing subsystem processes data in the following order:

1. Data Acquisition - Raw data is acquired and stored on magnetic tape in real time, along with calibration data taken before each run.

2. Calibration Program - Flight calibration data and flight data are retrieved from magnetic tape. The raw data is checked, converted to meaningful units using the calibration data, and stored on magnetic tape.

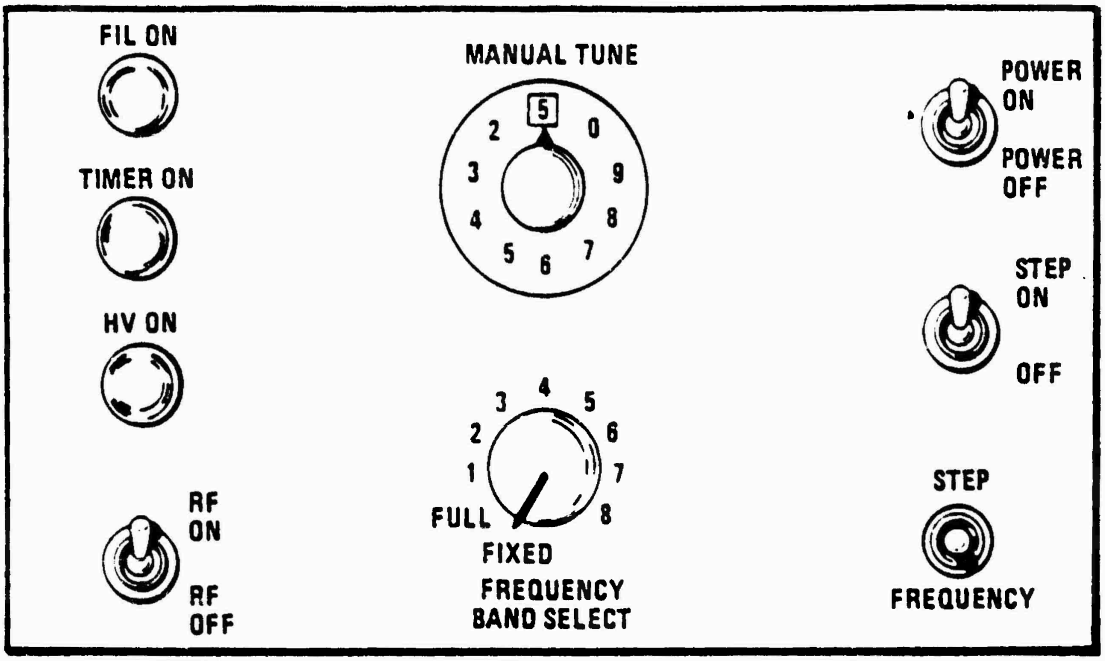

Figure 13. Remote Control Panel

3. Tape Merge - The calibrated data and airborne monitoring system (AMS) data are retrieved from magnetic tapes. A coordinate transformation is used to shift the reference axes from the PAMS antenna to the vehicle and a new output tape is created.

4. Plot Program - Data is retrieved from the Tape Merge magnetic tape, and plotted on a pen plotter.

In order to expedite data throughout and reduce the cost of running a test, evaluate the quality of results obtained and produce antenna plots of various types, the data processing equipment should be augmented with additional units which would eliminate many of the limitations and production bottlenecks inherent in the present configuration.

Operationally, the augmented system should accomplish operations 1, 2, the coordinate transformation of 3, and a quick look of 4 during the flight. The data could be displayed on a CRT in near real time during the flight. At the end of the flight, the displayed data would be copied from the CRT onto a high speed plotter and made immediately available.

When so implemented, the costs of conducting a flight test program will be significantly reduced because data quality can be assessed while the test is being conducted, thereby eliminating costly standby, recall, and retest time. Additionally, more test programs can be conducted on the range in a given time interval because

the data processing time is reduced, thereby reducing the fixed costs allocated to each test; and finally, the more timely return of processed and plotted data will reduce the evaluation costs of the range customer.

As operating experience has been accrued, and the need for system augmentation becomes more clearly focused, we have taken a look at various solutions to the operational problems. We believe that the addition of a Hewlett-Packard Automatic Spectrum Analyzer will provide the necessary augmentation, and at the same time, add a powerful new capability for spectrum surveillance and electromagnetic signature analysis.

This system adds capabilities for foreground and background processing which will reduce the processing time by an order of magnitude or greater. In addition, the system permits on-line editing and removes the base page restriction from the present computer complex. The spectrum analyzer will allow complete test and evaluation of the PAMS receiver system and can be used to perform RFI/EMI profiles about the Verona site. And finally, integration of the PAMS system with the spectrum analyzer will permit complete signature analysis of complex waveforms.

The proposed augmentation of the PAMS data processing equipment featuring the Hewlett-Packard 8580 Automatic Spectrum Analyzer is illustrated in figure 14. This addition will solve the present limitations arising out of the program size restrictions and relatively slow data reduction time.

The augmented system configuration will provide following benefits:

- Presentation of new real-time data in a graphics mode to allow the immediate evaluation of data and the reduction of flight time.
- Hard copy graphics immediately after flight.
- Simultaneous execution of multiple required programs.
- Simultaneous program development and modification while executing data reduction.
- Rapid random access to program files.
- More sophisticated and larger programs using overlays.
- Removes present base page programming restriction. During program development more time can be spent on solving problems and less on making program "fit" core size.
- Reduction of compilation and assembly time by two orders of magnitude. In addition, less errors arising out of paper tape punching operations.
- More rapid and accurate system calibration and performance assessment.

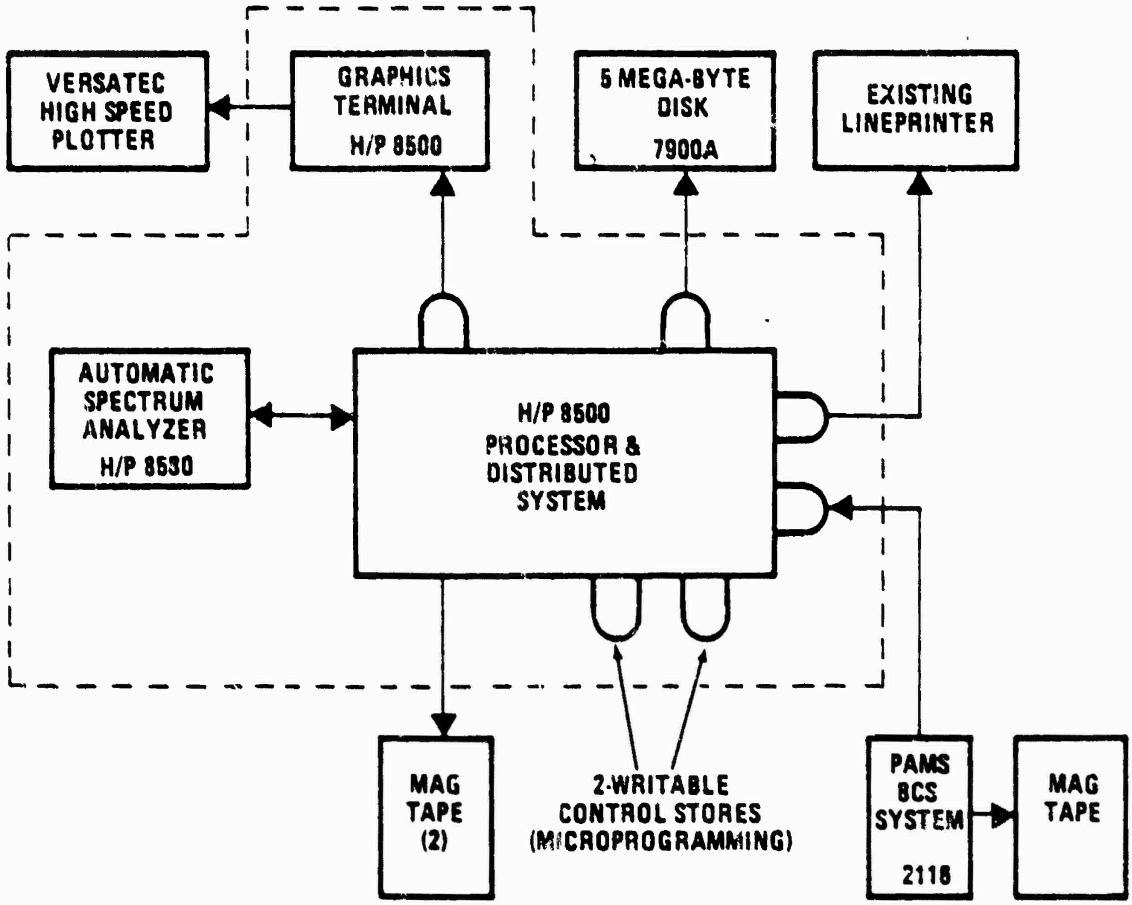

Figure 14. Proposed Configuration for Data Enhancement of PAMS System

Additionally, the Spectrum Analyzer will add significantly to the information capacity of the PAMS complex for example, statistical data can be organized and presented in both printed and graphic formats. Instructional data can be presented in a graphic form. Programming can be written in easy to use ATS BASIC as well as FORTRAN.

Other benefits of the new equipment arise from the distributed computing writable central store, disc memory, and real-time executive features available with the added equipment.

For example:

Distributed computing will add to the PAMS system the capability of simultaneous program development at the central processor while other programs are being executed on the remote PAMS terminal. With this communication package, the remote terminal will have the ability to load and store programs, and also use peripherals while new programs are being developed. Utility programs, such as full and partial file director listings, will be supplied.

Base page storage limitations will be greatly alleviated by this system. The augmented system will use the Automatic Spectrum Analyzer processor as the central processing system with the aid of the Real Time Executive Program. This in turn will communicate with the present PAMS HP 2116 processor, treating the PAMS computer as a remote terminal. Programs will be assembled on the central processor using a cross assembler, which will access a HP 2116 configuration file. Then, with the system cross loader, it will link and load the present PAMS software. This method will reduce the required storage for address links.

One of the main advantages of distributed computing is the ability of multiple processors to take advantage of the same set of high performance peripherals. Centralized data is also available to each processor. Each system can be taken down individually for maintenance while processing continues on the other system. Any future expansion can be more readily implemented.

The Real-Time Executive (RTE) is a multi-programming software system that allows several programs to operate concurrently.

Programs to be executed on the PAMS HP 2116 will be compiled and assembled using this system. Previous base page restrictions are removed, since linking is accomplished during the relocation where the linkages are placed on the corrected pages. In addition, the ability to overlay program segments is available and allows the development of more extensive programs even though the maximum core limit is the same.

Programs are executed on an automatic scheduled basis by priority. These programs may be scheduled for execution by:

1. Operator request,
2. program request,
3. a device interrupt, or
4. the completion of a predetermined time interval.

The RTE provides four user-defined program areas for the execution of programs:

1. Real-time core resident,
2. real-time disk resident,
3. background core resident, and
4. background disk resident.

The above areas are listed in the order of priorities. Suspension of program execution and swapping out of core is available in the real-time disk resident area if the area is required by a higher priority program.

A Writable Control Store (WCS) configuration will be used to enhance the speed of the PAMS programs. This WCS allows frequently used algorithms to be micro-programmed, increasing their speed by factors of from five to twenty times. This is accomplished in micro-coding. Other benefits gained with the WCS are:

- An increase in the available core space.

- Access to six internal registers not previously available.

Presently written PAMS programs will execute on the Automatic Spectrum Analyzer processor since the same instruction set is used. These programs, however, may be converted to micro-coded algorithms in order to increase the processing speed for near real-time data manipulation.

Microprograms will be added and stored on disk, to be loaded into the WCS at run time. These programs can then be modified dynamically during the run if required.

The WCS consists of 256, 24 bit words. Each 24 bit word allows for six micro instructions as shown below. Each micro instruction executes in 196 nanoseconds.

23 22 21 20	19 18 17 16	15 14 13 12	11 10 9 8	7 6 5 4	3 2 1 0
R Bus	S Bus	Function	Store	Special or Jump Target or Constant	Skip

The memory and I/O sections of the computer operate on a cycle of 980 nanoseconds, i.e., five times the length of the micro instruction rate.

A disc file also speeds up processing time as, for example, program compilation and assembly with disk procedures rather than paper tape procedures reduces time by several orders of magnitude due to the higher data transfer rate. Data transfer to the disk is at a rate of 312,000 bytes per second, rather than the 500 bytes per second limit of the paper tape punch. Using a disk adds a new dimension to system data storage. This device, in addition to having a faster data transfer rate, allows random direct access rather than the sequential access of magnetic or paper tape.

The present system requires multiple passes during the compilation and assembly of programs. This requires paper tape punching and reading which in turn increases the possibility of error. With the addition of the disk, paper tape will no longer be required for the tasks. In addition, an on-line edit package will be available for rapid program editing.

The disk memory is composed of two disks, one fixed and the other a removable disk cartridge. Each disk contains 2.5 million bytes or 1.25 million 16-bit words. With this disk controller, three additional disks drives may be added to give a total storage of 20 million bytes.

A high speed printer/plotter is required to obtain hard copy output at a speed compatible with the output data produced by the system. The proposed plotter produces output using electrostatic methods. Plotting is pre-formatted into output lines using dot matrices. Each plot pattern is completely formatted onto disk at computer speeds and then outputted at approximately two linear inches of paper per second. One 8-1/2 x 11 inch plot will be printed in approximately six seconds. Line printer output will be produced at approximately twice the speed of the present line printer. Since this line printer is a non-impact printer, the acoustic printing noise will be considerably reduced.

APPENDIX I

CALIBRATION AND ALIGNMENT SYSTEM FOR THE PRECISION ANTENNA MEASUREMENT SYSTEM

1.0 INTRODUCTION

This engineering report presents the results of an analysis on the calibration and alignment of the Precision Antenna Measurement System (PAMS). A new approach to the system calibration was formulated for automatic operation under computer control. The report also addresses the use of a collimation tower for both electrical and optical alignment of the PAMS and describes how the calibration system can be incorporated into the collimation tower concept. Conclusions are made based on the analysis and recommendations made for the implementation of the collimation tower and automatic calibration system.

2.0 BACKGROUND

The PAMS was developed for the purpose of evaluation and calibration of airborne RF radiating systems under dynamic flight conditions. The PAMS is slaved to an FPS-16 track radar and monitors and records the RF power and frequency of the system under test as a function of the aircrafts position. The PAMS operates over the frequency range of 0.1 GHz through 18 GHz and is capable of receiving AM, FM, CW, and pulse signals with any polarization. The system can monitor and record data on up to twelve frequencies simultaneously throughout the operating frequency range. The reduced data is plotted as a radiation pattern of the RF system relative to the heading of the aircraft in Effective Radiated Power (ERP). The data can be plotted in a two dimensional format, either rectangular or polar coordinates, or in a three dimensional format.

The following section discusses the PAMS calibration and presents a new method which improves system accuracy and enables completed calibration in a matter of minutes rather than days.

3.0 TECHNICAL DISCUSSION

As described above the PAMS monitors and records the signal level and frequency of an airborne RF system and then reduces and plots the data. Therefore, the two most important parameters are the amplitude and frequency accuracy of the system. In order to provide meaningful data, it is necessary to have an accurate calibration of power and frequency. In essence, the PAMS acts as a comparator. The raw data is compared with a reference and its true value determined. The present method for calibrating the system consists of manually measuring the power level and frequency of an input test signal and recording the output of PAMS. From this data a table is generated with the appropriate correction factors and then stored in the computer. In actual operation the raw data is compared against the look up table, corrected, and then stored in the data bank. Consequently, the system accuracy is primarily a function of the initial calibration.

3.1 CALIBRATION

The system is calibrated in the following manner. The antenna input is disconnected from the receiver and an appropriate signal generator substituted. The generator is calibrated for a 0 dBm output and its frequency recorded. The generator output is then set at -40 dBm and the output is measured by PAMS and recorded. The input level is reduced in 6 dB increments down to -94 dBm with each reading being recorded. The procedure is repeated for five separate frequencies across the operating band of the receiver. This procedure, while relatively accurate, is quite time consuming. In fact, to calibrate the entire system over its operating range, and including the calibration of the test equipment, requires approximately five days. Therefore, the system is calibrated and new gain tables generated in about three month intervals. This introduces a long term system error of an unknown magnitude. A maximum short term RMS error of 1.5 dB was measured during the initial acceptance test of the system; however, the long term effect has not been evaluated. This subject will be addressed in another engineering report on the PAMS system performance. However, it is noted here that the antennas and their associated transmission lines are the major contributors to the long term errors in the system. The PAMS antenna system was thoroughly measured in 1971 and neither the antenna gain nor antenna patterns have been checked since that time. What changes, if any, have occurred over the past three years are completely unknown. At the present time, the only way to check the antenna system is to remove the entire array from the pedestal and put it on a static antenna range and then perform the measurements of interest. As can be seen, this procedure would be both time consuming and expensive. In addition, the entire calibration could be voided if the array suffered any damage when it was reinstalled on the pedestal.

The need for a rapid and accurate method of calibration for the PAMS has been recognized for some time now. The following paragraphs will discuss an approach for a fast and accurate method of calibration of the PAMS including the antenna subsystem.

3.2 SYSTEM CONCEPT

The approach to be considered here incorporates a collimation tower which is completely instrumented for the calibration of the PAMS including the antenna characteristics. The primary purpose for utilizing a collimation tower is to permit the system to be checked through the antenna input. As mentioned previously, the antennas and associated transmission lines are neglected in the present calibration procedure. A collimation tower will eliminate this shortcoming and in addition will permit the antenna parameters such as gain, beamshape, and boresight to be evaluated as a part of the calibration cycle.

This concept utilizes all standard instrumentation with the only special hardware consisting of the data multiplexer and logic control. The instrumentation will be incorporated in a modular configuration for ease of maintenance and versatility. Figure 1 is a block diagram of the proposed calibration system. This approach to the system calibration will allow the operator to evaluate the receiver gain, dynamic range, and minimum detectable signal over the entire 0.1 GHz to 18 GHz range or over any particular frequency band of interest. The calibration can be

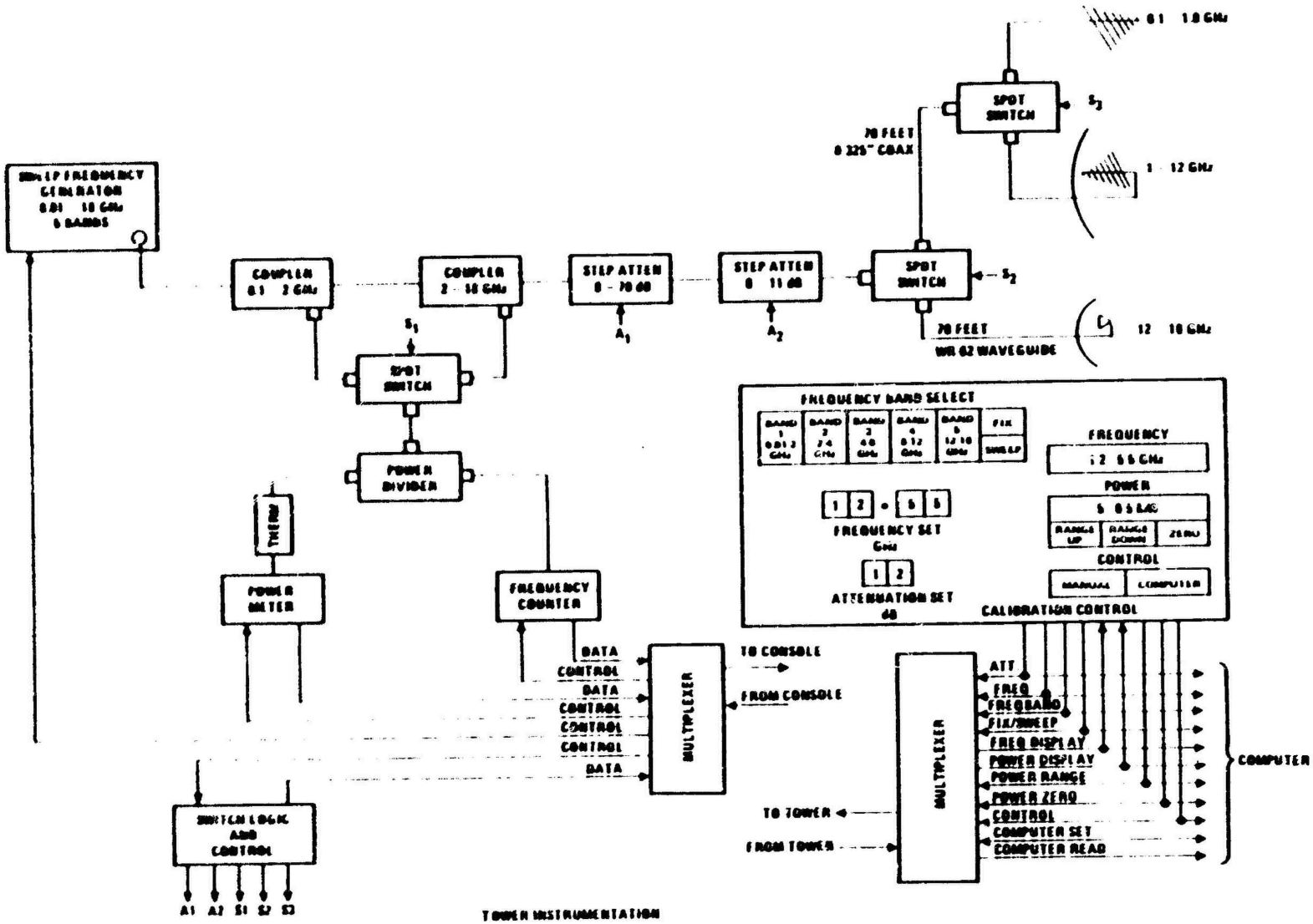

Figure 1. PAMS Calibration/Collimation System

accomplished under complete computer control or in a semi-automatic mode with the operator controlling the process. The calibration of the antenna system and transmission lines will be treated in later paragraphs.

3.3 INSTRUMENTATION

The instrumentation would be located at the collimation tower and operated remotely from the PAMS console and teletype located in Lab 7. A remote control panel will be incorporated into the PAMS console with all the controls required for automatic operation as well as two displays for the power and frequency readouts. For computer control of the calibration all the automatic functions at the console will be overridden with the exception of the two displays. In the computer mode all command data is inputted via the teletype terminal. The following description of the operation of the calibration system will assume that it is under control of the computer, the only difference being that the teletype is used rather than the control switches.

The signal generator covers the frequency range from 0.1 GHz through 18 GHz using multiple RF plug-in heads with a minimum RF output of ten milliwatts. The signal generator is configured to allow complete coverage across the band or any particular band of interest. Frequency selection is programmable using a BCD format which provides 1000 point frequency resolution for any one band. The operator activates the system by calling up the calibration program via the teletype. He inputs the frequencies to be calibrated, range of signal level, and resolution of the attenuation increments used to obtain range of signal level desired. The attenuation is achieved with two programmable step attenuators which provide 81 dB of attenuation in 1 dB increments. The correct antenna is selected automatically by the switch logic of the system. The transmitted signal is received and processed by the PAMS and then compared to the test reference. The reference is obtained in the following manner. The test signal is sampled by directional couplers and fed to an RF power meter and RF frequency counter. This data is outputted in a BCD format and multiplexed to the control panel via cable where both the power and frequency are displayed. The computer reads the input to the control panel and corrects for the insertion loss of the sampled signal level. This data is then used as the reference level for the amplitude calibration. The insertion loss of the sample loop is accurately measured during installation and the results recorded in the calibration program. When the level of the test signal is reduced by the step attenuators the computer reads the switch logic to determine the value of attenuation and then subtracts the value from the original reference level to obtain a new reference. This procedure is repeated for each signal level and frequency specified by the operator. The power and frequency data are tabulated and a delta (Δ) offset calculated for each measurement. The data is stored in the computer as a look up table to be used to correct each power level and frequency recorded during a flight test. In addition, the data can be outputted on the line printer to be used as a part of the flight test data package. The format for the hard copy data is illustrated in figure 2.

The multiplex system converts the parallel data from the power meter and frequency counter to a serial bit stream and sends the data via cable to the remote display panel. Here, the data is converted back to a BCD format to drive the

F_1(REF)	F_1(MEAS)	ΔF_1	P_{11}(REF)	P_{11}(MEAS)	ΔP_{11}
			P_{12}(REF)	P_{12}(MEAS)	ΔP_{12}
			.	.	.
			.	.	.
			.	.	.
			P_{IN}(REF)	P_{IN}(MEAS)	ΔP_{IN}
F_2(REF)	F_2(MEAS)	ΔF_2	P_{21}(REF)	P_{21}(MEAS)	ΔP_{21}
			.	.	.
			.	.	.
			.	.	.
			P_{2N}(REF)	P_{2N}(MEAS)	ΔP_{2N}
F_M(REF)	F_M(MEAS)	F_M	P_{MI}(REF)	P_{MI}(MEAS)	ΔP_{MI}
			.	.	.
			.	.	.
			.	.	.
			P_{MN}(REF)	P_{MN}(MEAS)	ΔP_{MN}

Figure 2. Calibration Data Format

remote displays for power and frequency. The computer samples this data and stores it in memory. The signal level is changed in three second intervals which allows 10 data samples to be acquired. The signal level is then incremented and the power and frequency displays updated and the new switch logic status read by the computer. With this test sequence, it is possible to measure 10 signal levels at each of 20 frequencies in any one band in approximately 10 minutes. This includes generating the look up reference table which will be used in the flight test. Under this criteria, the PAMS could be calibrated over its complete frequency range in 50 to 60 minutes. To accomplish the same task using the present procedure would take four to five days. With the calibration system, it would be possible to accurately calibrate the PAMS prior to and after each test flight. This procedure would essentially eliminate the effect of long term system errors. In addition, with calibration data before and after the test flight the magnitude of the short term errors could be evaluated and corrections made in the data printout if required.

3.4 COLLIMATION CONFIGURATION

The primary requirements for the antennas to be used on the collimation tower are narrow symmetrical beamwidths to minimize the effects of ground reflections and reflections from nearby buildings and obstacles, and high gain to overcome the free space attentuation so that low level RF signal sources can be used. These requirements can be basically achieved over the operating band with the exception of the 0.1 GHz to 1 GHz range. Here, the large wavelength makes the size of a highly directive antenna impractical for use on a collimation tower. For instance, in order to achieve a half-power beamwidth of 10 degrees at 250 MHz a 30 foot diameter parabolic reflector would be required. The best compromise for this band is an antenna whose characteristics are relatively constant as a function of frequency.

The antenna complement selected for the collimation tower is made up of three antennas with dual linear and/or circular polarization to cover the frequency range from 0.1 GHz to 18 GHz. For the 0.1 GHz to 1 GHz band a crossed log periodic dipole (LPD) with a nominal gain of 8 dB across the band was chosen. The free space attenuation in this frequency range is relatively low so that the low gain of the LPD is not necessarily a handicap. However, the very broad beamwidths will introduce measurement problems because of reflection. The range and the reflection problems will be treated in later paragraphs. To cover the 1 GHz to 12 GHz range, a ten-foot parabola with a crossed LPD feed was selected. The choice of a 10 foot reflector rather than a 6- or 8-foot dish was dictated primarily by the narrower beamwidth at the low frequency end in order to minimize the ground reflections. The gain of this antenna varies from 26 dB at 1 GHz to 47 dB at 12 GHz. For the 12 GHz to 18 GHz band a 3.5-foot dish with a quadra-ridge feed will be used to obtain both a narrow beamwidth and gains from 39.0 dB to 42 dB. In order to minimize the insertion loss from the signal sources to the antenna array, a 0.325-inch diameter air-articulated coaxial transmission line will be used for the two antennas covering the 0.1 GHz to 12 GHz range. For the 12 GHz to 18 GHz band, WR-62 waveguide will be employed.

The decision to use dual polarization rather than a single linear polarization was made so that both the vertical and horizontal channels in the PAMS receivers could be calibrated simultaneously or individually. In addition, this configuration allows both circular polarizations to be evaluated. The same information could be achieved using the single linear polarization by mechanizing the collimation array so that the polarization could be rotated by 90 degrees to achieve both vertical and horizontal components. This not only requires additional hardware but would more than double the calibration cycle.

The proper antenna selection is obtained automatically by the use of switch logic. The frequency set command, either from the control panel or the computer, is sensed by the switch logic which then activates the correct switch sequence. The same technique is used for selecting the directional coupler for the reference loop. The major instrumentation required for the calibration/collimation system illustrated in figure 1 is itemized in table 1.

TABLE 1. SYSTEM INSTRUMENTATION

DESCRIPTION	MANUFACTURER	PART NUMBER
Sweep Oscillator Set	Weinschel	4310A/K-16-H-01
Power Meter	Hewlett Packard	432C
Thermistor Mount	Hewlett Packard	8478B
Frequency Counter	Hewlett Packard	5340A
Directional Coupler (0.1 GHz - 2 GHz)	Hewlett Packard	778D
Directional Coupler (2 - 18 GHz)	Hewlett Packard	11691D
Programmable Step Attenuator (0 - 70 dB)	Hewlett Packard	33300
Programmable Step Attenuator	Hewlett Packard	33304
Power Divider	Weinschel	1506A
SPDT Switch (3)	Transco	909C70100
Multiplexer (2)	Actron	
Switch Logic and Control	Actron	
Calibration Control Panel	Actron	
Crossed Log Periodic Antenna (0.1 GHz - 1 GHz)	Scientific Atlanta	29C-0.1
10 Ft. Parabola and Crossed LPD Feed (1 GHz - 12 GHz)	Watkins Johnson	AR194-AS
3.5 Ft. Parabola with Quad Ridge Feed	Watkins Johnson	WJ8572-1

3.5 COLLIMATION RANGE REQUIREMENTS

The concept of a collimation tower is considered to be the optimum approach to the calibration and alignment of the PAMS. This technique enables all of the system parameters to be evaluated and correction factors generated without the need to take the equipment down. The calibration system described above enables the calibration cycle over the entire operating frequency range to be performed in approximately one hour. To calibrate a single band requires only 10 to 15 minutes. This makes it practical to go through the calibration before and after each test flight to insure maximum accuracy of the data.

The most important parameter in the collimation tower concept is the propagation path. It is necessary that the PAMS antennas be illuminated with a uniform amplitude and phase. Excessive amplitude deviations will introduce errors in the gain measurements and a non-uniform phase will give rise to asymmetrics and distort the measurement. It is relatively simple to insure that a fairly constant phase front is maintained across the aperture of the PAMS antennas by maintaining a distance R between antennas that follows the relationship

$$R \geq \frac{2D^2}{\lambda}$$

D = Dimension of aperture
λ = Free space wavelength
D and λ are in same units

This will result in a phase deviation on the order of $\lambda/16$ which is the commonly accepted criteria for phase deviation. This phase error will introduce gain errors less than 0.1 dB and only minor distortions in the sidelobe level. It is much more difficult to achieve a constant amplitude across the aperture due to reflections from the ground and surrounding obstacles.

Ideally one would want the antennas situated in such a manner that the path length of the reflected wave would be much greater than the direct wave. In this case the amplitude of the interferring signal would be reduced to a negligible level due to free space attenuation. Unfortunately, this would require antenna heights of several hundred feet which is out of the question. A second approach to the problem is to take advantage of the properties of the interference pattern. For a worst case condition of unit reflection coefficient, it can be shown that the variation in the field intensity across a test aperture, PAMS in this case, is given by

$$E = 2E_0 \sin \frac{2\pi h_1 h_2}{\lambda R}$$

where

h_1 = height of PAMS antenna

h_2 = height of collimation antenna

R = distance between antennas

λ = free space wavelength

From this expression it can be seen that there is a sinusoidal variation as a function of frequency and antenna heights for a fixed spacing. The first maximum occurs when

$$\frac{2\pi h_1 h_2}{\lambda R} = \frac{\pi}{2}$$

or

$$h_2 = \frac{\lambda R}{4h_1}$$

If the first maximum of the interference pattern is impinging on the PAMS antenna, the resultant variation across the aperture will not vary more than one-or two-tenths of a dB. In order to maintain this condition across the frequency range of PAMS, the height of the collimation tower antennas will have to be varied from 160 feet at 100 MHz to approximately one foot at 18 GHz. While the ground level range approach is practical for a static test range it is not suitable for the present application. The time required to reorient the collimation antennas as the frequency is changed would be so excessive that most of the advantages of the present concept would be lost. In addition, the cost to erect a suitable tower at Verona would be prohibitive.

There is an existing tower at the Verona Test Annex which could be utilized as the collimation tower. As shown in figure 3, the tower is located approximately 2250 feet from the PAMS site and is 70 feet high. The tower is accessible from the PAMS building and has AC power available at the site. The instrumentation could be stored in a standard Air Force shelter with the transmission lines running up through the center of the tower. There is a large hexagonal platform at the top with approximately 191 square feet of working area. The geometry of the proposed site is shown in figure 4. Instrumentation cable would have to be installed to handle the data transmission between the two facilities.

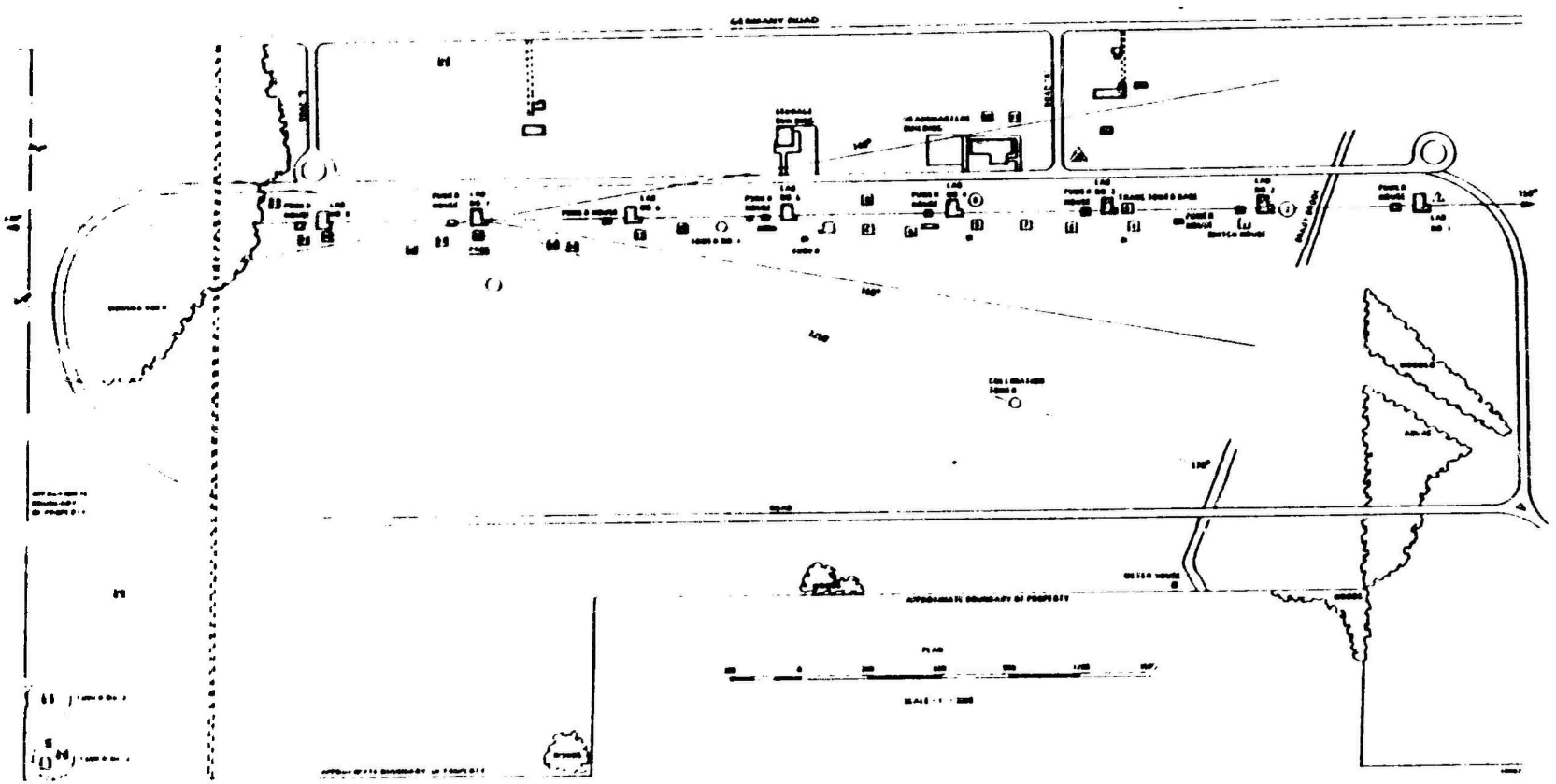

Figure 3. Plot Plan - Verona Test Annex

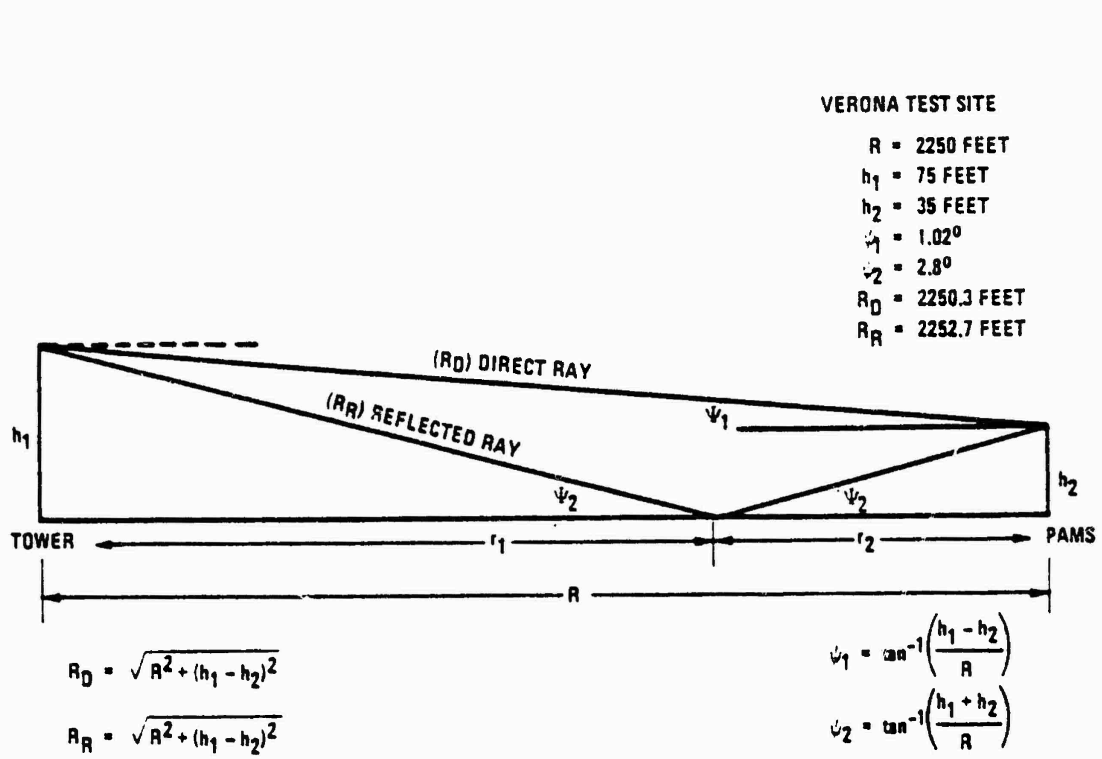

Figure 4. Site Geometry

3.6 RANGE REFLECTION CONSIDERATIONS

The primary difficulty associated with this site geometry and the existing tower for the collimation and calibration range is the ground reflection problem. This is a combination of the low grazing angles and the broad beamwidth of the 0.1 GHz to 1.0 GHz antenna in particular. In addition, because of the site geometry the direct path and reflected path are approximately equal in length. The actual difference being 2.69 feet. In the case of the low frequency antenna the beam shape is constant as a function of frequency and due to the broad beamwidth the power level at the point of reflection is only one or two tenths of a decibel lower than the main beam. Consequently, depending on the relative phase difference between the direct and reflected signal, the field strength at the PAMS aperture will vary from zero to twice the level of the transmitted signal. This will result in a gain error of 6 dB to $-\infty$ in the received signal. Figure 5 is a plot of the gain error as a function of the relative reflected power. Examining figure 5, it can be seen that in order to maintain a gain error of 0.25 dB requires that the reflected signal be suppressed by 31 dB below the direct signal. There are several methods which can be used to reduce the level of the reflected signal and these are discussed in the following paragraphs.

The field strength at the aperture of a receiving antenna is due to a resultant field which is made up of the direct ray and a reflected ray. The magnitude of the reflected ray is primarily a function of the antenna radiation pattern, magnitude of the reflection coefficient and the divergence factor. Secondary effects are introduced by the polarization of the transmitted signal.

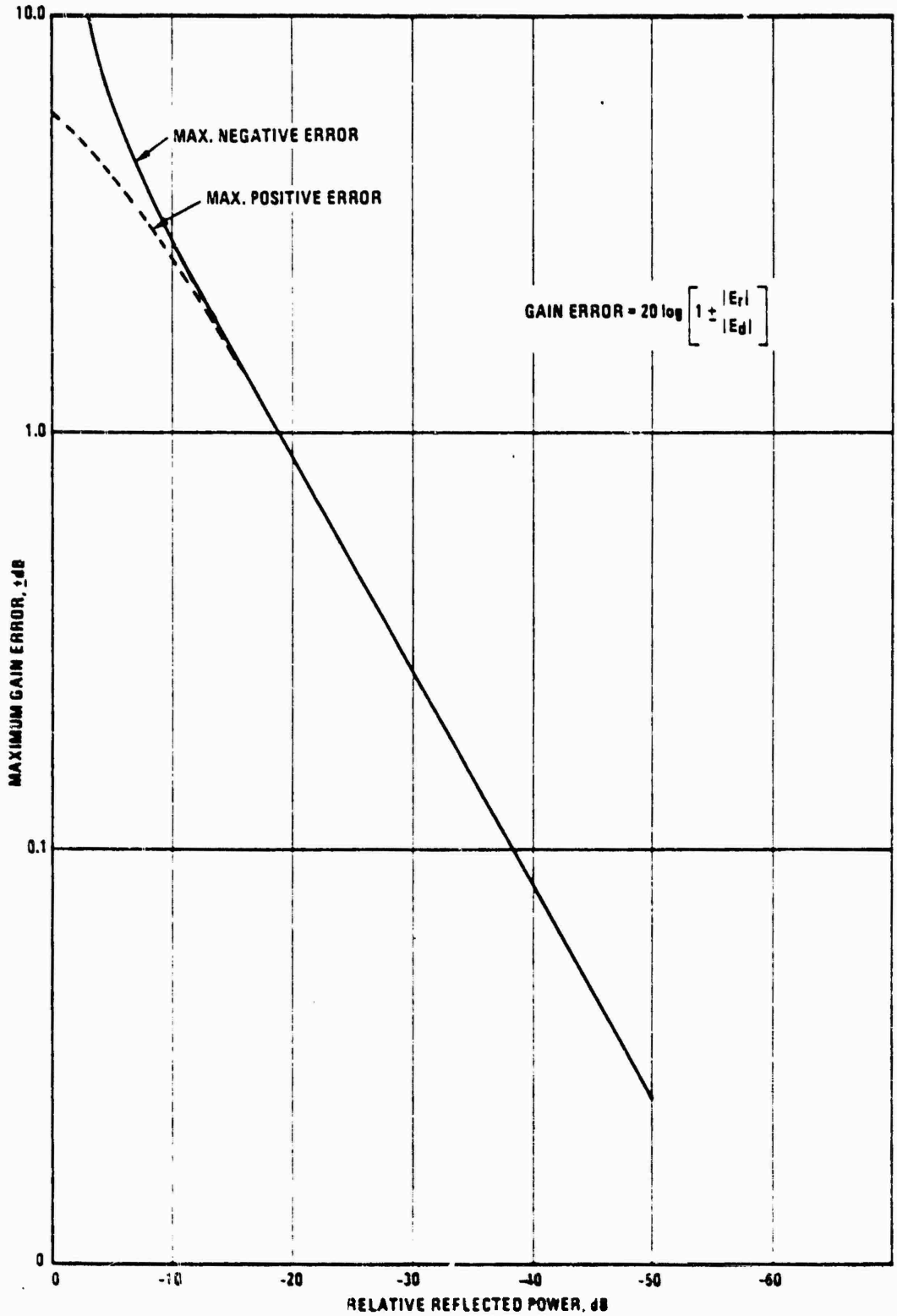

Figure 5. Gain Error

The reflection coefficient is very difficult to predict accurately because it is a function of polarization, frequency, grazing angle, surface roughness, soil type, moisture content, weather and season. The expressions for calculating the coefficient for vertical and horizontal polarization is given as:

$$\rho_V = \frac{n^2 \sin\psi - \sqrt{n^2 - \cos^2\psi}}{n^2 \sin\psi + \sqrt{n^2 - \cos^2\psi}}$$ Vertical reflection coefficient

and

$$\rho_H = \frac{\sin\psi - \sqrt{n^2 - \cos^2\psi}}{\sin\psi + \sqrt{n^2 - \cos^2\psi}}$$ Horizontal reflection coefficient

where

$n_2 = \epsilon_r - j60$

ϵ_r = relative permittivity of the ground

σ = conductivity of the ground

λ = free space wavelength

ψ = grazing angle

Due to the many parameters involved, the magnitude of the reflection coefficient can vary considerably. In fact, for the case of the vertical coefficient, it ranges from 1.0 to 0.0. The horizontal coefficient is somewhat more stable as it generally stays in the range of 1.0 to 0.8.

The divergence factor is the ratio of the field strength after reflection from a spherical surface to that of a plane surface. In our case we are dealing with a flat earth and the divergence factor is therefore unity. The relationship of these two factors to the resultant field is given by

$$E_d = E_0 \sqrt{1 + DR^2 + 2DR \cos(\theta - \phi)}$$

where

E_d = resultant field

E_0 = free space field

D = divergence factor

R = reflection coefficient

θ = path length difference in degrees

ϕ = phase shift due to reflection

This ratio of E_d to E_0 is called the earth gain factor and for the special case of D=1 we have

$$g(\theta) = E_d/E_0 = \sqrt{1+R^2+2R\cos(\theta-\phi)}$$

Examination of the above expression will show how the field strength varies as the electrical path length changes. If we assume that R=1 and 0=constant, then $g(\theta)$ will range from 0 to 2 as the cos $(\theta-\phi)$ changes from -1 to +1 and the electrical path length difference increases as a function of frequency. Also it can be seen that the nulls for horizontal polarization are deeper in general than those for vertical polarization since the magnitude for the horizontal reflection coefficient is generally greater than for the vertical reflection coefficient. For this reason the polarization used on the collimation range should normally be vertical or circular. When using horizontal polarization, precautions will have to be taken to minimize the deep nulls.

Of the parameters listed for the control of the field strength at the receiving aperture the most important is the antenna radiation pattern. This is due to the fact that the beamshape basically controls the amount of power available to be reflected. With proper beamshape control, it is relatively simple to maintain the level of the reflected wave to 25 dB to 35 dB below the direct wave.

Normally, the beamshape control for such a range as the one under consideration here is achieved with the use of parabolic reflectors to produce a narrow pencil beam with low sidelobes. In fact, considerable suppression of the reflected wave can be achieved with the use of moderately sized dishes for approximately 70 percent of the operating bandwidth of the collimation tower and PAMS.

For example, a 3.5 foot diameter reflector used for the 12 GHz to 18 GHz band will maintain the level of the reflected energy to approximately 25 dB exclusive of the PAMS receive antenna. This same level of performance can be obtained in the 1 GHz to 12 GHz band with a 10 foot diameter dish down to about 4 GHz. Below 4 GHz the beamwidth begins to broaden and the level of reflected energy will increase. Although larger diameter antennas could be used, the size required is not only impractical but extremely expensive. This is easily seen when it is

recognized that in order to keep the same performance as described above down to 1 GHz would require a forty foot parabolic dish. However, there is a technique available which can be used to reduce the level of the reflected power to the point where a relatively constant field can be maintained at the PAMS aperture. This approach involves the diffraction fences in the propagation path.

3.7 DIFFRACTION FENCES

The primary purpose of the diffraction fence is to prevent reflected energy from causing an interference pattern at the receiving aperture and producing fluctuating power levels. In other words the fences screen the receiver from energy which would, in the absence of the fences, be incident from points within the region of the range surface including the Fresnel zones which are illuminated by the relatively high levels of the transmitted pattern. This requires that the screens be placed in such a manner that they intercept a portion of the energy from the transmit antenna. This will result in perturbations in the receiving aperture due to edge diffraction effects. For a small frequency range, an acceptable level of ripple can be achieved by simple alterations to the fence configuration and its location on the range. However, for broad frequency ranges the use of multiple fences will most likely be required. This is due to the fact that the beamwidth, position of the near in sidelobes, and null positions are constantly shifting as a function of frequency. In addition, the size of the fresnel zones are also changing which affects the magnitude of the ground reflection. The use of zone plates and strips on the diffraction screens have not been considered here due to their frequency dependence and narrow band operation.

The full development of the theoretical analysis for edge diffraction and screening and its application to the problem at hand is beyond the scope and intent of this report. The approach is basically one of dividing a wave front into discrete increments in a systematic manner and computing the field in terms of the relative phases from each of these differential sources. These calculations are then repeated for each frequency of interest. Without detailed knowledge of both the transmit and receive antenna patterns and the reflection coefficient at the range site the calculations could be misleading.

In general, the addition of the diffraction screen will cause the field to appear as shown in figure 6. The magnitude of the ripple will be affected by the number of fences used, their location, and the angle of the screen with respect to the ground. Additional improvement can be achieved with the addition of broadband absorbent material across the top of the fences. It is also necessary to remove any potential sources of reflection near the receiving aperture. This will require that all metal railings and nearby metal structures be removed or covered with absorbent material.

As discussed above, it will be necessary to deploy diffraction screens on the collimation range when operating below 4 GHz because of the increasing beamwidth and decreased directivity of the transmit antenna. For convenience and ease of range maintenance, it is recommended that the screens be made a permanent part of the collimation range. The exact design of the fences will be deferred until the actual system hardware has been specified and approved. The location of the

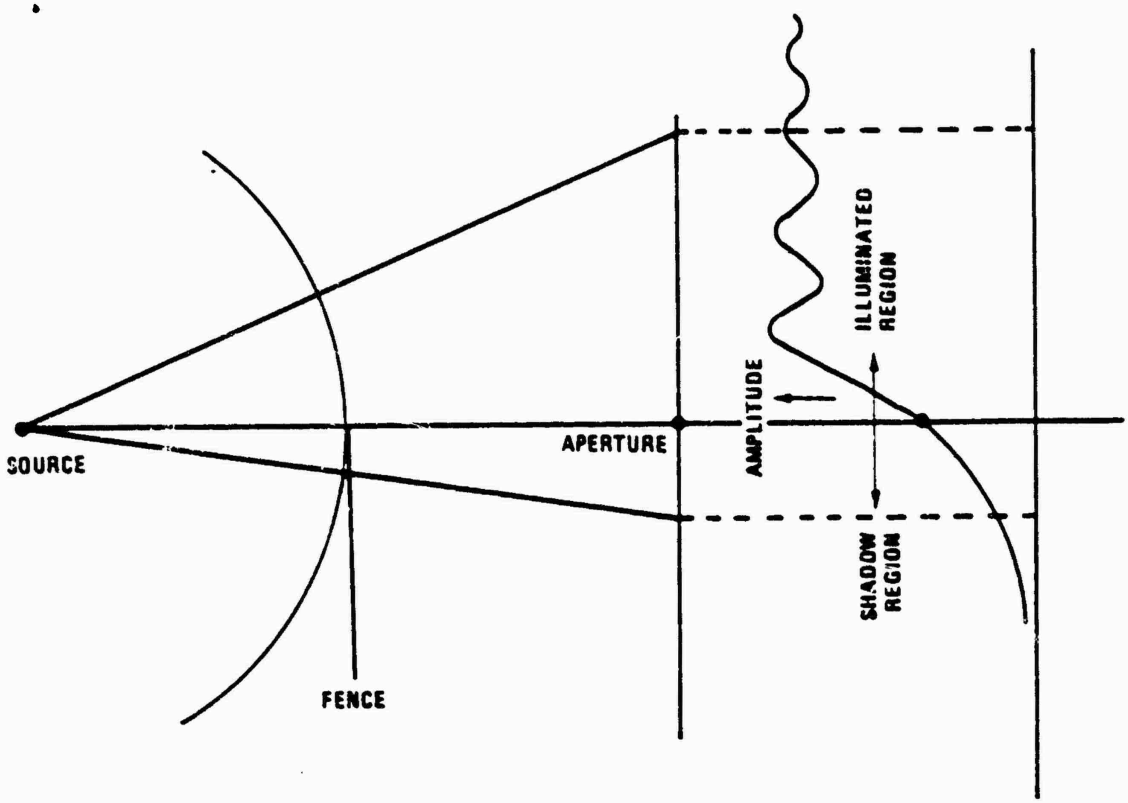

Figure 6. Resultant Field Amplitude with Diffraction Screen

fences on the range will be derived experimentally after the collimation system has been installed and the allowable ripple or gain error has been defined for the system.

The fences will have to remain in place on the collimation range throughout the year and therefore, will have to be fabricated from weather resistant materials. The necessity of being a permanent installation is dictated by the fact that initial placement is somewhat critical and the time required to deploy the screens each time they are required would be excessive.

3.3 ANTENNA ALIGNMENT

The last parameter of interest in the system calibration is the pointing accuracy of the PAMS antenna array. The pointing accuracy is a measure of the difference between the mechanical and electrical alignment of the antennas. It is not unusual to have the peak of the radiation skew to some extent as a function of frequency. Since PAMS monitors the amplitude of airborne emissions it is essential to know the degree of skew, if any, in order to calibrate out any amplitude error which could be introduced by antenna misalignment.

The boresight instrumentation will consist of a telescope mounted on the PAMS pedestal and a set of optical targets which will be located at the transmit antenna array on the collimation tower. To determine the pointing accuracy of the system, the PAMS array is optically aligned with the telescope using the targets on the collimation tower. The next step is to locate the position of the PAMS array for maximum signal amplitude as observed at the console. The difference in the two pedesal positions indicates the pointing accuracy. This procedure must be repeated for a minimum of three frequencies for each of the antennas which make up the PAMS array. These measurements will be sufficient to establish a trend so that the beam skew can be predicted and compensated for in the data acquisition program. In the case of a constant offset across the frequency band, a complementary offset will be introduced in the pedestal position. This test will not be required during each calibration cycle as the error is basically fixed by the antenna geometry. However, the pointing accuracy should be verified on at least a quarterly basis to insure that no perturbations have been introduced into the antenna array. It is further recommended that the pointing accuracy be checked after high wind and/or heavy snowfall has been encountered at the site.

The instrumentation necessary to implement the boresight capability is currently available at the Verona Site. The telescope and mounting hardware were delivered with the PAMS. The optical targets are presently located on the tower being considered for use.

4.0 CONCLUSIONS

The previous paragraphs have identified the need for a calibration and alignment system for the PAMS. It was shown that such a system could be built using basically standard test equipment and components. This approach not only allows the system to be installed at the Verona Test Site in a reasonable length of time, but also makes it possible to minimize the cost of the program. The only nonstandard hardware required for the collimation system is the multiplexer, control panel, and diffraction screens. An instrumentation cable will be required between the collimation tower and the PAMS facility. A cable with six individual shield pairs is adequate to handle the present instrumentation. However, this does not provide for much future expansion at the site. Therefore, it is recommended that a cable containing on the order of 15 to 27 shield pairs be installed.

The collimation range presents the greatest challenge in the program. The analysis in the previous section clearly illustrated that the ground reflections become very pronounced below 4 GHz and that diffraction fences would be required in order to achieve a relatively constant field at the PAMS aperture. The exact location of the screens will be derived experimentally by making a series of measurements on the range with the fences. The antennas recommended for the range are standard items and will not require development. A complete set of patterns and gain measurements will be needed in order to finalize the fence design and for use in the calibration software. A three and a half foot diameter dish is recommended for the 12 GHz to 18 GHz band. The best compromise for the 1 GHz to 12 GHz band is a 10 foot diameter reflector. This offers reasonable performance down to approximately 4 GHz before the variations in the field strength begin to introduce appreciable errors in the measurements. Although a 12 foot diameter dish would offer somewhat improved performance and extend the lower frequency

limit to approximately 3 GHz, the increased cost of the antenna and mounting structure requirement limits its selection. For optimum operation, it is recommended that the polarization be restricted to vertical and either right handed or left handed circular.

Due to the fact that the majority of the instrumentation for the project is standard equipment, the engineering effort would be primarily concerned with the design of the multiplexer, control panel, diffraction screens, software, and field tests. The programming effort will be initiated early in the program in order to have the software available and on line by the time the instrumentation is installed. The field measurements would be started as soon as the antennas have been completed.

APPENDIX II

ERROR ANALYSIS PROGRAM FOR THE PRECISION ANTENNA MEASUREMENT SYSTEM

1.0 OBJECTIVES

This report describes a design of an error analysis program for the Precision Antenna Measurement System (PAMS). The analysis objectives are as follows:

1. To identify the sources of system error.

2. To derive an overall system model.

3. To measure the system and random errors.

4. To derive the overall theoretical system error and the statistical variations of the error.

5. To formulate a figure of merit.

6. To calculate the actual overall system error from the measured data and ascertain the error fluctuations.

7. To compare the theoretical and actual system error.

8. To identify means for decreasing the system error.

2.0 ERROR IDENTIFICATION AND MEASUREMENT

2.1 ERROR IDENTIFICATION

The PAMS system offers a means for dynamically measuring the radiation pattern of an antenna mounted on an airborne vehicle by means of a ground based receiving system. The measurement is accomplished in three steps. First, the field strength of the radiated signal is measured relative to a ground based coordinate system. Second, the attitude of the airborne vehicle is measured. Third, the field strength data is transformed to a coordinate system fixed in the moving vehicle and the radiation pattern is derived relative to the moving vehicle.

A complete system error analysis can only be performed if adequate data, both theoretical and experimental, are available on the various portions of the system which contribute to the overall system error. However, when dealing with an actual large scale system such as PAMS, it is impossible to obtain the necessary data for a complete analysis. Furthermore, the contribution of some of the component errors to the total system error will be negligible in comparison to the error sources. Thus, to include every error source in the analysis will complicate the calculations and becloud the results needlessly. For all practical purposes, an error analysis will be complete when all first and second order errors are identified and these contributions to the total errors are determined.

The prescription for initiating an error analysis is to select the variables that are spelled out by the derived model. Any variation of these variables are classified as errors. The first step is to divide the sources of error into two groups, namely system and random errors. System errors are basic to the overall system and the various components which are consequences of the particular design or choice of components and have no random components. Bias and offset errors are typical examples of system errors. Random errors arise in the measurement of the received signal field strength as a consequence of the variations of component characteristics, variations of ambient conditions and effects of noise. The identification and calculation of random errors will comprise the major effort of this study.

The calculation of the random errors and their consequence draws on the methods of probability theory. A complete characterization of the noise requires a series of measurements and a myriad of data reduction calculations. A more reasonable approach is to make use of the insight afforded by the physics of the problem. A reasonable approach to follow is to assume a feasible noise process with known properties, make a set of controlled measurements and calculate the significant statistical error parameters. When the theoretical and measured error parameters agree within prescribed bounds, the assumed noise process can be assumed to be the correct noise process to be used in the complete error and/or smoothing calculations. The significant measurement parameters that contribute directly to the overall error are as follows:

a. Transmitted power

b. Received signal power

c. Signal frequency

d. Spatial orientation of the receiving antenna

e. Spatial orientation of the transmitting antenna

f. Relative orientation of the receiving and transmitting antennas

g. Mean noise power, covariance and noise amplitude distribution.

The next step in the analysis is to identify the errors in the system components. For purposes of the error analysis, the PAMS system can be divided into six components. Associated with each component are a number of parameters which affect the variables that contribute to the overall error indirectly. The components and the parameters associated with each component are listed as follows:

Receiver

1. Gain

2. Sensitivity

3. Selectivity

4. Noise figure

5. Signal-to-noise ratio

6. Channel tracking

7. AFC loop characteristics

8. Bandwidth IF and RF

Antennas

1. Gain as a function of frequency

2. Boresight orientation

3. Pattern shape

4. Polarization discriminator

Pedestal/Slip Ring Assembly

1. Signal loss

2. Signal distortion

3. Velocity and acceleration rate characteristics

4. Servo lead or lag characteristics

5. Auto rate, digital track and manual track versus zero alignment (both axis)

6. Mechanical alignment

Signal Processor

1. Sampling error

2. Error in hold output (approximation error)

3. Video filtering

4. Computer interfacing

5. Drive circuit characteristics

6. A/D approximation error

Insertion Losses (Antenna Terminals to Receiver Input)

Computer

2.1.1 Ancillary System Errors

Three ancillary pieces of equipment must be included in the proposed error analysis model. The FPS-16 Tracking Radar and the Airborne Monitoring System are used to measure direct measurement parameters (spatial orientation of transmitting antenna and relative orientation of the receiving and transmitting antenna). The Airborne Signal Source supplies the signal power that excites the transmitting antenna. The system errors and the random errors which are associated with the three equipment items must be considered in the calculation of the overall system error.

The parameters of interest for each of the three pieces of equipment are as follows:

FPS-16 Tracking Radar

1. Tracking accuracy
    a. Tracking error (determine loss of track lock)
    b. Skin tracking (determine loss of track lock)
2. Pointing error
3. Range accuracy
4. Interface errors
    a. Radar boresight orientation
    b. Servo loop lead or lag characteristics
    c. Velocity and acceleration rates

Airborne Signal Source

1. Amplitude stability
2. Frequency stability
3. Leveling capability
4. Environmental effects

Airbone Monitoring System

1. Roll, pitch, heading
2. Altimeter reading
3. Processing errors

4. Tape deck

   a. WOW

   b. Flutter

   c. Repeatability

   d. Parity

2.2 SYSTEM MODELING

A system error analysis is developed from a model of the physical system under investigation. System models are mathematical descriptions of the state of the system. The designer or user of the system can ascertain its performance from a knowledge of the system state. Deviations of the system performance from the design objectives are considered to be errors.

The model should predict the system state from input and output variables that are measurable quantities or attributes. The calculation of system and random errors must be possible from the model. An important requirement imposed upon the model is that it should reduce the system to the most significant parameters. Complex models are of limited value and an insight in the system's behavior usually is obtained from a simple model.

A guide to the development of a model is its ultimate application. Several applications are possible. The most important are (1) to facilitate the understanding of the system behavior, (2) to have a means to obtain design data for expanding the system, and (3) to establish a framework for detailed error analysis. These applications may impose different requirements on the model.

System models can be expressed in many forms. A differential equation is a common form. The solution requires a mathematical expression for the forcing functions, initial conditions and boundary conditions. Differential equations are of two types, linear and non-linear. Linear differential equations lend themselves to closed form solutions. Non-linear equations offer great difficulties. Usually, only partial solutions of specific aspects of the problem are obtained such as phase space solutions. If the variables are propitiously selected, linear differential equation offers the possibility of a complete solution.

The transfer function model offers a relatively simple solution for a system problem. However, the transfer function of the system characterizes only the zero-state response. The power of the transfer function, $H(s)$, is the usefulness of the expression

$$y(s) = H(s)\,X(s)$$

where $y(s)$ and $x(s)$ are the Laplace transforms of the output, $y(t)$, and input, $x(t)$, respectively. $H(s)$ is the Laplace transferrable to the impulse response, $h(t)$ by the relation

$$h(t) = \frac{1}{2\pi j}\int_{c-ja}^{c+ja} H(s)e^{st}dt$$

provided the system is time-invariant and c is constant defining the domain of convergence of the integral. Multiple input multiple output systems can be treated within the same formulism.

A third formulation of a system model is obtained by means of the state variable approach. This method is a refinement of the differential equation representation. In order to define the output of the system over some interval $t_0 \leq t < t_1$, it is necessary to know not only the input over this time interval but, in addition, a number of initial conditions that must be adequate to describe how any past inputs ($t < t_0$) affect the system output in the interval $t \geq t_0$.

The state of the system is the minimal amount of information about the effects of past inputs necessary to describe completely the output for $t \geq t_0$. The variables that contain this information are the state variables. Thus, given the state of the system at t_0 and the input from t_0 to t_1, we can derive both the output and the state at t_1 if it is assumed that the system is realizable.

Assume that a system can be described by a n^{th} order scalar differential equation. This equation can be transformed to a first-order vector equation (n simultaneous first-order differential equations) which is easier to solve. A linear time-variant system is describable by the vector differential equation

$$\frac{d}{dt}\underline{x}(t) = \underline{F}\,\underline{x}(t) + \underline{G}\,u(t) \tag{1}$$

and

$$y(t) = \underline{C}\,\underline{x}(t) \tag{2}$$

where $\underline{x}(t)$ is the state vector and the components x_i are state variables $v(t)$ is m-vector representing the inputs $\underline{F}$ and $\underline{G}$ are n x u and n x m matrices while $\underline{C}$ is a n x p matrix. $y(t)$ is the system output. When the system is time-variant, the dynamic system is described by

$$\frac{d}{dt}\underline{x}(t) = \underline{F}(t)\,\underline{x}(t) + \underline{G}(t)\,\underline{u}(t) \tag{3}$$

and

$$y(t) = \underline{C}(t)\,\underline{x}(t) \tag{4}$$

A formal solution of equations (1) and (2) can be easily obtained. These equations are inhomogenous differential equations which requires that the solution consist of a particular and a homogenous part.

The homogenous part is obtained by setting $\underline{u}(t) = 0$ with the result

$$\underline{x}(t) = e^{\underline{F}(t-t_0)}\, \underline{x}(t_0) \tag{5}$$

The term

$$e^{\underline{F}t} = \sum_{n=0}^{\infty} \frac{(Ft)^n}{n!}$$

Write $e^{\underline{F}(t-t_0)}$ in the form $\phi(t-t_0)$, the important relation follows

$$\frac{d}{dt}\, \underline{\phi}(t-t_0) = \underline{F}\, \underline{\phi}(t-t_0) \tag{6}$$

where $\underline{\phi}(t_0-t0) = \underline{\phi}(o) = \underline{I}$ is the initial condition. ($\underline{I}$ is the unit matrix).

The homogenous solution can be rewritten as

$$\underline{x}(t) = \underline{\phi}(t,t_0)\, \underline{x}(t_0) \tag{7}$$

$\underline{\phi}(t,t_0)$ is the state transition matrix. Finally, the solution to the inhomogenous equation is

$$\underline{x}(t) = \underline{\phi}(t,t_0)\, \underline{x}(t_0) + \int_{t_0}^{t} \underline{\phi}(t,t)\, \underline{G}(\tau)\, \underline{u}(\tau)\, d\tau \tag{8}$$

Since the system is a linear system, the system is characterized by its impulse response $\underline{h}(t,\tau)$ by the relation between the input and output

$$\underline{y}(t) = \int_{-\infty}^{t} \underline{h}(t,\tau)\, u(\tau)\, d\tau \tag{9}$$

Usually, the initial condition at $-\infty$ is zero, thus equation (8) can be written in the form

$$\underline{x}(t) = \int_{-\infty}^{t} \underline{\phi}(t,\tau)\, \underline{G}(\tau)\, \underline{u}(\tau)\, d\tau$$

substituting in equation (4) with the result

$$\underline{y}(t) = \int_{-\infty}^{t} \underline{C}(t)\, \underline{\phi}(t,\tau)\, \underline{G}(\tau)\, \underline{u}(\tau)\, d\tau$$

where

$$\underline{h}(t,\tau) = \underline{C}(t)\, \underline{\phi}(t,\tau)\, \underline{G}(\tau) \qquad t \geq \tau$$
$$= \underline{0} \qquad \text{elsewhere}$$

The result is very important since $\underline{h}(t,\tau)$ is uniquely defined in terms of the state variable matrices which are not unique.

It was demonstrated that the three methods for modeling a dynamic system are actually different aspects of the same method. The choice of method is dictated by the particular system being investigated.

The models described assumed that the systems are deterministic. The system errors can be calculated within this framework. However, for purposes of this error analysis, the random errors are of prime interest. In order to calculate the random error requires the introduction of random noise as a system input.

The introduction of random noise increases the problem by an order of magnitude. First, the noise process must be modeled making the mathematics of the solution less tractable. The choice of system to be used becomes more critical. For purposes of the state variable representation, the noise is characterized by the covariance function. Three typical examples which are the most useful and occur very commonly in physical system are as follows:

(a) Wiener or Brownian Process (nonstationary)

$$E\left[X_t X_s\right] = \sigma^2 s \quad s \leq t \quad \sigma^2 = \text{variance}$$
$$= \sigma^2 t \quad t \leq s$$

where E represents expectation.

(b) First-order Butterworth-Markov- (stationary)

$$E\left[X_t X_s\right] = \underline{P} e^{-\alpha(t-s)} \qquad \underline{P} \text{ and } \alpha \text{ are constants}$$

(c) White noise (stationary)

$$E\left[X_t X_s\right] = \sigma^2 \delta(t-s)$$

where $\delta(t-s)$ is the delta function.

t, s are time epochs.

In order to avoid being overwhelmed by mathematical difficulties, it will be assumed that the system is linear and time invariant. The assumption removes the necessity to deal with non-linear differential equations and avoids the effect of the non-linearity on the input noise process. The noise excitation will be assumed to be white noise or Butterworth. More sophisticated methods will only be introduced if the calculated errors differ in excess from the measured errors.

The modeling should be a state variable description of the system and the noise processes. This characterization provides a framework for system description which can be linear, time-invariant or time varying. Thus, flexibility is introduced in the analysis. Many statements can be made about system behavior. The description of the actual dynamics is more representative of the physical situation. This approach leads to solution techniques that are easily implemented on a computer which is especially important if error smoothing is introduced.

2.3 SYSTEM ERROR MEASUREMENTS

System errors are identified with a particular system and its components. These errors characteristically manifest themselves as errors due to drift, bias or offset errors and experimental errors. System errors due to drift and offset can be eliminated or compensated. However, experimental errors which are consequences of the measuring technique and sensors used determine the accuracy and precision of the measurements.

Although experimental errors result from the randomness in the measured output data, they must be differentiated from system random errors. In the content of this report, system random errors are a consequence of the noise-like excitation of the system. Such forms of excitation are random processes. On the other hand, whenever a series of repeated measurements are made with a measuring system, a variability in the output data is observed. This non-repeatability of the output data is called experimental error. Typical causes of experimental error are the inability to reset a dial to the same position for each measurement or the ability of a tracking radar to slew to the same azimuth for each measurement. Experimental errors are calculated from the output data while the bias and drift errors are measured directly.

The actual airborne antenna pattern measurement is a two step process. First, the signal radiated by the Airborne Signal Source is measured in respect to a ground based coordinate system by means of the Receiver-Antenna system which is slaved to a FPS-16 Radar. Secondly, the data is transformed to an airborne coordinated system using the data from the Airborne Monitoring System to orient the transmitting antenna in the new coordinate system.

Since the PAMS system is an open-loop system, the errors in each process can be measured separately. The errors introduced in the first step can be classified as direct measurement errors in the received signal power. However, the Receiver-Antenna System is slaved to the FPS-16 Radar, hence, the errors in the measurement of the range, elevation, elevation and azimuth angle of the moving airplane must be considered direct errors. However, errors introduced by the Airborne Monitoring System enter only indirectly in the overall error. The variables are introduced in the system by the axis transformation which is described in the Final Technical Report, PAMS Airborne Instrumentation, RADC-TR-74-174, page 127-139.

The measurement program will be outlined in detail in a subsequent section. The first set of measurements will serve as means to determine whether the system performance is according to specifications. The second set will function as a means for calibration. Finally, the errors will be measured.

2.4 DYNAMIC ERROR MEASUREMENTS

Dynamic errors result when the system is excited by a noise-like signal which may be random noise or random noise superimposed on the test signal. Measurements made on a system which is excited by a random noise source can reveal many important system characteristics. The noise band or the integrating effect of the system on the noise signal can be easily ascertained. The probability of error due to false detection can be measured. The probability of error as it depends on threshold setting can be determined. Finally, the system stability can be studied.

In the present system, a random noise excitation of suitable bandwidth can be introduced into the system as follows:

1. superimposed on the signal to be transmitted
2. the input signal to the transmitter
3. superimposed on the FPS-16 Radar outputs
4. superimposed on the appropriate signal in the Airborne Monitoring System.

In the present study, the system will be assumed to be linear, time invariant. The noise-like signals will be assumed additive. The detailed program will be described in a later section.

3.0 ERROR CALCULATION

3.1 THEORETICAL ERROR CALCULATION

The theoretical system error is defined in terms of the errors in the independent variables. These directly contribute to the overall error. The method for calculating the system is determined by the following factors:

a. specific system model

b. nature of input signal signals

c. system noise characteristics

d. definition of the error.

The system under study is an open-loop system. This received signal power may be described by a functional relation of the form

$$P_s = f(x_1, x_2, x_3, x_4, x_5) \tag{10}$$

where

x_1 = transmitted power

x_2 = signal frequency

x_3 = spatial orientation of the receiving antenna

x_4 = mean noise power

x_5 = convariance of the noise

The signal power is redefined in terms of the transmitted antenna spatial disturbance by means of the transformation

$$P_t = O_p(y_1, y_2, y_3) P_s \tag{11}$$

where the transformation operator is dependent on the following

y_1 = spatial orientation of the spatial orientation of the transmitting antenna in respect to vehicle

y_2 = vehicle orientation to the receiving antenna (range, azimuth, elevation)

y_3 = radar parallax

Equation (11) can be rewritten as

$$P_t = g\,(y_1, y_2, y_3, x_1, x_2, x_3, x_4, x_5) \tag{12}$$

or

$$P_t = g\,(z_1, z_2, z_3, z_4, z_5, z_6, z_7, z_8)$$

where the y's and x's were redefined in terms of the z's.

In Final Technical Report, PAMS Airborne Instrumentation, RADC-TR-74-174, page 71, it was demonstrated that the error in P_t, the power in a unit volume of the antenna pattern can be written as

$$\sigma^2_{\Delta P_t} = \sum_{k=1}^{N} \left(\frac{\partial g}{\partial z_i}\right) \sigma^2_{\Delta zi} + \tag{13}$$

$$\sum_{\substack{k=i \\ i \neq j}}^{N} \sum_{k=j}^{N} \left(\frac{\partial g}{\partial z_i}\right)\left(\frac{\partial g}{\partial z_j}\right) \rho_{\Delta z_i\, \Delta z_j}\, \sigma_{\Delta z_i}\, \sigma_{\Delta z_j}$$

where $\sigma_{\Delta z_i}$ is the error in the dependent variable z_i and ρ_{ij} is the correlation coefficient relating z_i and z_j variables. However, $\rho_{ij} = 0$ for those variables which are independent of each other.

In Appendix No. 1, the description of the errors were extended to include the situation in which some of the individual z_i are functions of other variables. As an example, the transmitted signal power can be demonstrated to be a function of the antenna gain, frequency, boresight orientation, pattern shape and polarization.

Equation A-6, Appendix No. 1 completely describes the procedure necessary to calculate the overall system error. Equation A-1 reduces to the case of equation (13), if the independent variables are not functions of other variables. These situations prevail as follows:

1. All variables are statistically independent and functionally independent. (The first term of equation (13) or equivalently the second term of equation A-6 prevail - $\rho_{ij} = 0$).

2. Variables are statistically dependent and functionally independent (equation (13) or the second and fourth term of equation A-6 prevail - $\rho_{ij} \neq 0$).

3. Variables are statistically independent but some of the independent variables are functionally relational (equation A-6 prevails - $\rho_{\Delta z_i\, \Delta z_j} \neq 0$).

Basic to the application of these equations is the requirement that it is possible to write an equation in the form of equations (11) and/or equation (12). If this is possible, the calculation of the error becomes mere formalism. In the event that this relation cannot be written from theoretical considerations, it is possible to use dimensional analysis techniques plus the use of measured data to obtain a functional relation.

The equations (13) and A-1 define the system error. No noise-like input signals were assumed. The introduction of noise as an input changes the method of error analysis because probability theory must be introduced.

The system error is described by equations (13) and A-1. In the development of these equations, it was assumed that all input signals are noise-free. Thus, given any variation in the independent variables, the overall error can be calculated with high precision.

The next step is the calculation of the dynamic errors. The dynamic error calculation now assumes that the input signal can include random noise processes which mandates the use of probability theory. The problem becomes much more complex. Two classes of techniques are available. First, the classical least squared error method is a possibility. Secondly, the linear filter estimation are available theory methods. These are the Wiener and the Kalman-Bucy procedures which are the most likely choice. These procedures can be considered parameter estimation techniques.

The uncertainty in the estimate of the parameter of concern is measured by an estimation covariance matrix. The error variance is a useful quantity especially when system is "corrected" during a measurement. The complete error analysis can be performed actually without simulating the linear filter by solving the covariance matrix equations.

These methods require a specific model and a known set of noise statistics. An inadequate model can degrade the power of these procedures. Thus, the impact of the specified model on the error and the error sensitivity must be determined. The assumed noise model determines the noise statistics. Finally, the error must be defined that operationally fit the measurement requirements.

3.2 MEASURED DATA ANALYSIS

The accuracy of the assumed model must be tested with actual measured data before it can be used to calculate the system error. The requisite measurements for collecting the data fall into two groups. First, the system and bias errors are measured. These measurements are made with stationary signal sources. The necessary corrections must be made to minimize the bias errors. The system error evaluation will be used to demonstrate the system performance. In order to insure that accuracy of these measurements, calibrated signal sources must be used plus a standard gain antenna. In fact, a collimation reference would be the most desirable. Typical measurement procedures will be described in Section VI.

The data reduction process will make use of classical estimation techniques. The parameters of importance for the variables being measured are he sample size, mean, variance and probability distribution. Pearson's method of moments and/or the method of maximum likelihood will yield results of sufficient accuracy. In addition, the confidence intervals will be established.

The output of these calculations will be a set of nomagraphs which can be used to predict system errors given the appropriate input data. Also, a mathematical framework will be available to extend the predictions when additional data becomes available.

The second group of measurements will concern themselves with the dynamic errors. This group of measurements can be accomplished in several ways as follows:

1. Add noise of known power spectral density and bandwidth to the transmitted signal from a stationary source.

2. Add simulated radar data to the appropriate inputs.

3. Track a moving plane with transmitter-antenna system slaved to the FPS-16 Radar.

Under the conditions, the PAMS measurement system is an open-loop system excited by random noise plus deterministic signals. Having effectively calibrated the system and compensated for bias errors, the dynamic errors can be ascertained. It will be necessary to assume the FPS-16 Radar was calibrated and the accuracies defined. It may be necessary to determine the statistics of the noisy radar output signals (range, elevation, and azimuth). The most significant parameter is the correlation function or the power spectral density.

The error can be determined using the Wiener or Kalman-Bucy methods. As a by-product of these two formulas, it will be possible to design smoothing filters or algorithms to reduce the overall dynamic system error.

The output of these measurements will be a second set of nomagraphs that will define the overall error under prescribed input conditions and degrees of smoothing.

If the model which was assumed was adequate, the theoretically derived results and the measured results will agree with prescribed accuracies. In addition, the results of these calculations will help define the system accuracies and precision.

Significantly, the data reduction procedures must aim for minimum complexity. Although very attractive, no complicated procedure should be considered unless the data and accuracies make them necessary and no simpler choice is available. Whenever a choice exists between two computational procedures, etc. choice should be based on accuracy and computational time.

3.3 ERROR WEIGHTING

Equations II-4 and A-6 have coefficients containing partial derivatives. These coefficients are weighting factors. It is by means of these coefficients that the relative magnitudes of the various system errors can be evaluated. The significance of the errors are established by a threshold which is set by trial procedures. The usual method is to arbitrarily set a lower limit to these magnitudes. Repeat by lowering the threshold and noting which errors are relatively insensitive. This weighting process can reduce the computations considerably.

The weighting of the input information is a very specialized process in the Kalman-Bucy theory. Any weighting has the effect of decreasing the information upon which the estimate is made. The error variance is inversely proportional to information.

3.4 NOISE ANALYSIS

The analysis of random noise is mathematically a very complex problem which is beyond the scope of the study. However, in the theoretical error calculation, random noise is one of the exciting signals. In order to facilitate this calculation, a practical procedure is to assume physically appropriate random noise processes as sources of excitation which are known to be associated with the class of problems. These noise processes have well-known statistics and are relatively easy to tract analytically. The three random processes which were described in Section 2.2 are likely candidates. These are the white noise (Gaussian) processes, First-Order Markoff or Butterworth and the Wiener Process. The first two are stationary random processes while the third is non-stationary.

The results of the theoretical error calculations will ultimately be compared to the measured results. Thus, the validity of the assumption as to the noise process will be measured. It is believed that only the stationary noise processes will be required. This belief can be substantiated from previous radar studies.

An integral part of the measurement program will be to establish the statistics of the noisy signals which are encountered. Typical noisy signals are the radar output signals (range, azimuth, and elevation) and the received signal. Given a signal which represents a desired signal plus noise, the noise characteristics must be known in order for the measured data to be useful. Four statistical parameters must be known in order to characterize the noise. These are the average value, mean-squared value, power-spectral density and/or calculation function. A by-product of the measurement of the average value and the mean-squared value is the determination of the stationarity of the process. Actually, if the average value and the mean squared value are time independent, the process can be said to be wide-sense stationary which is adequate for the present study. The power spectral density can be measured directly by standard laboratory analyzers. The correlation function is best obtained by calculation. The Fourier Integral of the power spectral density is the correlation function. The correlation function may be calculated directly from the measured time signals using the Tukey algorithms. The resulting parameters which characterize the measured random process can be used with the system to calculate a system error. The calculated theoretical calculations can be compared with the measured errors to obtain an evaluation of the system error. If the theoretical error calculated using the assumed noise model

agrees with experimentally allowed error variance, the measurement of the noise may not be necessary for the error calculations. On the other hand, if error smoothing is desired, then, the actual noise statistics must be known for the Wiener or Kalman-Bucy smoothing filter determination.

3.5 FIGURE OF MERIT

A figure of merit is usually a dimensionless quantity or a numeric which is used to compare the performance of a system against some standard. This quantity can be formulated in terms of principal parameters which describe the system functioning or evaluate the systems's output. Significantly, the figure of merit can concern itself only with those parameters which describe a particular aspect of the system performance being studied. For an example, assume that the azimuth angle output signal of a tracking radar is a sinusoid plus random noise. A physically meanful figure of merit can be variance of the signal voltage divided by the square of the mean value of the average of the output signal. This factor also can be considered the noise to signal ratio. Another figure of merit that is useful for some applications can be the signal correlation time divided by the signal bandwidth.

An objective of the system modeling study and the theoretical error calculation is the development of a suitable figure of merit. The quantity will be used to assign a value to an antenna pattern measurement which makes it possible to gage the utility of the measured pattern in terms of such quantities error of the system and the background noise. In addition, performance nomographs can be prepared with the figure-of-merit as a parameter. It may be useful to derive two figures-of-merit. One can be used as a measure of the system performance while, the second can be the measure of the measurement error.

4.0 SOFTWARE ERROR ANALYSIS

The Software Error Analysis will be concerned with two groups of errors which are as follows:

1. Data Processing Errors

2. Calculation Errors

Within the context of this study, data processing will consist of reading the various signal outputs, operating on the signals and feeding the processed signal into the computer input. The major sources of error in the data processing are the sampling errors and the synchronization errors.

Several of the output signals are analog types. These signal outputs are determined by taking time samples at specified time intervals. When dealing with time samples three sources of error present themselves.

Since some of the signals are imbedded in random noise, the statistical independence of the time samples and threshold setting used in the measurement must be determined. These considerations are especially important when considering the signal that represents the receiver power at the PAMS antenna. Time sample independence is determined from a knowledge of the autocorrelation function of the

random noise. The autocorrelation function of a noisy signal is determined from the noise power spectral density and the frequency bandwidth of the driving circuitry. The second consideration is the threshold setting which fixes the probability of error. This problem was discussed in PAMS Airborne Instrumentation, RADC-TR-74-174, Section II, 2.3.

An additional consideration is the sample size which is the number of time samples used to determine a data point. The number of samples should be sufficiently large to insure the statistical reliability of the results. Classic sampling algorithms are available for this determination.

The synchronization errors arise because the measured data is acquired in two processes. The Data Acquisition process collects data in real time from measurements made at the ground-based antenna platform, while the calibration process collects calibration and flight data in the moving vehicle. The Merge process combines this data for calculation of the antenna pattern. However, the time sampling intervals used in processing the signal strength data must be coherent with all the flight data. Any slip in the synchronization of the various signals manifests itself in an error in the resulting pattern. This problem can only be analyzed when the final system configuration is developed.

The second group of errors arise because of the numerical procedures used in the pattern calculations. The typical causes of calculation errors are round-off errors, overflow, use of single precision routines instead of double precision routines. The choice of a calculation routine is determined by the target system error and computer time required for calculation. The candidate routines usually represent a trade-off between the two factors. Ideally, the error introduced by the computations should be at least an order of magnitude less than the smallest component system error. This aspect of the computational error analysis will be relatively simple because the calculations under consideration are quite elementary.

5.0 CONCLUSION

A design for an error analysis of the PAMS Precision Antenna Measurement System was developed. The various errors were divided into two major groups which were system and dynamic errors. Within each group, two subgroups were defined. The errors which should be considered in the analysis were identified. In addition, the error measurement was discussed.

The calculation of the system error was delineated. The need and requirements for a system model was described. Also, the various considerations which are required for the model development was discussed. The theoretical error calculation, measured data analysis, error weighting, noise analysis and figure of merit was detailed. The analytical techniques that are appropriate were identified. Finally, the errors to be considered in the software error analysis were described.

APPENDIX NO. 1

VARIANCE OF COMPOUND ERRORS

The received signal, E_r, at the PAMS antenna can be assumed to depend on N variables. Functionally, the signal can be expressed as

$$\epsilon_r = \epsilon_o F(V_i) \qquad i = 1, \ldots, N$$

where the coordinate system is fixed at the receiving antenna. As an example the variables can be r, the slant range of the vehicle in respect to PAMS, θ, the azimuth angle, ϕ, the elevation angle, λ, the wavelength of the radiated signal, t_r, the receiver threshold, N_0, the noise power, and ϵ_2, a multipath function.

An error in ϵ_r can be expressed as

$$\Delta\epsilon_r = \sum_{i=1}^{N} \frac{\partial F}{\partial x_i} \Delta x_i \qquad \text{A-1}$$

where Δx_i are the errors in the independent variables. ϵ_o is normalized to unity.

In the system under consideration, the received signal should be defined in respect to a coordinate system fixed at the moving antenna. To obtain this result, it is necessary to transform the coordinate system from the PAMS antenna to the radiating antenna. Not all of the N independent variables are affected by a coordinate transformation. Such variables as wavelength, receiver threshold, etc. are independent of the coordinate system transformation.

Assume M of the N variables are transformable. Then equation A-1 can be rewritten as

$$\Delta\epsilon_r = \sum_{i=1}^{M} \frac{\partial F}{\partial x_i} \Delta x_i + \sum_{i=M+1}^{N} \frac{\partial F}{\partial x_i} \Delta x_i \qquad \text{A-2}$$

A coordinate transformation of the M variables can be written as

$$x_i = G_i (y_j) \qquad y=1, \ldots P$$

and

$$\Delta x_i = \sum_{j=1}^{P} \frac{\partial G_i}{\partial y_j} \Delta y_i \qquad \text{A-3}$$

Substituting into equation A-2 with the result

$$\Delta\epsilon_r = \sum_{j=1}^{P} \sum_{i=1}^{M} \frac{\partial F}{\partial x_i} \frac{\partial G_i}{\partial y_j} \Delta y_j + \sum_{i=M+1}^{N} \frac{\partial F}{\partial x_i} \Delta x_i \qquad \text{A-4}$$

Equation A-4 is the desired expression for the error in the measured received signal in terms of the errors in P variables which depend on the coordinate system selected and N-M variable which are independent of the coordinate system.

The variance of the received signal is expressed as

$$\sigma^2_{\Delta\epsilon_r} = E(\Delta\epsilon_r)^2 - \left\{ E(\Delta\epsilon_r) \right\}^2 \qquad \text{A-5}$$

where $E(\Delta\epsilon_r)^2$ is the mean or expectation of the square of the error and $E(\Delta\epsilon_r)$ is the mean of the error.

Then,

$$E(\Delta\epsilon_r) = \sum_{j=1}^{P} \sum_{i=1}^{M} \frac{\partial F}{\partial x_i} \frac{\partial G_i}{\partial y_j} E(\Delta y_j) + \sum_{i=M+1}^{N} \frac{\partial F}{\partial x_i} E(\Delta x_i)$$

The square of the error becomes

$$(\Delta\epsilon_r)^2 = \sum_{j=1}^{P} \sum_{i=1}^{M} \sum_{m=1}^{P} \sum_{\ell=1}^{M} \frac{\partial F}{\partial x_i} \frac{\partial G_i}{\partial y_j} \frac{\partial F}{\partial x_\ell} \frac{\partial G_\ell}{\partial y_m} (\Delta y_j)(\Delta y_m)$$

$$+ \sum_{j=1}^{P} \sum_{i=1}^{M} \sum_{r=M+1}^{N} \frac{\partial F}{\partial x_r} \frac{\partial F}{\partial x_i} \frac{\partial G_i}{\partial y_j} (\Delta y_j)(\Delta x_r)$$

$$+ \sum_{i=M+1}^{N} \sum_{i=M+1}^{N} \frac{\partial F}{\partial x_i} \frac{\partial F}{\partial x_j} (\Delta x_i)(\Delta x_j)$$

Rewriting

$$(\Delta \sigma_r)^2 = \sum_{j=1}^{P} \sum_{i=1}^{M} \left(\frac{\partial F}{\partial x_i} \frac{\partial G_i}{\partial y_j} \right) (\Delta y_j)^2$$

$$+ \sum_{\substack{j=1 \\ j \neq m,\ \ell \neq 1}}^{P} \sum_{L=1}^{M} \cdot \sum_{M=1}^{P} \sum_{\ell=1}^{M} \frac{\partial F}{\partial x_i} \frac{\partial G_i}{\partial y_j} \frac{\partial F}{\partial x_\ell} \frac{\partial G_\ell}{\partial y_m} (\Delta y_j)\ (\Delta y_m)$$

$$+ \sum_{i=M+1}^{N} \left(\frac{\partial F}{\partial x_i} \right)^2 (\Delta x_i)^2$$

$$+ \sum_{\substack{i=M+1 \\ i \neq j}}^{N} \sum_{j=M+1}^{N} \frac{\partial F}{\partial x_i} \frac{\partial F}{\partial x_j} (\Delta x_i)\ (\Delta x_j)$$

$$+ \sum_{j=1}^{P} \sum_{i=1}^{M} \sum_{r=M+1}^{N} \frac{\partial F}{\partial x_r} \frac{\partial F}{\partial x_i} \frac{\partial G_i}{\partial y_j} (\Delta y_j)\ (\Delta x_r)$$

Substituting into equation A-5 and rearranging, the desired result is obtained.

$$\sigma^2_{\Delta\epsilon_r} = \sum_{j=1}^{P}\sum_{i=1}^{M}\left(\frac{\partial F}{\partial x_i}\frac{\partial G_i}{\partial y_j}\right)^2 \sigma^2_{\Delta y_j} + \sum_{i=m+1}^{N}\left(\frac{\partial F}{\partial x_i}\right)^2 \sigma^2_{\Delta x_i}$$

$$+\sum_{j=1}^{P}\sum_{\substack{i=1\\ j\neq m,\ i\neq \ell}}^{M}\sum_{m=1}^{P}\sum_{\ell=1}^{M} \rho_{\Delta y_j \Delta y_m} \frac{\partial F}{\partial x_i}\frac{\partial G_i}{\partial y_j}\frac{\partial F}{\partial x_\ell}\frac{\partial G_\ell}{\partial x_m}\sigma_{\Delta y_j}\sigma_{\Delta y_m} \qquad \text{A-6}$$

$$+\sum_{\substack{i=M+1\\ i\neq j}}^{N}\sum_{j=M+1}^{N} \rho_{\Delta y_j \Delta x_j}\frac{\partial F}{\partial x_i}\frac{\partial F}{\partial x_j}\sigma_{\Delta x_i}\sigma_{\Delta y_j}$$

$$+\sum_{\substack{j=1\\ j\neq i}}^{P}\sum_{i=1}^{M}\sum_{r=M+1}^{N} \rho_{\Delta y_j \Delta x_r}\frac{\partial F}{\partial x_r}\frac{\partial F}{\partial x_i}\frac{\partial G_i}{\partial y_j}\sigma_{\Delta y_j}\sigma_{\Delta x_r}$$

Where the ρ are the correlation coefficients of the indicated pairs of the independent variable errors as indicated by the subscripts. The correlation coefficients varies from $-1 \leq \rho \leq 1$.

When each ρ is zero, the last three terms are zero for the case when all the independent variable errors are uncorrelated. It is reasonable to expect that the fourth term should normally be zero because it is highly unlikely that the errors in the independent variables that are dependent on the choice of coordinate system will be correlated to the variables independent on the particular coordinate system.

The number of variables that define equation A-6 is P+(N-M). Hence, the number of terms in equation A-6 is

$$\binom{V}{1} + \binom{V}{2} = \frac{V!}{(V-1)!} + \frac{V!}{2!\,(V-1)!} = V + \frac{V(V-1)}{2} = \frac{V^2+V}{2}$$

When all the variable errors are uncorrelated, the number of terms is V. If N=7, M=3, P=5 then V=8. The number of terms in equation A-6 becomes 36. It becomes apparent that variables must be carefully selected in order to keep the mathematics trackable.

APPENDIX III

SITE EVALUATION AND PROPAGATION ANALYSIS FOR THE PRECISION ANTENNA MEASUREMENT PROGRAM

This report presents results of a preliminary study performed by Atlantic Research Corporation for Actron to evaluate effects of the Precision Antenna Measurement System (PAMS) site and signal propagation on system performance. The scope of the study included a preliminary analysis of the site for the purpose of identifying potential sources of RF interference, and defining propagation effects which would affect performance of the PAMS. Potential sources of RF interference include emissions from communications, radar, and navigation systems operating in the vicinity of the Verona test site as well as possible contributions from power lines, automobile ignition systems or other significant incidental sources. Propagation effects which were considered include reflections from obstacles or terrain, signal blockage by obstacles or terrain, multipath effects, polarization, weather, ground constants, etc.

1.0 BACKGROUND

The Precision Antenna Measurement System (PAMS) provides the capability for dynamic measurement of airborne antenna radiation patterns or, alternatively, of the effective radar cross section of airborne vehicles. With the airborne antenna radiating, the aircraft follows a predetermined flight profile, aided and controlled as necessary via voice radio communications with the PAMS facility. The auxiliary radar continuously skin tracks or beacon tracks the aircraft and provides target range, azimuth, and elevation data to the PAMS equipment in real-time. The PAMS antennas, being slaved to the tracking radar, also track the aircraft and receive the emissions from the airborne antenna. Dynamic changes in the PAMS-to-aircraft viewing geometry will, if properly programmed, permit PAMS to observe all desired portions of the mainlobe and sidelobe structure of the airborne antenna's radiation pattern from measurements of the amplitude of the signal received at each viewing angle. The measured data is then merged or recombined as necessary during subsequent data reduction to produce the desired antenna pattern plots. The two auxiliary equipments enhance the overall utility of the PAMS system. The PAMS Airborne Monitoring System (AMS) is a pod-mounted instrumentation grouping which includes a two-gyro stable platform to monitor aircraft attitude. The attitude data, a timing reference, and altitude data are recorded by a digital tape recorder for post-flight merging with the ground-derived data. The availability of this additional data from the AMS has both operational advantages (e.g., eliminating the requirement for the pilot to closely control aircraft attitude) and pattern determination accuracy advantages. As will subsequently be discussed, PAMS can operate satisfactorily without AMS data, but flight pattern options are much more limited under these conditions plus the accuracy of the measurements is altered.

The second PAMS auxiliary equipment, the Airborne Signal Sources (AS^2) are used to excite airborne transmitting antennas and antennas which are a part of passive avionic systems and, therefore, normally do not radiate. The signal sources have a less direct bearing on aircraft flight profile selection than the

AMS. When employed, their principal impact is that the data acquisition rate (sampling rate) for PAMS may be affected in a manner that requires a lower aircraft flight velocity than might otherwise be used.

In order to utilize the PAMS most effectively, it is essential to know what limitations, operational constraints and degradation are imposed by the site and the resulting signal propagation. What is required in the present study is a rigorous analysis of the effects of the site and propagation on the overall operation of the PAMS, and a careful definition of the limitations resulting from the environment in the vicinity of the site.

2.0 RF ENVIRONMENT SITE SURVEY

All electrical and electronic equipments contribute to the PAMS total RF environment. Equipments such as communication, navigation and radar transmitters, which are intended to produce RF signals, are generally the most significant contributors to RF environment. However, there are numerous other sources such as power supplies, generators, electrical systems, switches, relays, digital checkout and control equipments, etc.

There are a number of active RF systems at Verona covering an extremely broad frequency spectrum. Figure 1 shows a site plan for the Verona Test Annex. Table I identifies the RF radiating equipments, indicates their location, and provides their approximate distance from PAMS. Actron has performed a preliminary analysis of the conditions of RF interference present at the PAMS site as a result of these RF systems. The results, which were based on free space propagation loss and RF alignment of the antennas associated with the potentially interfering source and PAMS, are shown in table II. Reference to table II indicates that some very large interfering signal powers (up to 68 dBm) are available at the input to PAMS and these signals must be considered in terms of the impact which these interfering signals will produce to PAMS. Such an investigation is beyond the scope of this preliminary study. Section 3 contains recommendations for a detailed evaluation of the effects of the RF environment on PAMS operation.

3.0 PROPAGATION ANALYSIS

Propagation considerations of interest include reflection from or blockage by objects or terrain surrounding the Verona site, propagation path loss, and multipath effects. Each of these are discussed below.

3.1 TERRAIN AND OBSTACLE REFLECTIONS AND SCREENING

The effects of terrain and other obstacles such as buildings, towers, etc, in the vicinity of the Verona site must be evaluated in terms of possible blockage or undesired reflections for either the FPS-16 or the PAMS. Signal blockage would result in a loss of signal which would be incorrectly interpreted as a null in the antenna pattern. In order to avoid this problem, it is necessary to define those regions of space in the vicinity of the Verona Site where blockage will occur, and avoid using them for antenna pattern measurements. Atlantic Research has a computer program which will be used to calculate line-of-site coverage (or alternately regions of signal reflection or blockage) as a function of range and

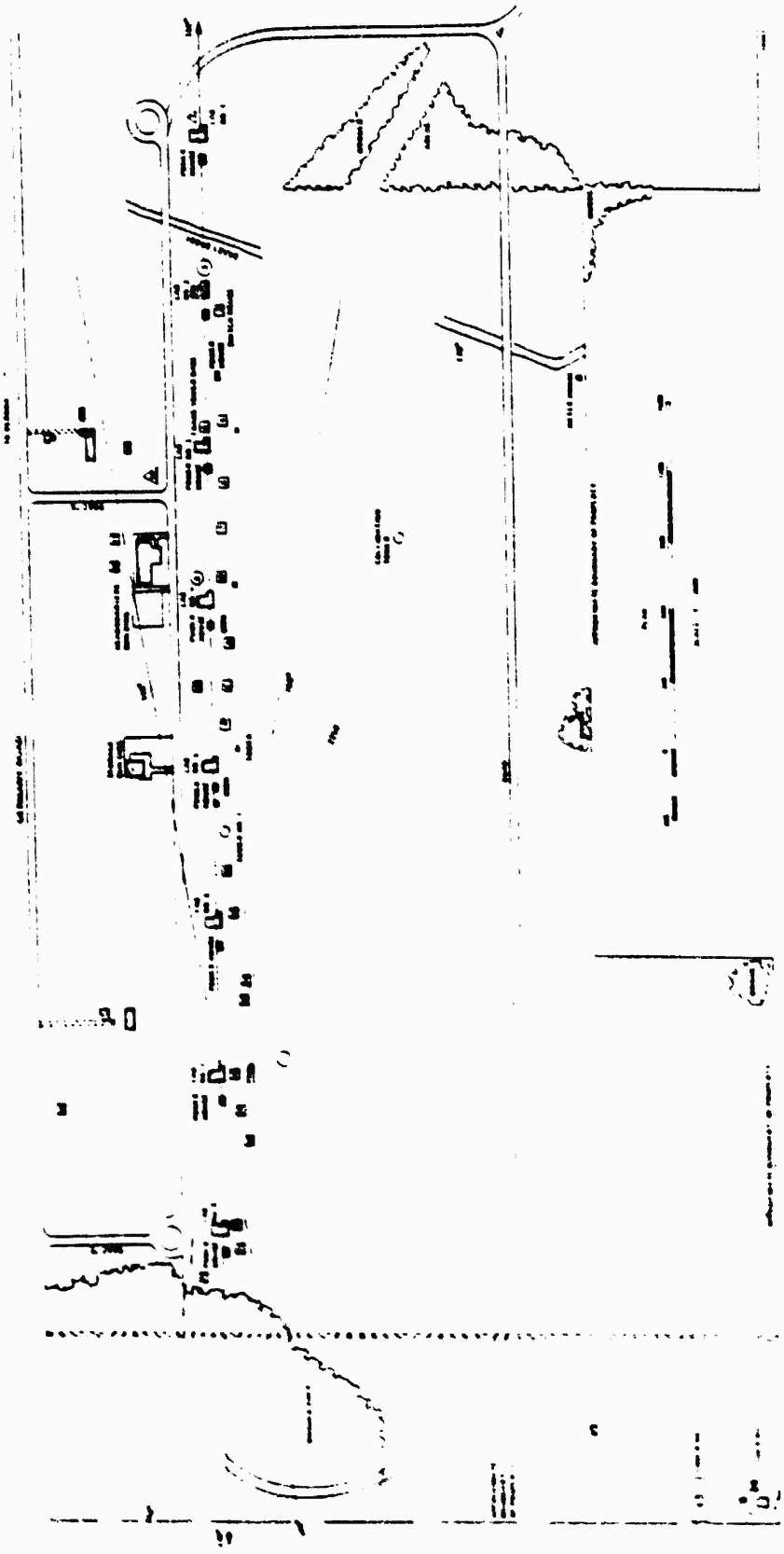

Figure 1. Plot Plan - Verona Test Annex

TABLE I. EMITTER LOCATIONS

Bldg.	Site	Emitter	Unit	Dist. to PAMS (ft)
1	1	1	FPS-74	4060*
	1	2	MRC-113	3260*
2	2	1	MRC-98	3410*
3	4	1	SPS-8	2810*
	5	1	SPS-30	2735*
	6	1	TPS-40/MPS-16	2530*
4	7	1	FPS-6	2215*
	8	1	FPS-65	2065*
	9	1	FPS-67	2095*
Hdqtrs.	10	1	URN-3	2220*
	11	1	GRC-27	2220*
	11	2	GRC-27	2220*
	11	3	GRC-27	2220*
	11	4	GRC-27	2220*
	11	5	GRC-27	2220*
	11	6	GRC-27	2220*
	11	7	GRC-27	2220*
	11	8	RT-723	2220*
	11	9	RT-723	2220*
	11	10	RT-723	2220*
Tower 1	12	1	K-Band	965
	12	2	Q-Band	965
6	13	1	FPS-16	640*
	11	1	SG1-B	400*
	15	1	HF XMTR.	156
7	16	-	PAMS	0
	17	1	MPQ-29	130*
	18	1	MSQ-1A	320*
	18	2	MSQ-1A	320*
8	19	1	TROPO	670*
	20	1	TROPO	605*
	21	1	SCR-584	770*
Tower 2	26	1	FRT-60	3000*
	26	2	S-Band Breadboard	3000*
	28	-	H.F. Trans. TWR	150
Mobile 1	30	1	**TPS-1D	4000*
Mobile 2	31	1	**TRAIL III	4000*
A	32	1	NIKE "X"	1450*
B	33	1	NIKE "X"	1695*
C	34	1	NIKE "S"	1570*

* Operate in the PAMS frequency range.
**These are mobile units - 4000 feet was assumed distance from the PAMS site.
Only those sites known to have an active source are listed.

TABLE II. BEACON EQUATION DATA OUTPUT

SITE	EMITT	PT(DBM)	PT(DBM/C)	GT(DB)	GR(DB)	F(DB/C)	R(DBFT)
1	1	44.2623	30.0000	28.00	29.50	68.9432	72.1705
4	1	57.3121	30.7918	37.00	31.50	70.8814	68.9741
5	1	65.7349	33.9794	42.00	31.50	70.8814	68.7391
6	1	56.3445	30.0000	42.00	29.00	74.4691	66.0624
7	1	68.5151	36.9897	40.00	29.50	68.9432	66.9075
8	1	61.3090	33.0103	36.00	23.00	62.2789	66.2984
9	1	60.1838	33.0103	35.00	23.00	62.2789	66.4237
10	1	7.6780	8.7506	7.50	21.70	61.2215	66.9271
11	1	-21.4336	-10.0000	.00	6.00	48.3826	66.9271
11	2	-22.4357	-10.0000	.00	6.00	49.3847	66.9271
11	3	-23.1417	-10.0000	.00	6.00	50.0921	66.9271
11	4	-23.7214	-10.0000	.00	6.00	50.6704	66.9271
11	5	-23.9925	-10.0000	.00	6.00	50.8714	66.9271
11	6	-24.7150	-10.0000	.00	6.00	51.6640	66.9271
11	7	-24.7951	-10.0000	.00	6.00	51.7047	66.9271
11	8	-20.4249	-16.0206	.00	6.00	41.8122	66.9271
11	9	-20.8936	-16.0206	.00	6.00	41.8263	66.9271
11	10	-21.9818	-16.0206	.00	6.00	42.9101	66.9271
13	1	68.2814	30.0000	42.00	29.50	74.9638	56.1236
14	1	62.4315	14.9897	25.50	30.00	69.6860	52.0412
17	1	56.5750	14.7712	35.00	30.00	78.7904	42.2789
18	1	65.1011	24.7712	35.00	29.50	68.9432	50.1030
19	1	57.2010	6.7712	21.00	6.00	49.6432	54.5215
20	1	54.0526	6.7712	34.00	32.00	77.9525	55.6351
21	1	57.4810	24.7712	33.00	29.50	68.9432	57.7295
22	2	44.5501	21.7712	34.00	30.50	69.5424	69.5424
40	1	39.6434	26.0206	27.00	23.00	62.2118	72.0412
41	1	23.8414	6.6242	18.00	32.50	75.9176	72.0412
42	1	52.5492	23.9794	43.00	30.00	79.0845	63.2274
43	1	51.1811	23.9794	43.00	30.00	79.0848	64.5834
44	1	52.6774	24.9897	30.00	31.50	70.3703	63.9180

elevation from a reference location. In order to utilize the program, it is necessary to specify the location and height of terrain and obstacles with respect to the reference locations. Figure 2 illustrates sample terrain contours and the corresponding computer type display which is provided by the Terrain Effects Routine. The figure represents a screening profile along a particular radial from a reference location. The clear area is free from reflections or blockage, whereas, the area indicated by X's is subject to reflections or blockage. It is recommended that a detailed study and evaluation be performed to determine the screening profiles.

3.2 MULTIPATH PROPAGATION

Another source of error for the PAMS results from multipath. For the purpose of this discussion, the term error is used to refer to the difference between the free space pattern of an antenna mounted on an aircraft, and the pattern of the same antenna/aircraft measured in the PAMS air/ground environment. It should be recognized that for many applications the PAMS environment is typical of an actual operating environment. In this case the PAMS variations from the free space pattern should not be regarded as errors but rather should be considered to be representative of actual operational performance. However, in order that results obtained with PAMS be correctly interpreted, it is important to be able to define the effects of multipath and other propagation abnormalities on the antenna patterns. The types of multipath which must be considered result from specular and diffuse reflections from the ground and other nearby objects; and from distant terrain features such as hills, etc. Figure 3 illustrates the problem and defines the parameters of interest.

Referring to figure 3, the following relationships exist:

$$d = d_1 + d_2 = d_1 + \frac{h_2}{h_1} d_1 \tag{1}$$

$$d_1 = \frac{d}{1 + \frac{h_2}{h_1}} \tag{2}$$

$$\tan \gamma = \frac{h_1}{5280\ d_1\ \text{miles}} \tag{3}$$

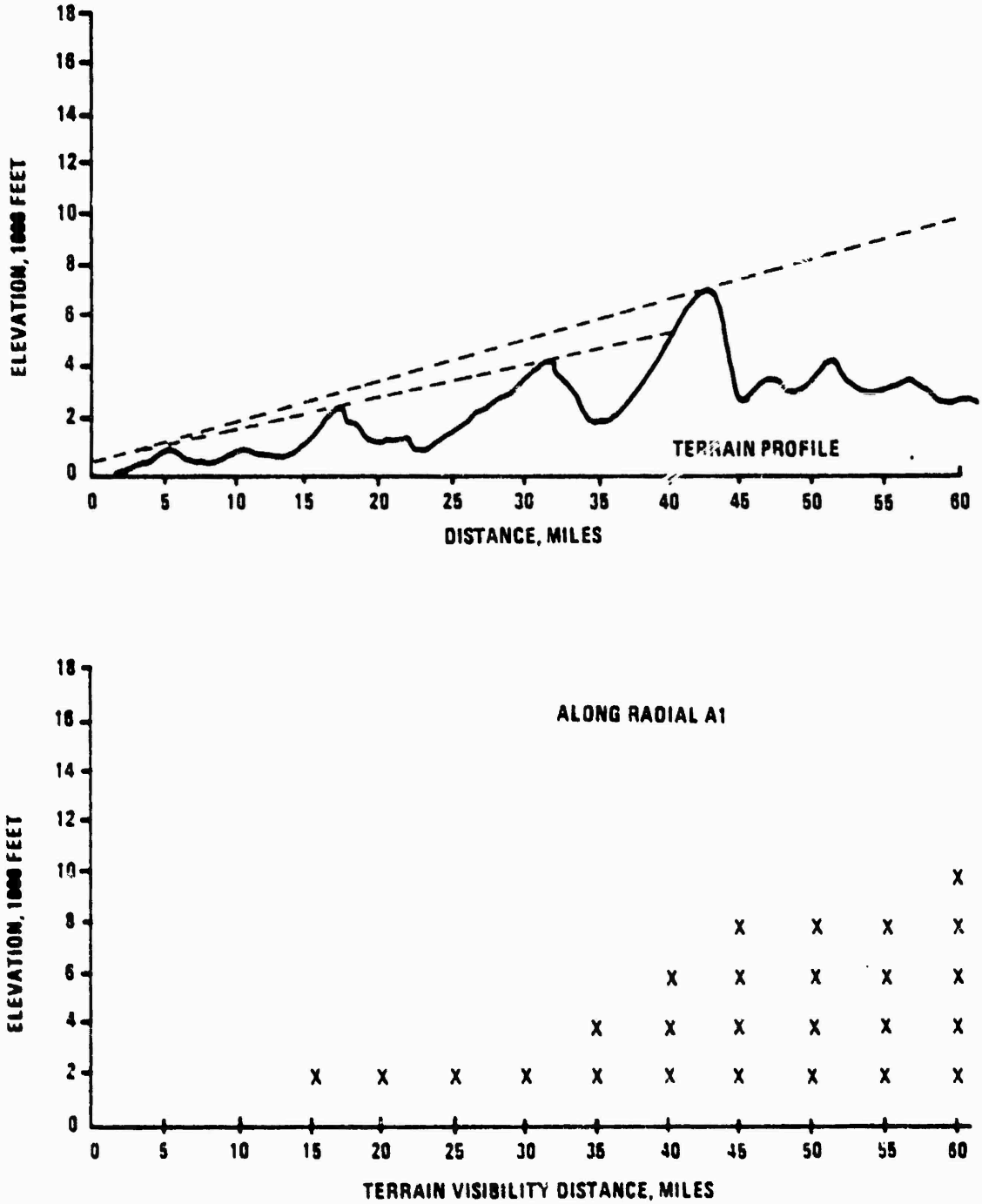

Figure 2. Output Display of Range Terrain Effects Routine

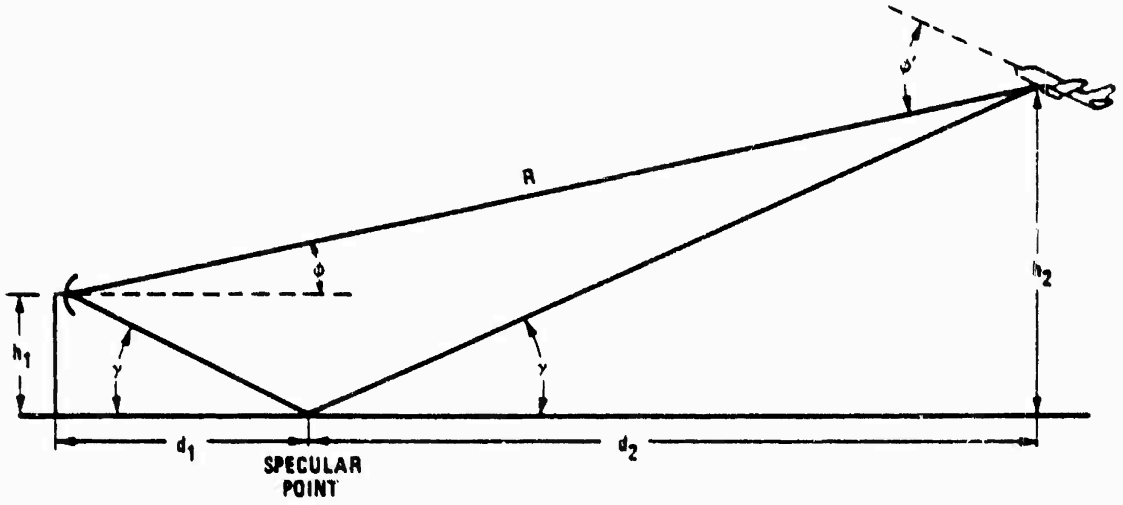

Figure 3. System Geometry

For a plane surface, specular reflection will occur for grazing angles such that (1)

$$\tan \gamma \geq \frac{0.01777}{(f_{MHz})^{1/3}} \tag{4}$$

This condition will be satisfied for many conditions of interest for the PAMS.

Because the reflected signal has traveled over a greater distance, it is delayed more than the direct path. The path length difference, expressed in degrees at a given frequency (f MHz) is given by

$$\phi = \frac{1.385 \times 10^{-4} \; h_1 h_2 \; f \; \text{MHz}}{d \; \text{miles}} \tag{5}$$

The reflected signal will combine with the direct signal, and the relative phase will depend on specific geometry. The resultant signal level will vary with aircraft position, and a moving aircraft will produce modulation on the signal. In general, nulls resulting from multipath fading will be spaced at least one-half wavelength apart.

The model for multipath propagation as depicted by figure 3 assumes that a single ray is propagated from the source and the earth's reflecting surface is flat. Actually, a bundle of rays is propagated from the source. Since the rays leave the source at different angles, a divergence or spreading of the rays result. This

effect increases with increasing distance. Since the rays are incident upon the convex side of the earth's spherical surface, additional divergence occurs because of the curvature of the surface.

The divergence factor D can be calculated from geometric considerations, figure 3-A. The factor D compares the density of the rays in a small cone reflected from the spherical earth near the principal point of reflection with the density that rays of the same cone would have if they were reflected from a plane reflector at the same point. The field strength is proportional to the square root of the ray density. Actually, D is the square root of the ratio cross section of the cone after reflection from a plane to the cross section of the cone after reflection from the sphere.

The divergence factor D is

$$D \approx \frac{1}{\sqrt{1 + \frac{2r_1 r_2}{a\,(r_1 + r_2)\sin\phi_2}}}$$

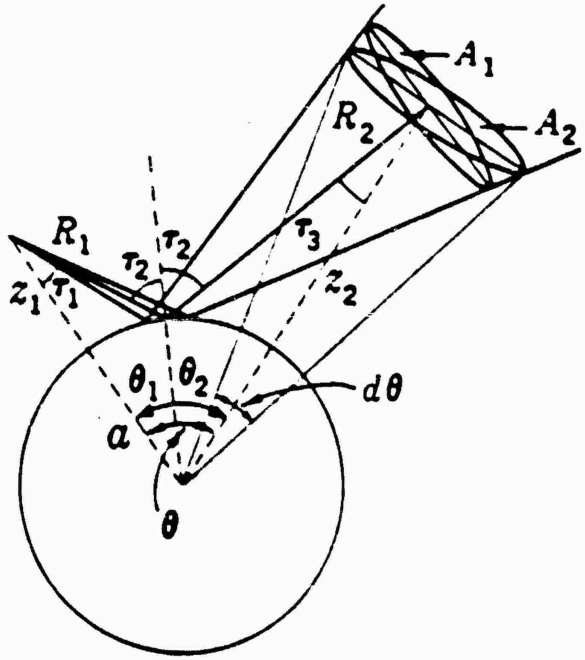

Figure 3-A. Geometry for the Divergence Factor D

Geometry for the Divergence Factor D

$$A_1 = (R_1+R_2)^2 \sin \tau_1 \, d\tau_1 \, d\phi$$

$$A_2 = (a + z_2)^2 \sin \theta \cos \tau_3 \, d\theta \, d\phi$$

$$D = \sqrt{\frac{A_1}{A_2}} \approx \frac{1}{\sqrt{1 + \frac{2r_1 r_2}{a(r_1 + r_2)\sin \phi_2}}}$$

$$R_1 = (a + z_1) \cos \tau_1 - a \cos \tau_2$$

$$R_2 = (a + z_2) \cos \tau_3 - a \cos \tau_2$$

$$d\theta = \frac{\partial \theta}{\partial \tau_1} d\tau_1$$

$$\psi_2 = \frac{\pi}{2} - \tau_2$$

$$\frac{z_1}{a} = \frac{z_2}{a} \ll 1$$

$$a \sin\theta \approx a\theta \approx (R_1+R_2)$$

$R_1 \sim r_1 \quad R_2 \sim r_2 \quad r_1$ and r_2 are ground ranges

The symbols and necessary assumptions are defined in figure 3-A. This factor is unity at high grazing angles ϕ_2 and decreases to zero as ϕ_2 decreases. This factor becomes important at small angles, low heights of source and receiver and short ranges.

At microwave frequencies, it is not valid to treat the earth as a plane reflecting surface; rather the rough character of the earth's surface must be taken into account. A sizeable literature has grown up around the problem of scattering of electromagnetic waves from rough surfaces and numerous models are available.

The effective roughness of a surface to a reflected wave depends on the surface height variance σ_g^2, wavelength λ and the grazing angle γ. The Rayleigh criterion, which may be used to specify surface roughness, is defined as:

$$g = \frac{4\pi\sigma_g}{\lambda} \sin\gamma. \tag{6}$$

For $g \ll 1$ the surface is considered smooth.
For $g \gg 1$ the surface is considered rough.

It has been firmly established both theoretically and experimentally that two distinct components arise from rough surface reflection - a specular component and a diffuse component. The specular component behaves much like mirror reflection at a point being predominant when $g \ll 1$ and being coherent and very slowly fading. Most of the energy contributing to the specular component is reflected from within the first few Fresnel zones surrounding the specular point. The diffuse component consists of energy reflected over a relatively wide area of the surface. It predominates for $g \gg 1$. For the parameters of interest both components are important.

The direct path component is obtained from the radar range equation. The received power is:

$$P_D = \frac{P_T G_T G_R \lambda^2}{(4\pi R)^2 L(R)} = \frac{1}{2} E_D^2 \tag{7}$$

where:

P_T = transmitted power

G_T = transmitted antenna gain

G_R = receiver antenna gain

λ = wavelength (meters)

R = distance between transmitting and receiving antennas (meters)

$L(R) = e^{-\alpha R}$ attenuation loss

E_D = received signal amplitude

Considering horizontal and vertical polarization separately:

$$P_D^H = \frac{P_T \lambda^2 G_T^H(\theta,\phi)\ \left[G_R^H(\theta';\phi')\cos^2\alpha_R + G_R^V(\theta';\phi')\sin^2\alpha_R\right]}{(4\pi R)^2\, L(R)} \tag{8}$$

$$P_D^V = \frac{P_T \lambda^2 G_T^V(\theta,\phi)\ \left[G_R^H(\theta';\phi')\sin^2\alpha_R + G_R^V(\theta';\phi')\cos^2\alpha_R\right]}{(4\pi R)^2\, L(R)}$$

where:

P_D^H = direct path power received with horizontal polarization.

P_D^V = direct path power received with vertical polarization.

$G_T^H(\theta,\phi)$ = transmitting antenna gain for horizontal polarization.

$G_T^V(\theta,\phi)$ = transmitting antenna gain for vertical polarization.

$G_R^H(\theta';\phi')$ = receiving antenna gain for horizontal polarization.

$G_R^V(\theta';V')$ = receiving antenna gain for vertical polarization.

The total direct signal power is

$$P_D = P_D^H + P_D^V. \tag{10}$$

Following Beckmann and Spizzachino[2], the specular component is introduced by multiplying the standard Fresnel reflection coefficients Γ_0^H, Γ_0^V for reflection from a plane surface by a specular coefficient ρ_S, where:

$$\rho_S = \exp\left\{-\frac{1}{2}\left(\frac{4\pi\sigma_R}{\lambda}\sin\gamma\right)^2\right\} = e^{-g^2/2} \tag{11}$$

At microwave frequencies, the ground conductivity (typically $\sigma > 10^{-3}$mho/m) is negligible so that Fresnel coefficients for dielectric media are acceptable[3] and

$$\Gamma_O^H = \left| \frac{\sin\gamma - (\epsilon/\epsilon_O - \cos^2\gamma)^{1/2}}{\sin\gamma + (\epsilon/\epsilon_O - \cos^2\gamma)^{1/2}} \right| \tag{12}$$

$$\Gamma_O^V = \left| \frac{\epsilon/\epsilon_O \sin\gamma - (\epsilon/\epsilon_O \cos^2\gamma)^{1/2}}{\epsilon/\epsilon_O \sin\gamma + (\epsilon/\epsilon_O \cos^2\gamma)^{1/2}} \right| \tag{13}$$

where ϵ is the ground dielectric constant.

If operation over seawater is to be considered, appropriate modifications in the Fresnel reflection coefficients must be made.

The received specular signal amplitude is given by

$$E_S = \rho_S \Gamma_O^H B_S^H + \rho_S \Gamma_O^V B_S^V \tag{14}$$

where

B_S^H = horizontal component signal level not including reflection effects

$$= \left[\frac{2P_T \lambda^2 G_T^H(\theta,\gamma) \left[G_R^H(\theta';\gamma') \cos^2\alpha_R + G_R^V(\theta';\gamma') \sin^2\alpha_R \right]}{(4\pi R_S)^2 L(R_S)} \right]^{1/2} \tag{15}$$

B_S^V = vertical component signal level not including reflection effects

$$= \left[\frac{2P_T \lambda^2 G_\Gamma^V(\theta-\gamma) \left[G_R^H(\theta';V') \cos^2\alpha_R + G_R^V(\theta';\gamma') \sin^2\alpha_R \right]}{(4\pi R_S)^2 L(R_S)} \right]^{1/2} \tag{16}$$

R_S = specular path length

$$= R\left[1 + \frac{4h}{R}\left(\frac{h}{R} + \sin\phi\right)\right]^{1/2}$$

γ = wave grazing angle

$$= \tan^{-1}\left[\frac{h - R\sin\phi}{R\cos\phi}\right]$$

h = transmitting antenna height

R = direct path length

ϕ = aircraft elevation angle.

The differential time delay, τ_S, relative to the direct path component is just

$$\tau_S = \frac{R_S - R}{C} = \frac{R}{C}\left\{\left[1+\frac{4h}{R}\left(\frac{h}{R}+\sin\phi\right)\right]^{1/2}-1\right\}. \tag{17}$$

The differential Doppler shift, $\delta\omega_o$, on the carrier frequency is

$$\delta\omega_o = \frac{\dot{R}}{C}\sin(\gamma-\phi)\,\omega_o. \tag{18}$$

where

$\dot{R}$ = $\frac{dR}{dt}$ = change of range with time or range rate

C = speed of light = 3×10^8 meters/second

ω_o = carrier frequency in radians per second.

Analysis of the diffuse component is complicated by the fact that a large area of the scattering surface participates in the reflection process and the antenna gain patterns can vary considerably over this area. Approximate calculations have been performed by Staras[4] and Bello[5] based on the assumptions:

- Specular point is much closer to the receiver than to the transmitter ($d_2 \gg d_1$ in figure 3)
- antenna gain patterns do not vary appreciably over the reflecting surface
- surface is rough, $g \gg 1$
- elevation angle, ϕ, much larger than R.M.S. surface slope.

The first two assumptions are reasonably well satisfied by the PAMS. However, the last two assumptions may be violated much of the time. The results of these calculations show that the ratio of diffuse component power, N_D, to direct component power, P_D, is

$$\frac{N_D}{P_D} = \left|\Gamma_o\right|^2 \frac{G_T(\theta,-\gamma)G_R(\theta',\gamma')}{G_T(\theta,\phi)G_R(\theta',\phi')} \tag{19}$$

That is, except through dependence on Γ_o, N_D/P_D is independent of λ, γ, and g. This has been confirmed experimentally[6].

It is necessary to make some modification so that the model can be used at small g and γ. It is known that the diffuse component vanishes as g approaches zero and varies roughly as the inverse of the specular component at small g(6). Therefore, we introduce a diffuse coefficient ρ_D similar to ρ_S given by

$$\rho_D = \exp\left\{-\frac{1}{2}\left(\frac{\lambda}{4\pi\sigma_g \sin\gamma}\right)^2\right\} = e^{-1/2g^2} \tag{20}$$

For this case, it may be possible to approximate the diffuse component power by the following expression:

$$N_D = \frac{\rho_D}{2}\left|\Gamma_O^H\right|^2 (B_S^H)2 + \frac{\rho_D}{2}\left|\Gamma_O^V\right| 2\ (B_S^V)^2 \tag{21}$$

It should be noted that this calculation is based on the Kirchoff approximation and ignores the effects of multiple scattering and depolarization.

In order to see the effect of multipath on the received signal it is necessary to look at the signal format in more detail. If the general case of AM and FM modulation is considered, the direct path signal, $S_D(t)$; has the form:

$$S_D(t) = E(t) \sin\left\{\omega_o t + \beta \sin\left[\omega_m(t)\, t\right]\right\} \tag{22}$$

where:

ω_o = carrier frequency

$\omega_m(t)$ = $\omega_1 + St$ = instantaneous modulation frequency

ω_1 = modulation frequency

S = frequency sweep rate

β = modulation index (nominally = 1)

E(t) = envelope function

Now consider a multipath signal $S_M(t)$ of the form

$$S_M(t) = A\, S_D\left(t - \frac{\delta R(t)}{c}\right)$$

where

A = attenuation factor

$\delta R(t) = R_O + Vt$ = differential path length relative to direct path component

R_O = differential range

V = differential range rate

Using this in Equation (22) gives

$$S_M(t) = AE(t\,(1-V/C)-\tau) \times \sin\Big\{(\omega_o' t-\omega_o \tau) + \beta \sin\Big[(\omega_1 t(1-V/C)-\omega_1 \tau)+S\Big[(t-\tau)^2 - 2V/C(t-\tau)\,t + (V^2/C^2)t^2\Big]\Big]\Big\}$$

where

$\tau = R_O/C$ = delay time

$\omega_o' = \omega_1(1-V/C)$ = Doppler shifted carrier

If V/C is taken as zero except when multiplied by the carrier frequency, this is simplified to

$$S_M(t) = AE(t-\tau) \sin\Big\{(\omega_o' t-\omega_o \tau) + \beta \sin\Big[\omega_1+S(t-\tau)\Big]\,(t-\tau)\Big\} \tag{23}$$

There remains a time delay, τ, in the envelope, an RF phase shift, $\omega_o \tau$, on the carrier, a Doppler shift, $\delta\omega_o = \omega'\omega_o$, on the carrier, a shift in the modulation frequency, $S(t-\tau)$, and a time delay, τ, on the modulation.

This is still quite a complicated function. If one attempts to add Equation (23) to Equation (22) and express the resultant as an envelope and phase, the result is a completely unmanageable expression. However, for the specular ground-reflection component, the differential Doppler shift is quite small, $\delta\omega_o \approx 5$ Hz to 100 Hz, and the time delay is restricted to $\tau < 0.1$ microsecond. In particular, for the geometry shown in figure 3 with $h_1 = 10$ m, $R = 1$ km, $\phi = 0.1$ rad, $R = -100$ knots = -500 m/sec and $\omega_o = 5$ GHz, then $\tau = 73$ nanoseconds and $\delta\omega_o = 25$ Hz.

For the specular case and $\beta = 1$, Equation (23) further simplifies to

$$S_S(t) = AE(t) \sin \left\{ \omega_o' t - \omega_o \tau + \sin\left[\omega_1 (t-\tau)\right] \right\} \tag{24}$$

This can now be combined with Equation (22) to give the resultant $S_R(t)$:

$$S_R(t) = S_D(t) + S_S(t) = A(t) \sin\ \omega_o t + \phi_R(t) \tag{25}$$

where:

$A(t)$ = envelope of the resultant

$\phi_R(t)$ = phase of the resultant.

The envelope can be calculated and is

$$A(t) = E_D(t) \left\{ 1 + A^2 + 2A\cos\left[\delta\omega_o t - \omega_o \tau - z\cos(\omega_1 t - \omega_1 \tau/2)\right] \right\}^{1/2} \tag{26}$$

where:

A = attentuation factor shown in Equation (24)

$z = 2\sin(\frac{\omega_1 \tau}{2})$.

For the specular component with $\tau = .1$ microsecond and $\omega_1 = 100$ kHz, $z = 0.01$ and the expression for $A(t)$ reduces to

$$A(t) = E_D(t) \left[1 + A^2 + 2A\cos(\delta\omega_o t - \omega_o\ )\right]^{1/2}$$

and the resultant envelope is distorted by the function

$$\left[1 + A^2 + 2A\cos\ (\delta\omega_o t - \omega_o\ )\right]^{1/2}$$

It should be emphasized that the approximations used in obtaining Equation (24) are no longer valid, if τ is larger than a few microseconds. Although an analytic expression is not available for the resultant of a direct path signal plus a long time delayed multipath, it is possible to get a rough idea of the nature of such a signal. The envelope will be roughly the superposition of $E_D(t)$ with $AE_D(t-\tau)$. For the times during which both signals are present, there will be beats at the difference between the two modulation frequencies, $\omega_1(t) - \omega_1(t-\tau) = S\tau$. In addition, while both signals are present, all of the effects occurring in Equation (26) will appear (i.e., beats at the Doppler frequency δW, and RF phase shift $\omega_o \tau$, and a sinusoidal amplitude modulation at the modulation frequency, ω_1).

The analysis presented above demonstrates that the problem of modeling multipath is a formidable task. In order to avoid some of the obvious complexities inherent in modeling multipath, but on the other hand not to simplify the problem out of existence, the following assumptions and considerations were made.

- Ray theory is valid. This is somewhat true if we can assume that the reflecting surface is large and leads to specular reflections.
- The effects from discrete multipath are present only in certain regions in space that are defined by the particular geometry.
- No diffuse reflections take place.
- There is only one significant multipath component.

If the above assumptions are made, the vector diagrams as shown in figure 4 can be constructed where:

E_D = resultant field

E_O = free-space field

E_R = reflected field

θ = path length difference

ψ = phase shift encountered by the ray upon reflection from the earth.

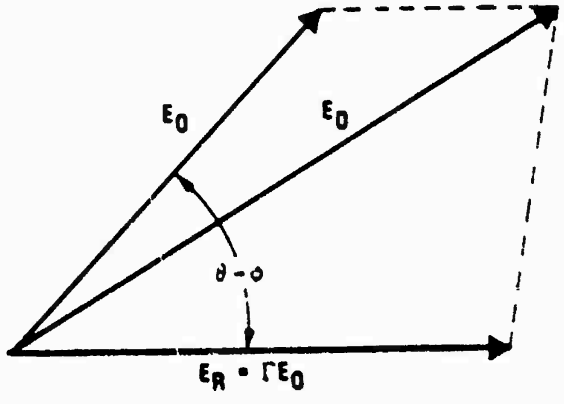

Figure 4. Vector Diagram of Ground - Reflected Multipath

From the vector diagram the ratio of the resultant field to the free-space is given by:

$$g(\theta) = \frac{E_D}{E_O} = \sqrt{1 + \Gamma^2 + 2\Gamma \cos(\theta - \psi)} \tag{27}$$

where

Γ = absolute value of the reflection coefficient.

The reflection coefficient is given by

$$\Gamma e^{j\psi} = \frac{N^2 \sin\gamma - N^2 - \cos^2\gamma}{N^2 \sin\gamma + N^2 - \cos^2\gamma} \tag{28}$$

where

γ = the grazing angle and

$N^2 = e_r - j\frac{\sigma}{\omega e_O}$

When ground reflections do not take place $E_D = E_O$ and $g(\theta) = 1$

If the multipath propagation results from a large discrete object such as a building, the result will be a region in space where the multipath effects are experienced as illustrated in figure 5. As long as the assumptions provided above are satisfied, Equation 27 can also be used to determine the ratio of the resultant field to the free-space field for the discrete multipath problem.

For the PAMS, the errors resulting from multipath are directly related to the parameter $g(\theta)$. The following paragraph presents a discussion of the errors which can result for various configurations.

The effects of two path propagations can have a significant influence on the apparent pattern of an antenna used in air-to-ground applications. For example, figure 6 shows an experimental radiation pattern for a half-wave vertical dipole used for UHF air-to-ground communication over sea water. The presence of lobes and nulls is obvious and multipath conditions such as those shown in the figure could result in significant errors in the measurement of antenna patterns.

The errors which result will depend on the specific flight path used in the test. For example, figure 7 shows the variations in received signal which result from an aircraft flying a radial path at a constant altitude. Reference to this figure

From the vector diagram the ratio of the resultant field to the free-space is given by:

$$g(\theta) = \frac{E_D}{E_O} = \sqrt{1 + \Gamma^2 + 2\Gamma \cos(\theta - \psi)} \tag{27}$$

where

Γ = absolute value of the reflection coefficient.

The reflection coefficient is given by

$$\Gamma e^{j\psi} = \frac{N^2 \sin\gamma - N^2 - \cos^2\gamma}{N^2 \sin\gamma + N^2 - \cos^2\gamma} \tag{28}$$

where

γ = the grazing angle and

$N^2 = e_r - j\frac{\sigma}{\omega e_O}$

When ground reflections do not take place $E_D = E_O$ and $g(\theta) = 1$

If the multipath propagation results from a large discrete object such as a building, the result will be a region in space where the multipath effects are experienced as illustrated in figure 5. As long as the assumptions provided above are satisfied, Equation 27 can also be used to determine the ratio of the resultant field to the free-space field for the discrete multipath problem.

For the PAMS, the errors resulting from multipath are directly related to the parameter $g(\theta)$. The following paragraph presents a discussion of the errors which can result for various configurations.

The effects of two path propagations can have a significant influence on the apparent pattern of an antenna used in air-to-ground applications. For example, figure 6 shows an experimental radiation pattern for a half-wave vertical dipole used for UHF air-to-ground communication over sea water. The presence of lobes and nulls is obvious and multipath conditions such as those shown in the figure could result in significant errors in the measurement of antenna patterns.

The errors which result will depend on the specific flight path used in the test. For example, figure 7 shows the variations in received signal which result from an aircraft flying a radial path at a constant altitude. Reference to this figure

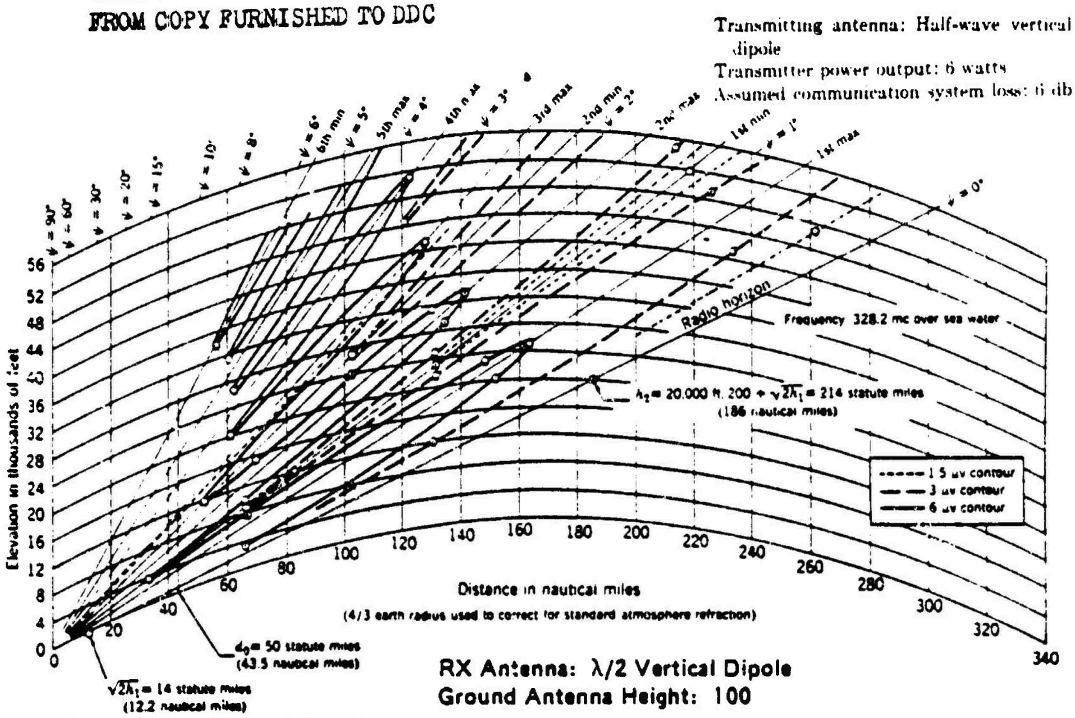

Theoretical UHF Radiation Patterns

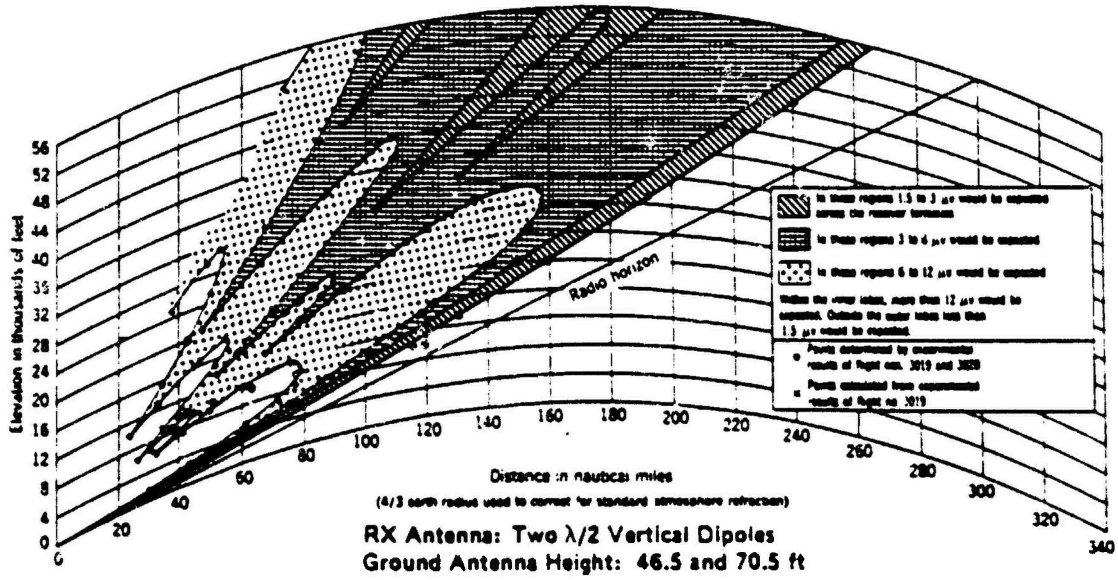

Experimental UHF Radiation Patterns

Figure 6. UHF Radiation Patterns

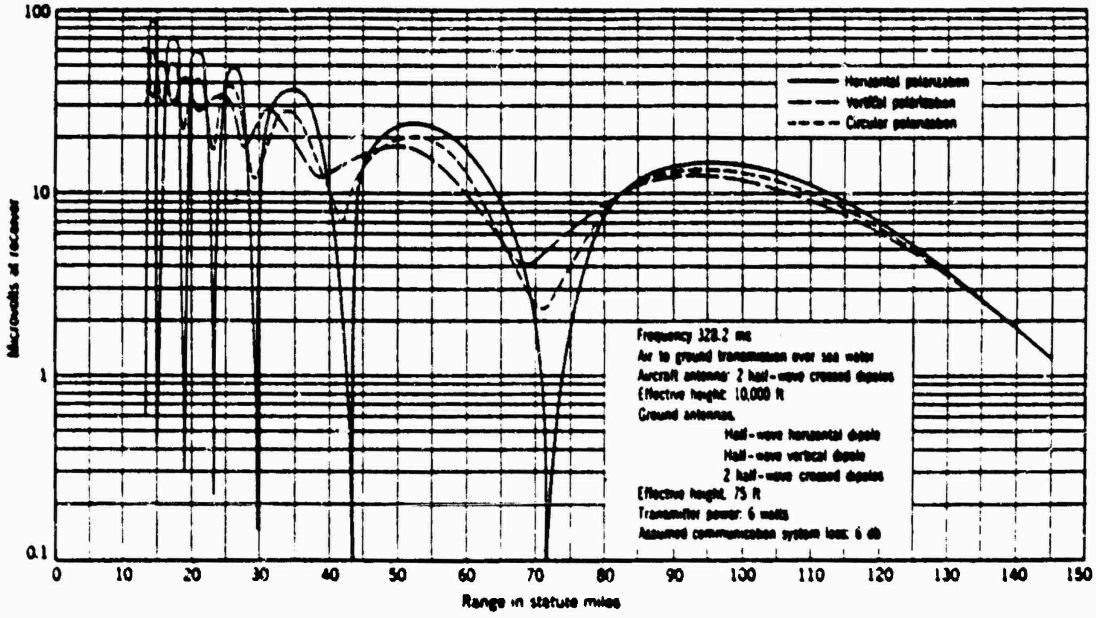

Theoretical Comparison of UHF Patterns

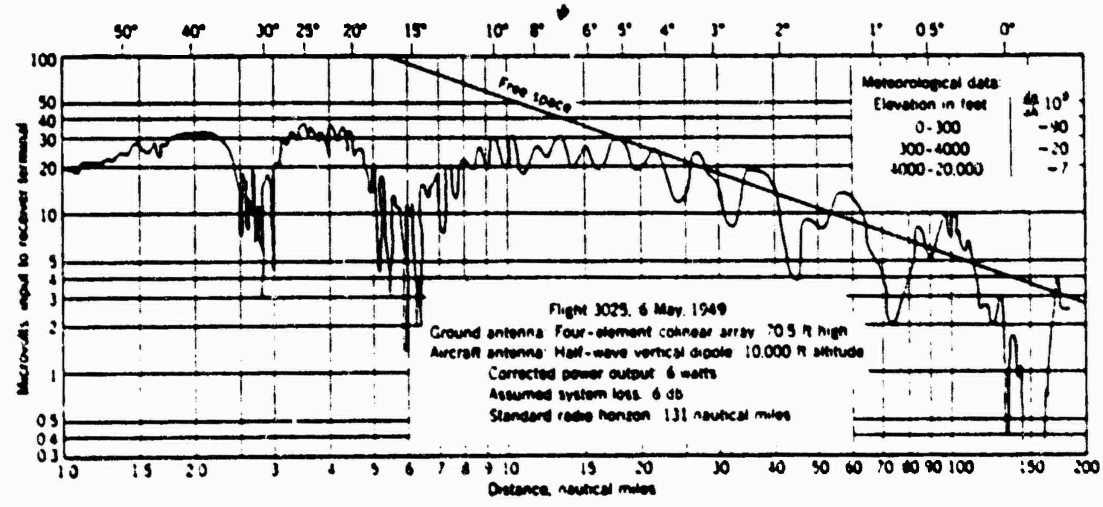

Experimental UHF Pattern Over Sea Water

Figure 7. UHF Multipath Signal Variations

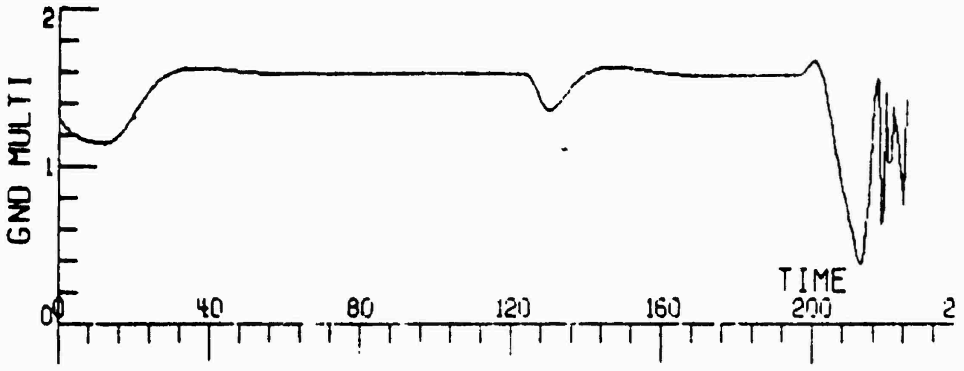

Ground Multipath Maximum = 0.05°, Discrete Multipath Maximum = 0.25°

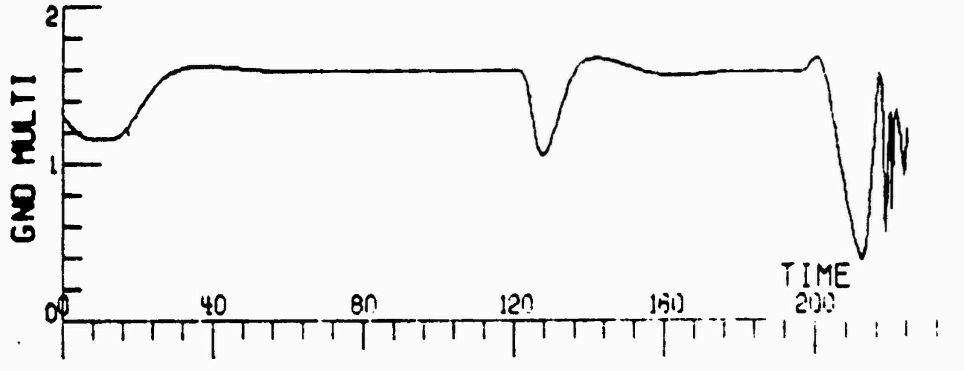

Ground Multipath Maximum = 0.12°, Discrete Multipath Maximum = 0.25°

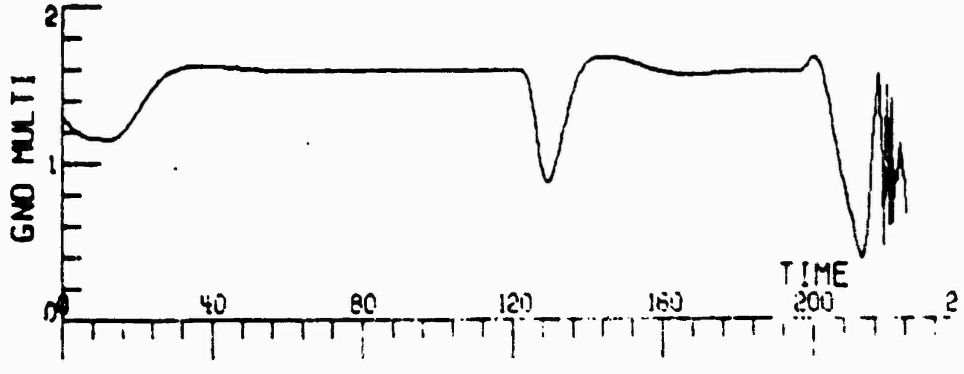

Ground Multipath Maximum = 0.075°, Discrete Multipath Maximum = 0.5°

Figure 8. Effects of Ground and Discrete Multipath

and surface are necessary so that the multipath channel may be simulated by digital computer. The simulation is, in turn, necessary for comparison to experimental data for verification of the model. The geometry of the situation is modeled deterministically; the resulting error characteristics are described in statistical terms. The use of statistical means and probability distributions brings up a point on the general use of statistical methods. Very often the use of statistical methods is viewed as an inability to solve a problem "exactly." In fact the opposite is true. A random quantity can be considered as found when not only its mean value but the entire probability distribution about this mean value is known. In certain rare and usually idealized cases this probability distribution is such that the mean value is, in the limit, the only value the quantity may assume and in this case the quantity is no longer random. In this special case of a single value instead of an entire distribution, we have a (so-called) "exact" solution; this is of course much easier to find than the statistical solution which includes the exact solution as a special case. From this point of view the two opposites are not "statistical" and "exact solution," but "general, statistical solution" and "idealized limited case."

In the multipath environment it is very often possible to make simplifying assumptions which will lead to tractable mathematical models. In lieu of experimental data one must reason "a priori" and derive the autocorrelation function which is defined as

$$R_X(\tau) = \text{Lin}\ \frac{1}{2T}\int_{-T}^{T} X(t+\tau)X(t)dt \tag{29}$$

If experimental data is available on the time history of the error it is possible to derive the power spectral density (using Fast Fourier Transform techniques) and then to approximate it by a meromorphic function so that the autocorrelation function can be derived. If the error sources are to be used in a real-time computer simulation the autocorrelation function can be used to determine the "whittening-filter." The basic idea of the procedure is to calculate the transfer function of a linear filter which would convert white noise into noise with the specified correlation function and then to use the transfer function of the linear filter expressed as a recursion relationship to compute the discrete errors. The filter, in order to generate a stationary random output, must be operating in the "steady state" i.e., it must have had an input of white noise for all $n \geq -\infty$. However, for computational purposes the input sequence must begin at n=0. Therefore the correct "initial conditions" must be derived so that the covariance matrix is the same as if the filter were operating in the steady state. This method while not only being an accurate method for generating random errors is also computationally efficient since the errors are computed recursively.

Every effort should be made to accurately model the electromagnetic wave in space, both the direct and reflected components. In simple cases, the geometric optics method may be valid for the problem. Very often, however, the physical optics

approach based on a solution of the wave equation will have to be used. However an exact solution of the wave equation for an actual problem is usually so difficult that it is impractical, therefore approximation methods must be used.

By modeling the multipath geometry and electromagnet wave accurately the resulting errors can be derived and simulated on a digital computer. This approach involves a deterministic evaluation of the geometry and wave in order to derive the stochastic error sources.

4.0 CONCLUSIONS

Results of the preliminary study presented in this report indicate that electromagnetic interference (EMI) could result in significant errors (20 dB or more) in the PAMS measurements. These errors will be a function of both frequency and direction and could result in apparent lobes at specific frequencies and directions. If the electromagnetic environment existing at the PAMS site is known, errrors resulting from EMI can be easily avoided by proper selection of test frequencies and flight profiles.

Propagation effects resulting from terrain or obstacle reflections or screening can also result in significant effects on PAMS measurements. Multipath propagation conditions can produce variations, which may be on the order of 20 dB, from the free space pattern. Although propagation effects are significant, it is emphasized that they are typical of operational conditions. Therefore, what is required is a "calibration" of the propagation effects in different flight test areas around the PAMS site so that the results obtained may be properly interpreted.

5.0 REFERENCES

1. RCTA report, A New Guidance System for Approach and Landing, Vols. 1 and 2, December 18, 1970.

2. Beckmann, P. and Spizzachino, A., The Scattering of Electromagnetic Waves from Rough Surfaces, Macmillan Co., New York, 1963.

3. Stratton, J.A., Electromagnetic Theory, McGraw-Hill, New York, 1941.

4. Staras, H., Rough Surface Scattering on a Communication Link, Rad. Sci., Vol. 3 (new series), June 1968.

5. Bello, P.A., Aeronautical Channel Characterization, IEEE Trans. on Communications, COM-21, 5 May 1973.

6. Barton, D.K., and Ward, H.R., Handbook of Radar Measurement, Prentice-Hall, Englewood Cliffs, N.J., 1969.

APPENDIX IV

RADAR CROSS SECTION (RCS) CAPABILITIES OF THE PRECISION ANTENNA MEASUREMENT SYSTEM (PAMS)

1.1 INTRODUCTION

This engineering report presents the results of an analysis on the radar cross section capability of the Precision Antenna Measurement System (PAMS). The report covers the present RCS capabilities and investigates methods for expanding the system to include the measurements of cross section distribution and density as well as J/S ratios. Some conclusions are drawn from the analyses and recommendations made.

2.1 BACKGROUND

The PAMS was developed by Actron for the Rome Air Development Center [1] for the evaluation and calibration of RF radiating systems and RCS measurements under dynamic conditions. The PAMS is slaved to an AN/FPS-16 track radar and monitors and records the RF emitting characteristics of the electronic systems under test as a function of vehicle position and attitude. In addition, the PAMS can receive scattered and reflected energy from the vehicle when the FPS-16 is operating in the skin track mode.

The system operates over the frequency range of 0.1 GHz through 18 GHz in either a CW, AM, FM, or pulse mode with any polarization. The system can monitor and record data on up to 12 frequencies with either both linear or both circular polarizations simultaneously throughout the operating range. The data is reduced and plotted as a radiation pattern relative to the vehicles heading in Effective Radiated Power (ERP). When required, the RCS of the vehicle can be plotted in db above a square meter.

In order to determine the vehicle attitude, auxiliary equipment was developed. The Airborne Monitoring System measures and records heading, roll, and pitch throughout the flight test. This data is merged with data acquired on the ground to present the actual conditions of the vehicle during flight.

3.1 RADAR CROSS SECTION TECHNICAL DISCUSSION

As described above, the PAMS monitors and records amplitude and frequency data from both active and passive targets. This report will be concerned with both the passive - radar reflections - and dynamic - jam to signal ratio (J/S) - modes of operation.

3.1 1 Radar Cross Section (RCS)

Radar cross section is simply the determination of the reflectivity of a target when the target is illuminated with an electromagnetic wave of a given polarization and

frequency. In other words it is the area which intercepts that amount of power which when scattered equally in all directions, produces a return at the receiver equal to that from the target and is expressed as

$$\text{RCS} = \sigma = \frac{\text{Power reflected toward source/unit solid angle}}{\text{Incident power density}/4}$$

and the experimental definition is given by

$$\sigma = \frac{(4\pi)^3 R^4 P_r}{P_t G_t G_r \lambda^2} \qquad (1)$$

where

R = Range in meters
P_r = received power in dbm
P_t = transmitted power in db
G_t = received power in dbm
G_r = gain of receive antenna in db
λ = free space wavelength in meters

Radar cross section is designated in square meters or by square wavelengths. However, due to the large variation of RCS over a wide dynamic range, the common format used to express RCS is decibels above one square meter. The PAMS software is configured for this format of RCS.

Typically, with most complex radar targets such as aircraft, ships, and terrain the RCS does not have a simple relationship to physical area. However, in general the larger the target size, the larger the cross section is likely to be.

3.1.2 Dynamic Radar Cross Section

This report will be concerned with the RCS of a target in free flight. Dynamic reflectivity measurements have become increasingly important in the last several years due to the difficulty in scaling some of the new exotic absorbing materials, conductivity, and other measurement parameters. In addition, there is the need to compare data taken in a dynamic environment with that of a controlled static environment. It is also desirable to be able to predict the characteristics of an unknown dynamic target using the parameters of a known fixed target. Dynamic measurements also eliminate the need for target supports and the errors associated with them, and ensures that the distance between the transmitter and the target is great enough so that a plane wave can be assumed at both the target and receiving antenna.

When making dynamic radar cross section measurements, it is mandatory that the targets attitude be known throughout the measurement period in order to know the exact aspect angle of the target and correlate perturbations in the data. Four parameters of the target aircraft which must be known are the heading, pitch, roll, and altitude. In addition the azimuth and elevation angles as well as the slant range from the radar to the target are required to completely define the aspect of the vehicle relative to the illuminating radar. This problem has been solved with the Airborne Monitoring System (AMS) developed by Actron for the Rome Air Development Center [2]. The AMS has a two-axis platform to derive the heading, pitch, and roll of the aircraft, a barometric altimeter, and a signal processor to convert the analog data to a digital format for storage on a seven track digital stepping recorder. A time code generator is included to put timing marks on the tape for correlation with data acquired by the PAMS. After the flight the tape is merged with the PAMS data acquisition tape to provide exact aspect information.

3.1.3 Active Radar Cross Section Measurement

It has already been stated that RCS is the result of illuminating a target with an electromagnetic wave, part of which is absorbed by the target as heat and the remainder scattered in many directions. The energy backscattered toward the receiver is the RCS which is addressed by this report. There is another distinction which must be made. This is the difference between an RCS measurement and RCS distribution. The difference is based on the resolution cell size of the illuminating signal. Any target which fits within a resolution cell is considered a point target and the measurement is referred to as a total radar cross section. If the target is larger than a resolution cell, the results are classified as an RCS distribution measurement. Both chaff and aircraft can fall into either classification depending on the size of the resolution cell. However, this report will be primarily concerned with the total cross section measurement. The configuration of PAMS is shown in figure 1, and the geometry of the aspect angle and direction is shown in figure 2.

As can be seen from figure 1, the PAMS has a bi-static geometry, i.e., the transmitter and receiver are separated by some distance; however, if the baseline distance is small with respect to the range from the transmitter to the target a pseudo monostatic condition will exist. When the baseline becomes significant with respect to the target range the bi-static angle β (shown in figure 1) has to be incorporated into the range equation (1) and the range parameter R^4 has to be modified to $R_T^2 R_R^2$ where R_T is the range to the target from the transmitter and R_R is the range from the target to the receiver antenna. The bi-static cross section will be different from the mono-static case where the transmit and reflected rays are parallel to each other. In the bi-static case the reflected energy has a different aspect angle and is made up of a different set of scatterers due to the complex geometry of an aircraft and polarization transformations. Consequently, it is necessary to ensure that the range is great enough to minimize the effect of the bi-static angle. There is no fixed minimum range since the reflected energy is dependent upon the target geometry as well as the range. Therefore, it will be necessary to review the requirements and target geometry prior to each test with the present PAMS configuration.

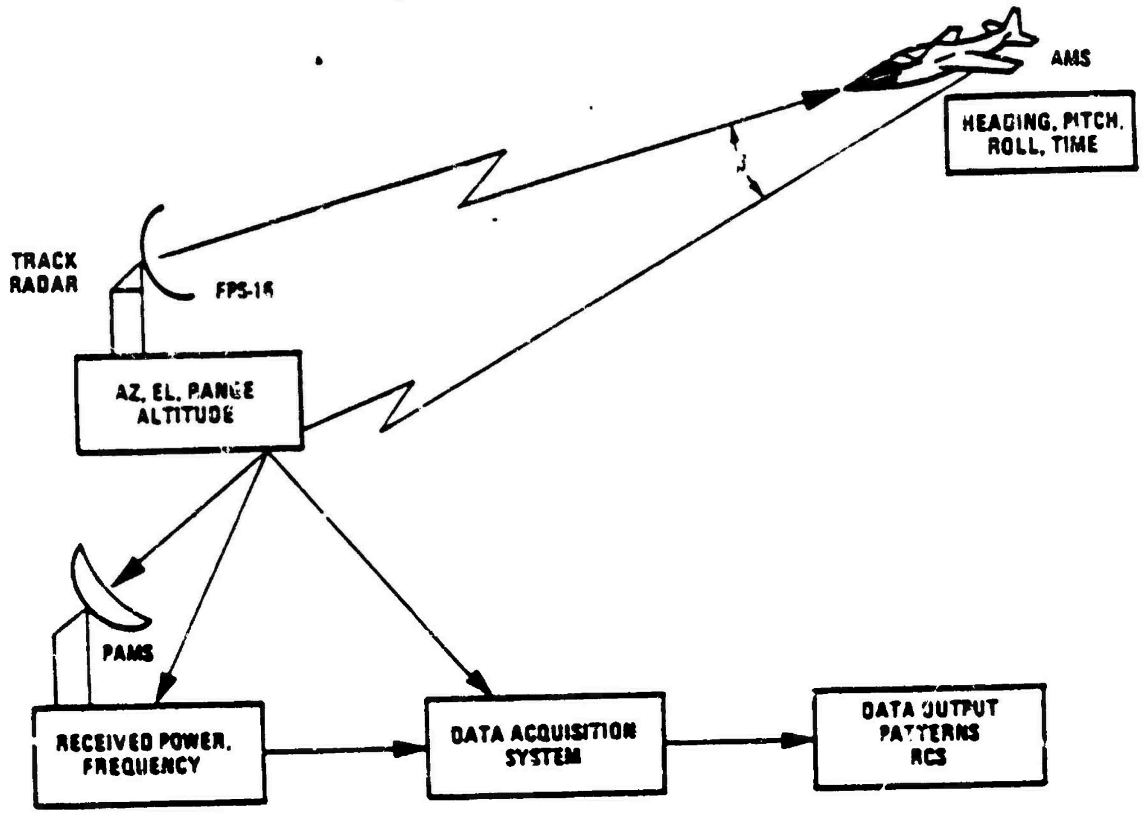

Figure 1. PAMS Configuration

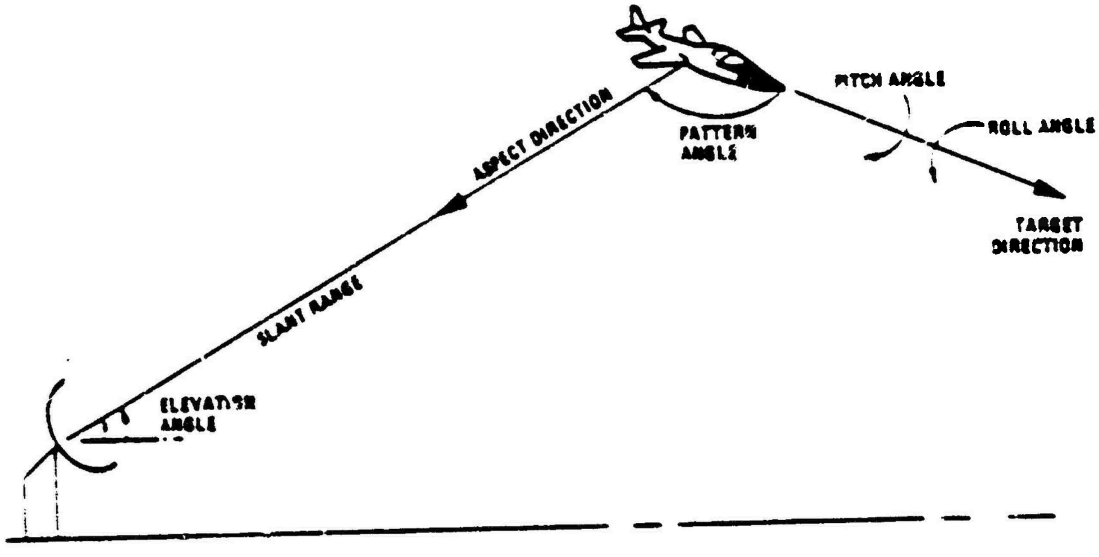

Figure 2. Target Aspect Direction

The following paragraphs will discuss the effects of frequency and polarization in radar cross section, calibration requirements, and J/S measurements.

3.1.4 Frequency and Polarization

It is well known that radar cross section is a function of target shape, material, aspect angle, frequency, and polarization of the transmit and receive antennas. The target has frequency dependent characteristics due to the target conductivity, absorbing properties, and size relative to the wavelength used in the measurement. With the frequency diversity capability of today's modern radars it is very desirable to relate a target's cross section as a function of frequency. This data will give rise to the detectability of the target over a frequency range of interest and will give the system designer data for enhancing the RCS or decreasing the detection probability depending on specific requirements. The capability of the PAMS to perform measurements over the frequency range from 0.1 GHz to 18 GHz makes it a useful tool to analyze the frequency characteristics of a target.

The polarization of transmitted wave also plays an important role in RCS measurements. In fact when a target is viewed at a single aspect angle and a single frequency the RCS is highly dependent on polarization. This dependence has led to numerous investigations and measurement programs to determine exactly what role the polarization plays in RCS. Some of the earliest contributors were Sinclair [3] and Kennaugh [4]. Sinclair related the scattered or returned field E^r, to the incident field E^t by the equation

$$E^r = KAE^t \tag{2}$$

where K is a function of the range and A is the scattering matrix with the form

$$A = \begin{pmatrix} A_{11} & A_{12} \\ A_{21} & A_{22} \end{pmatrix} \tag{3}$$

The a_{ij} term is a function of aspect angle and frequency and is generally complex. When the same antenna is used for both transmit and receive $A_{12} = A_{21}$. The analysis assumed that the distance between the target and the radar was such that the transmitted field was a plane wave. Kennaugh later extended the analysis to include the concept of null polarizations. It was shown that when an arbitrary target was illuminated by two particular polarizations the back scattered energy would be orthogonal to the incident polarization resulting in a null. The relationship of the null polarizations to each other provided a basis for target designation. He extended this work to include linear, isotropic, and symmetrical targets.

Further work by Huynen [5] has resulted in a technique to evaluate the polarization properties of target in the field. For this he defines a target scattering matrix

$$T = \begin{pmatrix} t_{11} & t_{12} \\ t_{21} & t_{22} \end{pmatrix} \begin{pmatrix} H-H & H-V \\ V-H & V-V \end{pmatrix} \qquad (5)$$

where H - V is a complex number which is proportional to the received horizontally polarized component of the returned signal (both amplitude and phase) when the target is illuminated with a vertically polarized wave. The measurement of the target scattering matrix requires amplitude and phase measurements on a pair of orthogonal returns from each of two orthogonal illuminating polarizations. In general, any pair of orthogonal polarizations may be used, e.g., right and left hand circular polarization, right and left diagonal, as well as vertical and horizontal. The instrumentation has to have the ability to measure both amplitude and phase of the back scattered return. In addition, the system requires the capability of transmitting two orthogonally polarized signals in sequence, and the capability to receive and record the orthogonal components of the polarized returns simultaneously. Field measurement of the scattering matrix requires a minimum number of two separate illuminations. Data by Huynen indicates that the accuracy of field measurements is approximately one to two decibels in amplitude and on the order of 20 degrees in phase. The PAMS lacks only the capability to measure the phase of the incoming wave for the determination of the target scattering matrix. A method of incorporating phase measurement into the PAMS will be discussed in Section 4 of this report.

3.1.5 Calibration

As was previously stated, cross section data is usually presented in decibels relative to one square meter. Therefore it is necessary to calibrate the system so that all subsequent measurements made with respect to the designated target are referenced to one square meter. Generally, calibration is accomplished by measuring a geometry whose characteristics are precisely known. The one geometry which fits these requirements is the sphere mainly because the sphere is the only shape whose cross section is constant regardless of the aspect angle at which the sphere is viewed. A sphere whose radius "a" is large with respect to the measurement wavelength will intercept the power contained in an area πa^2 of the incident wave and the cross section of the sphere is therefore πa^2. Therefore, the RCS of any sphere is exactly one-fourth the total surface area provided the radius is large compared to wavelength. Figure 3 illustrates the normalized cross section of a conducing sphere as a function of its radius.

Although it would be desirable to have one square meter spheres for each test frequency it is obvious that this would be economically impossible due to the broad spectrum of frequencies available with PAMS. Therefore it will be necessary to use a few standard spheres and incorporate correction factors into the calculations.

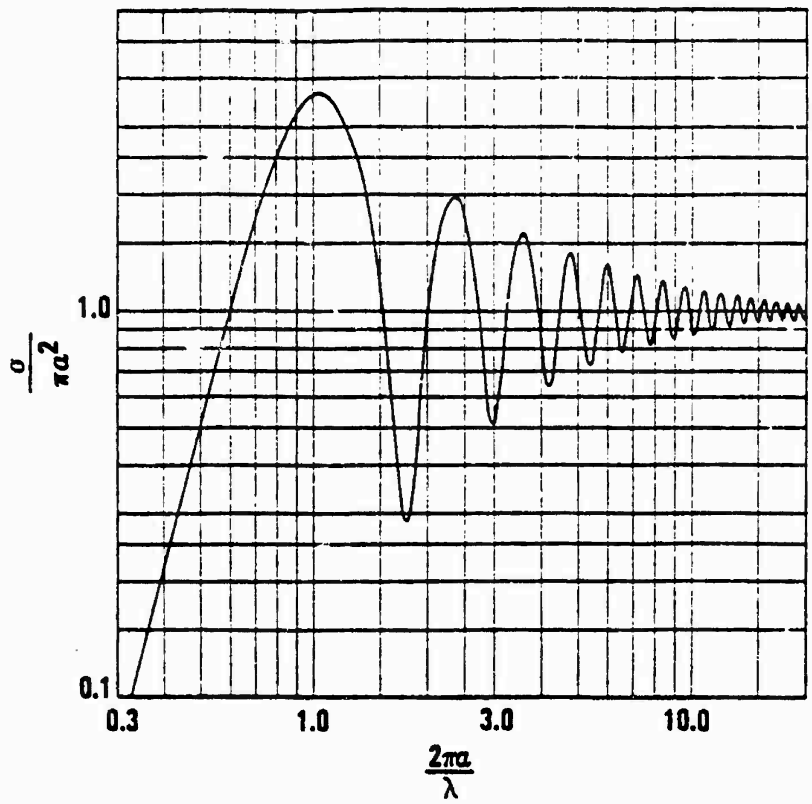

Figure 3. Normalized Cross Section of a Conducting Sphere

To properly calibrate the PAMS for RCS, a test sphere should be measured before and after each test flight. In addition to the primary calibration it is useful to have a secondary standard which could be used to check the calibration during the test program. This can be accomplished by using an isolated tower, water tank, etc., which is convenient and permanently located at a distance of several miles. If the value of the secondary or transfer standard is plotted relative to the sphere, the standard can be used to check the initial calibration throughout the test - provided there are no significant changes in the weather.

3.1.6 J/S Measurements

The ability to measure J/S ratios is needed to evaluate airborne jammers and system performance with respect to the location of the jamming antennas. In order to successfully evaluate jamming systems it is necessary to have the ability to accurately separate the J and S parameters. The technique used depends on what type of jammers are used, i.e., repeaters or transponders. There are three methods which can be used to obtain the J and S values [6]. The first two deal with the repeater technique and the third is used with transponders. The first method is to double pulse the target. The first pulse is repeated by the jammer yielding the

J + S value while the second pulse strikes the target with the repeater inhibited which yields the value of S only. This method loses some of its accuracy for low J/S values. However, in the case of repeater jammers, low J/S ratios are of little consequence. The second method uses an internal delay in the repeater to keep it from responding to the track radars initial track pulse, thereby permitting the J and S parameters. This technique can introduce frequency spreading due to the delay, thereby reducing the transmitted power. Therefore, precautions must be taken to ensure that the power reduction is minimal or laboratory measurements will have to be made on this to derive a correction factor which must be added to the measured data. The most efficient J/S measurements are obtained with transponders that can be interrogated by the track radar. The transponder can be adjusted to delay its response for a required period after the receipt of the interrogating pulse train. This permits the J and S to be extracted without the introduction of accompanying errors. This approach yields the best results and is, in general, very repeatable. The evaluation of noise jammers can be accomplished by keeping the track radar out of the frequency band of the jammer. This introduces some offset in the J/S measurement/ however, in most cases this should not be serious. If it is necessary to perform the S measurement inside the noise jammers bandwidth it will be necessary to key the jammer on and off so that the S parameter can be derived. In all the cases described above the results are related to the radar used in the test. If the results are to be applied to a specific threat radar they must be adjusted mathematically before they can be used.

In the past all measurements made with the PAMS have neglected the effect of atmospheric attenuation. However, in the case of J/S measurements the atmospheric attenuation should be taken into account since the J signal is reduced by $1/R^2$ while the S signal varies as $1/R^4$. Consequently, the results can have significant error introduced at the higher frequencies. In order to evaluate the effect of the attenuation we will modify equation (1) as follows:

$$P_r = S = \frac{P_t G_t G_r \lambda^2 \sigma}{(4\pi)^3 R^4} e^{-2\alpha R} \tag{6}$$

where the term $e^{-2\alpha R}$ is the attenuation for two way transmission [7]. In order to derive the value of the attenuation coefficient α we take two measurements on a calibration standard at ranges R_1 and R_2, where $R_2 > R_1$. This gives a ratio of S_1/S_2 which is expressed as

$$S_1/S_2 = \frac{R_2^4 e^{-2\alpha R_1}}{R_1^4 e^{-2\alpha R_2}} \tag{7}$$

and solving for α we get

$$\alpha = \frac{\ln\left(\frac{S_1 R_1^4}{S_2 R_2^4}\right)}{2(R_2 - R_1)} \qquad (3)$$

This can be calculated by the PAMS data acquisition system after the initial calibration has been made. We can now evaluate the effect of atmospheric absorption on the J/S ratio. Taking the equation for J we have

$$J = \frac{P_J G_J G_R \tau^2}{(4\pi R)^2} e^{-\alpha R} \qquad (9)$$

then taking the ratio of J/S we have the following

$$J/S = \frac{P_J G_J 4\pi R^2}{P_T G_T \sigma} e^{\alpha R} \qquad (10)$$

Equation (10) shows the effect of the attenuation introduced by the atmosphere. To convert this measurement to a free space condition requires the factor $e^{-\alpha R}$ be added to the results. For frequencies above I band the atmospheric conditions can introduce an unknown variance of ±3 db into measurement.

The following section describes the changes which will enhance the RCS and J/S measurement capability of the PAMS. In addition to hardware modifications the system will require additional software to support the measurements.

4.1 PAMS SYSTEM MODIFICATIONS

The preceding sections have discussed a number of radar cross section parameters and J/S measurements. This section will discuss some of the improvements which can be made to PAMS to enhance its overall capability in measuring, calibrating, and evaluating airborne electronic systems.

4.2 PAMS PRESENT CONFIGURATION

In its present configuration the PAMS can be used in a variety of measurement programs without any hardware modifications. Typically the following applications are well within the present capability of the system. (However, new software will have to be developed and existing software modified to incorporate new constants and measurement techniques).

1. RCS vs Aspect on aircraft
2. Total RCS of chaff
3. Frequency diversity
4. Polarization diversity
5. Glint on aircraft
6. Bistatic responses on aircraft and chaff

The principal limitation of the present configuration of PAMS is the lack of range resolution, particularly in chaff measurement applications. However, of all the modifications which will be discussed here, that is the simplest to incorporate. Range gating can be accomplished simply by adding PIN diode switches in the receiver input. The switch can be turned on (high attenuation position) by using a sample of the transmitted pulse for triggering a gate pulse generator to drive the switch. The switch can be turned off (low attenuation position) by using a signal from the range gate return from the FPS-16 track radar. This will ensure out of gate rejection of unwanted signals by up to 80 db, depending on the switch characteristics. This will provide the range resolution required for strong RCS signals at short ranges.

4.3 TWO PEDESTAL CONFIGURATION

As previously described in earlier sections the PAMS is slaved to an FPS-16 track radar which provides both position data and range and acts as the illuminating signal for RCS measurements. The configuration of the FPS-16 and PAMS results in a bistatic geometry with a baseline of approximately 600 feet. This system works moderately well as long as the range to the target is great enough to minimize the bistatic angle. The one drawback is that it operates over a very narrow frequency range in G Band. To cover a broad frequency would result in a multiplicity of radars each operating over a narrow band. While this approach would extend the usefulness of the system, the instrumentation interface problems could become extremely complicated and there would still be holes in the frequency coverage.

The problem was analyzed and two approaches evaluated. The first of these was the modification of the present system to incorporate both transmit and receive functions. This would be accomplished by removing one or more of the receiver drawers and replacing them with transmitter systems. While this approach had certain advantages in reducing the timing, control, and synchronization problems, it would require a number of other modifications. Principal among these would be the requirement to change over to higher power handling transmission lines and antenna feeds. This would be a major modification and broadband high power antenna feeds are difficult to realize over the entire frequency spectrum of PAMS. In addition, there was the problem of having to operate with the same antenna characteristics. This was particularly true where narrow beamwidths were required at the lower frequencies for RCS distribution measurement. There was also the loss of frequency coverage due to the loss of one or more receivers to make room for the transmitters. Consequently this approach was abandoned in favor of a two pedestal system.

The two pedestal concept offered some significant advantages which more than outweighed some of the added interface difficulties. Principal of these was the ability to use the full receiver capability of the PAMS. In addition, up to four transmit frequencies could be employed simultaneously. Another advantage which was made possible by the two pedestal system was the ability to incorporate higher gain antennas with the transmit system. This would result in either a reduction in required transmitter power for a given range or an increase in range for a given power level.

The recommended location for the transmit pedestal is next to the PAMS on the same platform. This has the effect of reducing the bistatic angle essentially to zero and results in a quasi-monostatic system. The interface between the two systems is also simplified when they are colocated in this manner. The main disadvantage from this geometry is the loss of coverage by the PAMS which would eliminate, particularly, overhead and nearby parallel flybys from flight planning. This deficiency could be eliminated by designing the transmit system to be lowered out of the way when not in use. However, the economics involved make this approach somewhat questionable. The overall range requirements will dictate the final configuration; therefore, the system geometry will not be pursued any further here.

The addition of a separate system for the transmitters results in a three pedestal configuration with both the PAMS receive and transmit systems being slaved to the FPS-16 track radar. The parallax correction program will have to correct for the parallax in both pedestals. Consequently, extreme care must be taken to ensure that the servo loops of both units are matched in order that the two pedestals track each other smoothly. If there is any overshoot or delay between the two, significant errors will be introduced into the measurement.

It is anticipated that the transmit system will utilize tuneable magnetrons in the 50 KW to 100 KW peak power class. A universal modulator will provide the operating power for the magnetrons along with the capability to set the pulse width and pulse repetition rate over a reasonable set of limits. The actual radiated power requirements for the system are investigated in the following paragraph.

4.4 POWER REQUIREMENTS

A brief analysis was made to determine typical power levels required to measure radar cross section in the range from 2 square meters to 20 square meters out to a range of 35,000 yards. A frequency of 6 GHz was chosen as being representative of a large number of measurements. For this frequency the PAMS antenna has a gain of approximately 31 db, and a transmit antenna of 40 db was assumed. The calculations were made using equation (1) and did not include any correction for atmospheric effects. The results are shown in figure 4. The same data was plotted in a different format to show the RCS in square meters as a function of transmit power for four fixed ranges and is illustrated in figure 5. The ability to utilize higher gain antennas was emphasized in the calculations. Had the same gain be used for the transmit antenna as that for the receive antenna the power would have to be increased by a factor of eight. However, caution must be exercised when specifying transmit gain in order to avoid very narrow beamwidths when the measurement does not require them. Too narrow a beamwdith can introduce glint and scintillation into a total RCS measurement due to the target slipping

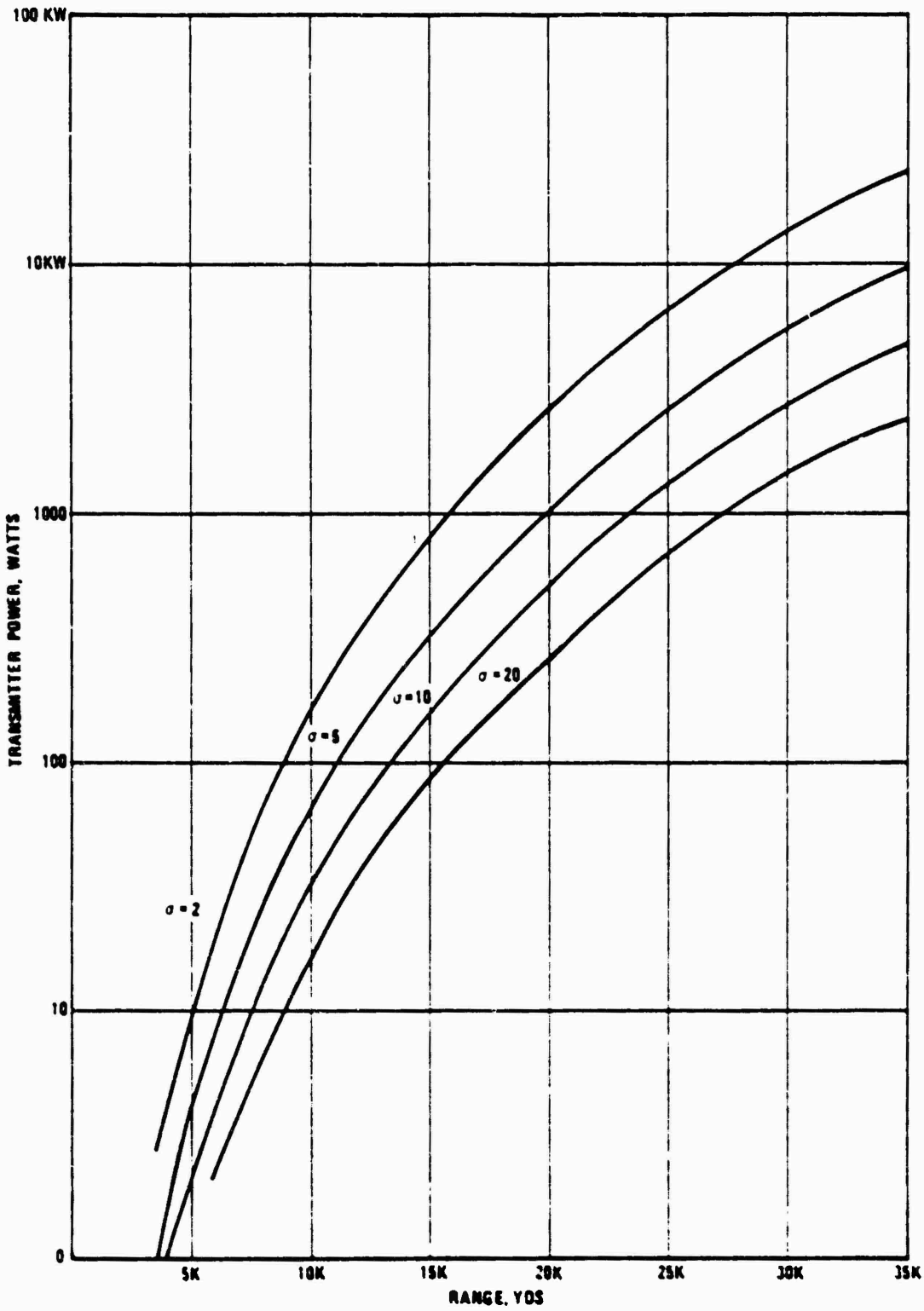

Figure 4. Power Requirements as a Function of Radar Cross Section and Range

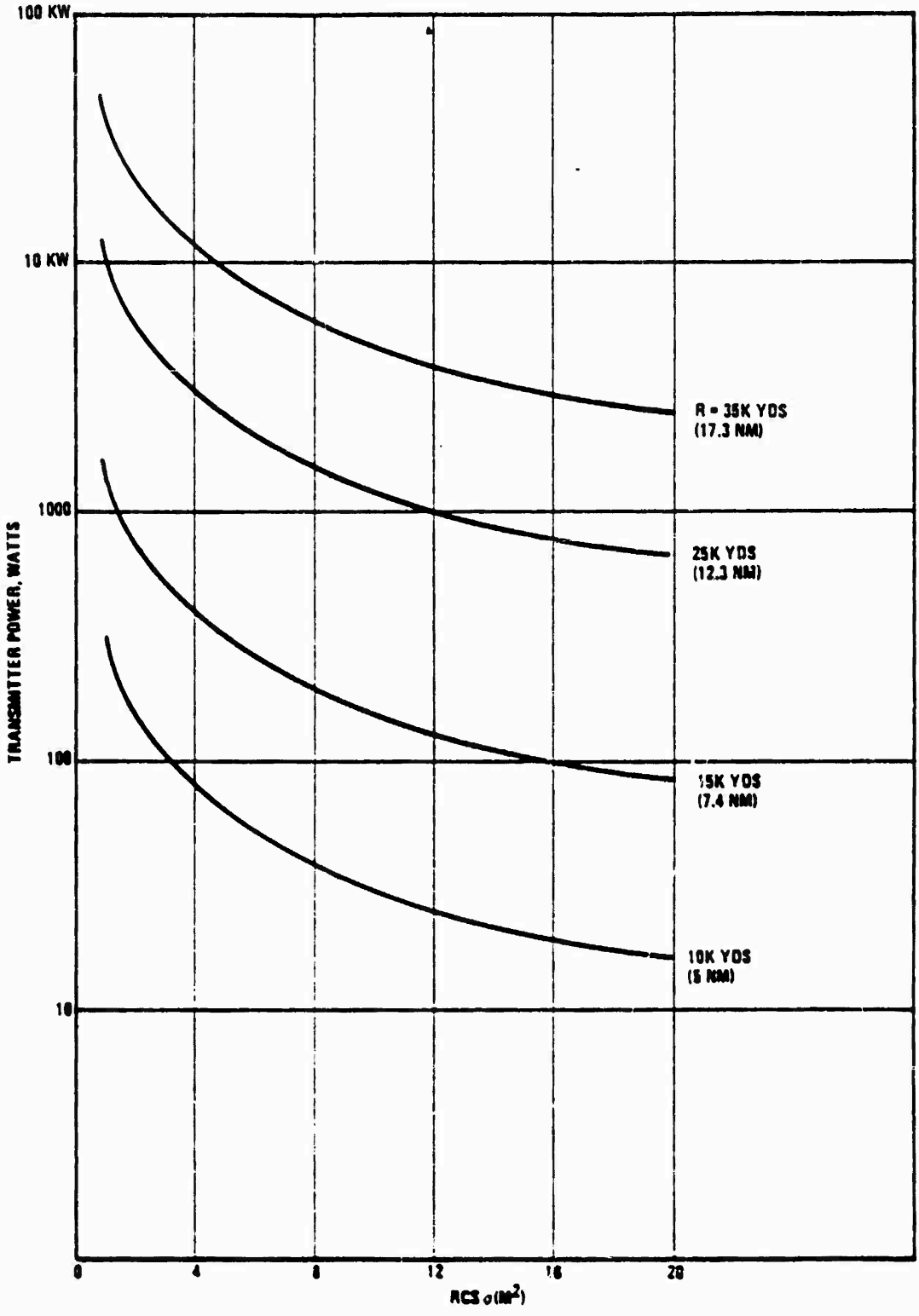

Figure 5. Power Requirements as a Function of Radar Cross Section and Range

in and out of the pattern coverage. The two-pedestal concept does allow for the use of high gain, narrow beam antennas when RCS distribution measurements are required on aircraft or chaff. A systems study will have to be performed when the long range requirements for the system are specified in order to make tradeoffs with performance and cost to arrive at the optimum configuration.

4.5 PHASE MEASUREMENTS

The PAMS does not currently have the capability to perform phase measurements. This deficiency limits the type of measurements which can be performed with the PAMS. Without the ability to measure phase it is not possible to perform high resolution doppler measurements or to define the scattering matrix. To add this capability to the PAMS will require some extensive modifications to the existing system. The basic requirements for a phase measuring system is illustrated in figure 6. This concept is related to that of an MTI radar with the exception of the pulse to pulse sequence between the horizontal and vertical feeds. The transmitter section is indicated as shown inside the dashed line of figure 6. The rest of the block diagram is part of the PAMS receiver. If scattering matrix data is not required, the switch between the horizontal and vertical antennas can be left in the desired polarization.

It was assumed that the transmitter would employ a magnetron. Since a magnetron is a pulsed amplifier which has no phase coherence between consecutive pulses, a phase reference must be established for each pulse. This is accomplished by taking a sample of the transmitted pulse and mixing it with the output of a stabilized local oscillator (stalo) and then using the resultant pulse to phase lock the coherent oscillator (coho). The coho then becomes the reference oscillator for the received signals. The received signals are mixed with a local oscillator which is phase locked to the stalo and then compared in phase with the coho in a phase detector. The output of the phase detector is proportional to the phase difference between the two input frequencies to the mixer preamp, while the output of the amplitude detector is proportional to the target echo signal referenced to the coho signal. Calibration of the amplitude of the reference coho signal in terms of radar cross section at a given range provides radar cross section data for the target.

In order to obtain the scattering matrix of a given radar target, amplitude, and phase data for horizontal and vertical polarization combinations must be measured [5]. This can be accomplished by alternately feeding the vertically and horizontally polarized antennas. Scattering matrix data can be gathered on a two-pulse basis by exciting the vertically polarized antenna on one pulse, and the horizontally polarized antenna on the next pulse, each time obtaining vertically and horizontally amplitude and phase data.

As can be seen from figure 6, the incorporation of phase measurement capability entails some extensive modifications. An alternate method to achieve some phase measurement capability would be to use one of the dual channels in the receiver as a reference channel by coupling off a portion of the transmitted signal and then phase locking the second channel to the reference. Phase detection capability would still have to be added; however, the modification is still less complex. One

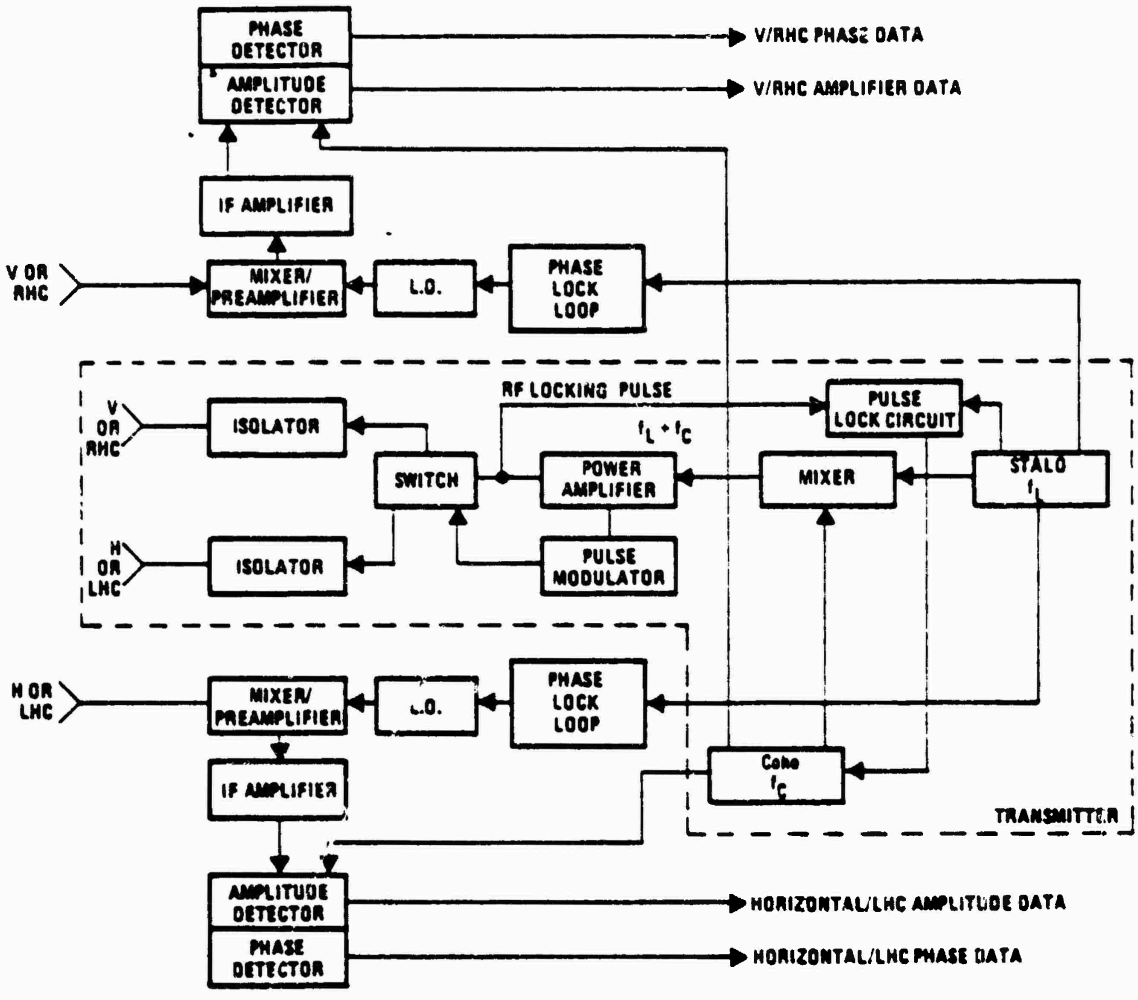

Figure 6. Phase Measurement System

disadvantage with this approach is that the polarization diversity is lost. Whether or not this would be acceptable is totally dependent on the particular requirements of a flight test program.

There is one more modification that may be considered. It does not incorporate phase measuring capability; however, it extends the polarization diversity of PAMS to include right and left hand diagonal polarizations. This can be accomplished by replacing the existing polarization network with the one pictured in figure 7. The switching network which is shown allows any two orthogonal polarizations to be selected. The switches could be programmed to provide a commutator effect with all major polarizations being sampled during the test. The combination of hybrids and switches provide excellent isolation between the two channels.

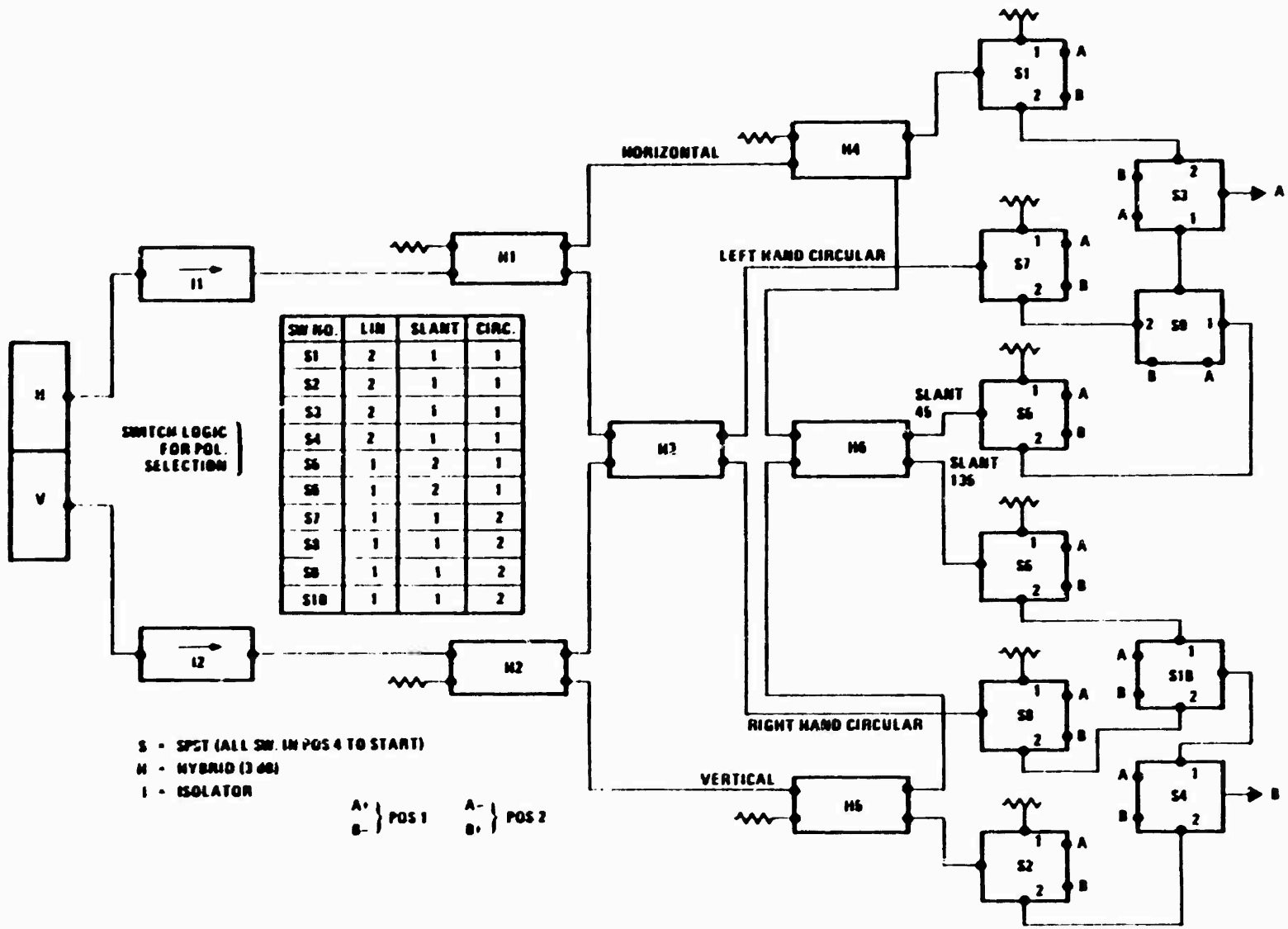

SW NO.	LIN	SLANT	CIRC.
S1	2	1	1
S2	2	1	1
S3	2	1	1
S4	2	1	1
S5	1	2	1
S6	1	2	1
S7	1	1	2
S8	1	1	2
S9	1	1	2
S10	1	1	2

Figure 7. Polarization Network

The optimum configuration for enhancing the radar cross section measurement capabilities will be dependent upon mission requirements for the next several years. Some or all of the modifications described in this section could be incorporated into the PAMS when the need for a particular measurement capability arises.

5.1 CONCLUSIONS

This report has covered the primary requirements for a number of various measurements involving the determination of radar cross section. In addition the ability of PAMS to perform these measurements was evaluated for its present configuration. Several modifications to extend the enhance the PAMS RCS capabilities were analyzed. For the majority of cross section measurement, phase data is not required. Only those cases involving high resolution doppler measurements and the determination of the target scattering data was phase information an absolute necessity.

The optimum configuration both from an operational as well as an economic standpoint appears to be the addition of a separate transmitter pedestal colocated with PAMS. The addition of range gating and polarization diversity enhancement results in a system capable of performing the majority of reflectivity measurements that will normally be required. The ability to handle phase measurements can be incorporated into the system when the need arises.

REFERENCES

1. Precision Antenna Measurement System - Final Technical Report RADC-TR-73-233 AD 915-581L
2. PAMS Airborne Instrumentation - Final Technical Report RADC-TR-74-174 AD 922-537L
3. G. Sinclair, "Modification of the Radar Range Equation for Arbitrary Polarization," Ohio State University, Antenna Laboratory Report 302-19, Sept. 1948.
4. E. M. Kennaugh, "Polarization Properties of Radar Reflections," Ohio State University, Antenna Laboratory Report 389-12, March 1952.
5. J. R. Huynen, "Measurement of the Target Scattering Matrix," Proceedings of the IEEE, Volume 53, No. 8, pp 936 - 954, August 1965
6. J. Seale, NATC Patrixent River, Md. Private Communications
7. M. I. Skolmk, "Introduction to Radar Systems," pp 540 - 546, McGraw Hill Book Co., 1962

BIBLIOGRAPHY

1. Radar Reflectivity Measurements Symposium Vol 1 RADC TDR-64-25 AD 601-364 April 1964
2. Radar Reflectively Measurement Symposium Vol. II RADC-TDR-64-26 AD 601-365 April 1965
3. Proceedings of the IEEE - Special Issue on Radar Reflectivity
4. J. W. Crispin, Jr. and K. M. Siegel "Methods of Radar Cross Section Analysis", Academic Press, 1968
5. M. I. Skolnick, "Radar Handbook", McGraw Hill 1970
6. D. K. Barton, "Radar System Analysis", Prentise-Hall Inc, April 1965
7. D. E. Kerr, "Propagation of Short Radio Waves", Vol. 13 Rad Lab Series, McGraw Hill 1951